

### **MACC O-INT WP3.1**

## **“Meningitis linked to mineral dust transport in the Sahel”**

### **Second delivery Report**

E. Cuevas<sup>1</sup>, C. Pérez<sup>2,3</sup>, J.M. Baldasano<sup>3</sup>, C. Camino<sup>1</sup>, S. Alonso-Pérez<sup>1,4</sup>, S. Basart<sup>3</sup>

<sup>1</sup> Meteorological State Agency of Spain (AEMET)

<sup>2</sup> The Earth Institute at Columbia University (IRI-NASA)

<sup>3</sup> Barcelona Supercomputing Center (BSC-CNS)

<sup>4</sup> The Spanish National Research Council (IDAEA-CSIC)

<sup>5</sup> International Research Institute for Climate and Society, Columbia University (IRI)

**April 2011**

This report summarizes the activities and major findings of the health specific user community test case (**Work-Package 3.1: “Meningitis linked to mineral dust transport in the Sahel”**) conducted within **O-INT (MACC)** and constitutes the following deliverable: **“Long-term retrospective analysis of dust and AI with meningitis epidemics data”** (M-20; 2011-Jan-30)

## **Index**

- 1. Introduction and motivation: Meningitis epidemics and atmospheric dust in the Sahel**
- 2. Main goals in the Framework of MACC**
- 3. Data and Methods**
- 4. Background: meteorological conditions**
- 5. NMMb/BSC-Dust model verification over Niger**
- 6. Results and discussion**
- 7. Findings and proposals for MACC**

**Acknowledgments**

**Bibliography**

1. **Introduction and motivation: Meningitis epidemics and atmospheric dust in the Sahel**

According to the World Health Organization (WHO, 1998), meningococcal disease is a contagious bacterial disease caused by the meningococcus *Neisseria meningitidis*, a *Gram-negative diplococcus bacterium*. There are three main clinical forms of meningococcal disease. Meningococcal meningitis (MM) is the more common entity, especially during epidemics. Meningococcal meningitis, commonly designated as cerebrospinal meningitis, is the only form of bacterial meningitis that causes epidemics with high case fatality rates. It is spread by person-to-person contact through respiratory droplets (throat secretions) of infected people (WHO, 2000). Epidemics can occur in any part of the world. However, the largest epidemics occur mainly in the semi-arid areas of sub-Saharan Africa, designated the African “meningitis belt” (Molesworth et al., 2002b). This is the area between Senegal and Ethiopia including Benin, Burkina Faso, Northern Cameroon, Chad, Gambia, Ghana, Mali, Niger, Northern Nigeria, and Sudan (see Figure 1.1.).

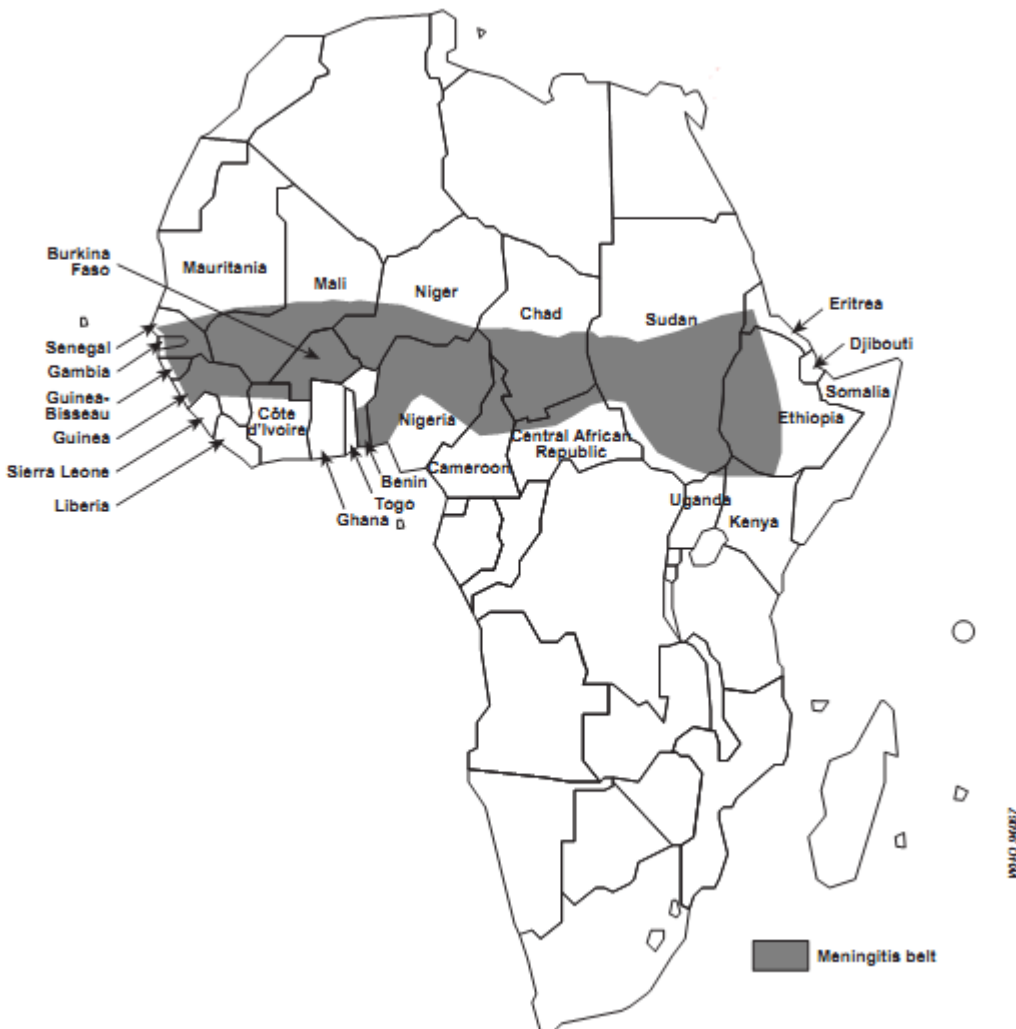


Figure 1.1.; African meningitis belt (from WHO; 1998)

Every year countries within the Sahelo-Sudanian band are badly affected with major MM disease outbreaks. Epidemics occur in seasonal cycles between the end of November and the end of June, depending on the location and climate of the country, and decline rapidly with the arrival of the rainy season (Molesworth et al., 2002a). In the meningitis belt countries, the estimated incidence

for the 20-year period 1970-1992 was about 800,000 cases (WHO, 1998). There was a substantial increase in reported meningococcal disease in Africa in 1996, being 188,341 the total number of meningitis cases reported during the period January-October 1996, of which nearly 20,000 were fatal (WHO, 1998).

Concerning the relationship between meningitis epidemics and environmental conditions, it is believed that low absolute humidity and dust may enhance meningococcal invasion by damaging the mucosal barrier directly (irritating the epithelial lining of the upper respiratory track), allowing bacteria penetration, or by inhibiting mucosal immune defences (WHO, 1998). Furthermore, a present controversial hypothesis suggests that dust particles might serve also as carriers for meningococcus bacteria facilitating the person-to-person transmission.

The first results aiming to link MM outbreaks and dry and dusty conditions in Africa were published by Lapeyssonie (1963). Later, there have been some studies aimed to model the spatial MM risk distribution according to environmental factors such as rainfall, absolute humidity, aerosols and soil conditions (Molesworth et al., 2003; Savory et al., 2006). However these studies provided fix MM risk maps, not accounting for the year-to-year variability of the number of Meningitis cases and timing.

The strong increase in MM disease occurrence in Mali has been analysed by Sultan et al. (2005). By using weekly number of cases of MM disease in Mali and large-scale fields (NCEP reanalysis) of surface wind speed, they have clearly found a strong relation between climate and the seasonal pattern of MM cases in Mali. They have identified the week 6 of the year (February) as the onset of disease outbreak and related to the intensity and timing of the Harmattan winds. This study implies an indirect relationship of MM outbreaks with dust conditions.

Thomson et al. (2006) have found a direct relationship between MM outbreaks and dust. However this relationship was not completely well understood because dust column integrated measurements from satellite (Absorbing Aerosol Index-AAI- from TOMS) were used in the study, which not always reflects the surface dust conditions (Ginoux and Torres, 2003) really affecting the population.

As it has been stated by Sultan et al. (2005), for studying the relationship between MM outbreaks and environmental factors, it is necessary to discriminate between local properties and potential large-scale effects on disease patterns. Among the first group that may play an important role in MM outbreaks, they have identified the immune receptivity of individuals, a poor socioeconomic level, medical aspects (as the transmission of a more virulent serotype), and social interactions, such as tribe migrations, and meetings. Of course, these factors are out of the scope of this test-case study. We will focus on large-scale environmental factors.

Remote sensing techniques (Aerosol Optical Depth –AOD- from AERONET or Absorbing Aerosol Index (AAI) or AOD derived from satellite -borne instruments) only provide total column dust observations, from which there are serious limitations to infer the actual dust concentration near ground that actually affect the population. On the other hand there is big gap of in-situ surface dust concentration and meteorological observations in the Sahel region. They are very scarce, with very limited spatial representation, and also limited in time. For all these reasons our aim in this test-case working package is to show the new capabilities we could gain with the use of high resolution dust model (NMMb/BSC-Dust; Pérez et al., 2009) long-term reanalysis, in order to improve the

knowledge of the relationship between MM outbreaks and environmental factors. These findings could aim to the establishment of operational dust forecasting products and services, in the European framework within MACC or post-MACC projects, in order to improve and long-term support the meningitis warning systems being developed by some international institutions under the WHO umbrella.

## 2. **Main goals in the Framework of MACC**

The main goals of the present study are: 1) show the relationship between meningitis epidemics and some environmental parameters, and 2) demonstrate the advisability of the use of surface dust concentration and meteorological variables obtained from high resolution dust model reanalysis in the “meningitis belt” to study the meningitis outbreaks.

The outputs of this deliverable are the following:

- a. Provide findings from a joint analysis of long-term (20 years; 1986-2008) number of meningitis cases (provided by the International Research Institute for Climate and Society, Columbia University), long-term high resolution dust model reanalysis (30 years; 1980-2010, namely the NMMb/BSC-Dust model), long-term NCEP and ECMWF meteorological reanalysis, and long-term dust-related remote sensing information (AERONET and satellite-borne sensors) in a specific test region (southern Niger) within the meningitis belt.
- b. Propose actions and activities (to MACC Project) concerning the feasibility and interest of developing future operational services and products (within the European framework) ad-hoc designed to support a short-medium range warning system for meningitis epidemics in the Sahel region, as a first step, and seasonal dust forecasting as a second step.

## 3. **Data and Methods**

Meningitis cases are included in the weekly reports of notifiable diseases and are aggregated at different spatial scales from the health local authorities to the country level. Meningitis reports, which include number of cases and deaths, are delivered periodically by the WHO’s Department of Communicable Disease Surveillance and Response. The present study is based on scrutinised, validated and standardized weekly number of meningitis cases disaggregated at district levels for the whole Niger, from 1986 to 2008, provided by the International Research Institute for Climate and Society (IRI; University of Columbia). The highest prevalence of the MM outbreaks is observed in the districts of southern Niger (Figure 3.1.). For this reason we have grouped the weekly number of meningitis of selected districts in one region (southern Niger). This region will be the geographical domain of our test case analysis (Figure 3.2.). The information of number of meningitis cases used in this study corresponds to the following districts of Southern Niger: AGUIE, BIRNI-N’KONNI, BOUZA, DAKORO, DOGON-DOUTCHI, DOSSO, FILINGUE, GAYA, GUIDAN-ROUMDJI, ILLELA, KEITA, KOLLO, LOGA, MADAOUA, MADAROUNFA, MAGARIA, MATAMEYE, MAYAHI, MIRRIAH, OUALLAM, SAY, TAHOUA, TESSAOUA, TILLABERI, and ZINDER. In Figure 3.2 the position of the validation sites used in this work have been included.

For determining the study area, we used Geographic Information System (GIS). The study area was obtained by calculating the total number of cases of meningitis over the whole period of available data, and interpolating maps using GIS analysis tools and Inverse Distance Weighted (IDW) method.

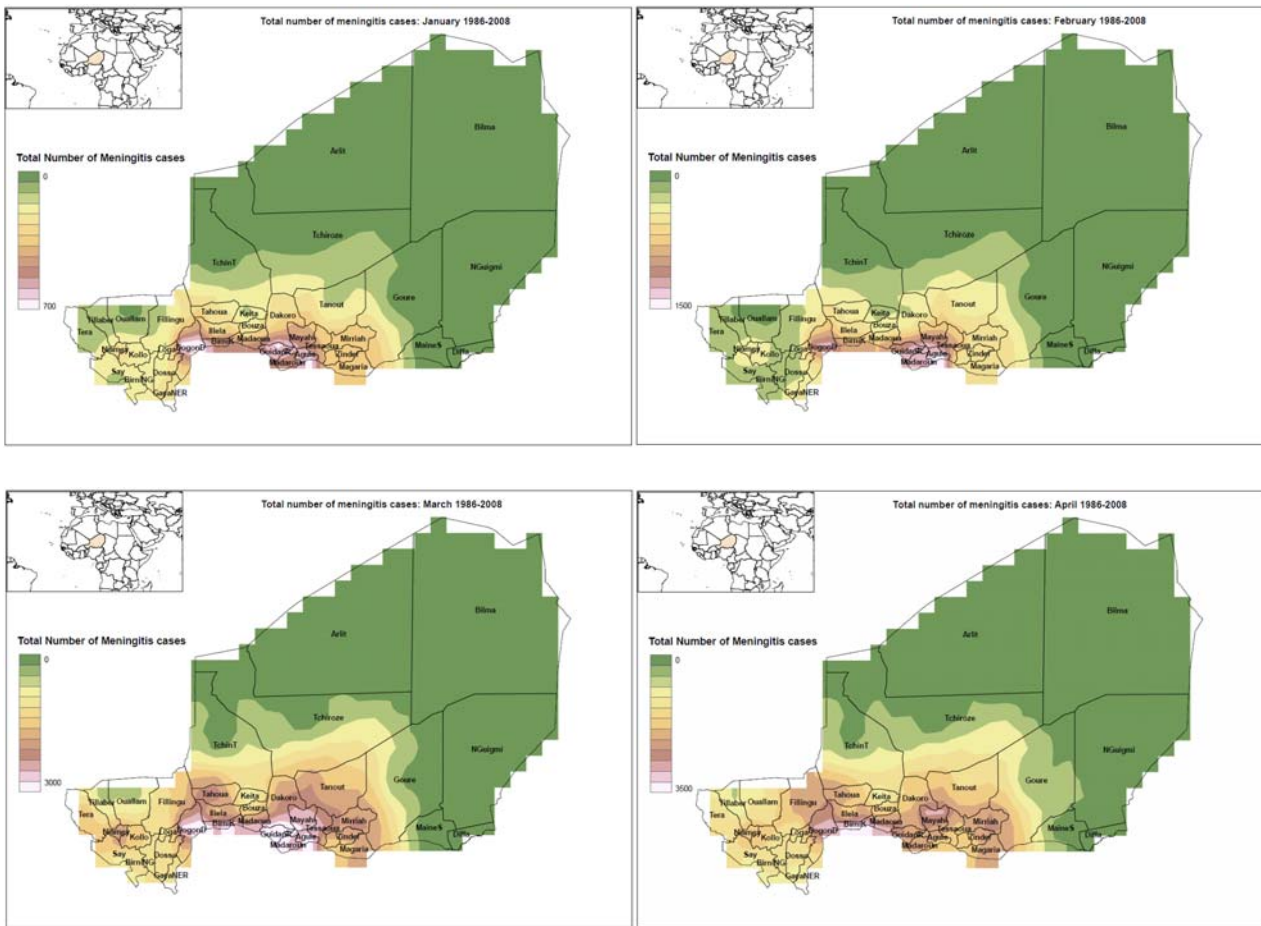


Figure 3.1.; Total number of meningitis cases in Niger during the period 1986-2001 for January, February, March and April, respectively.

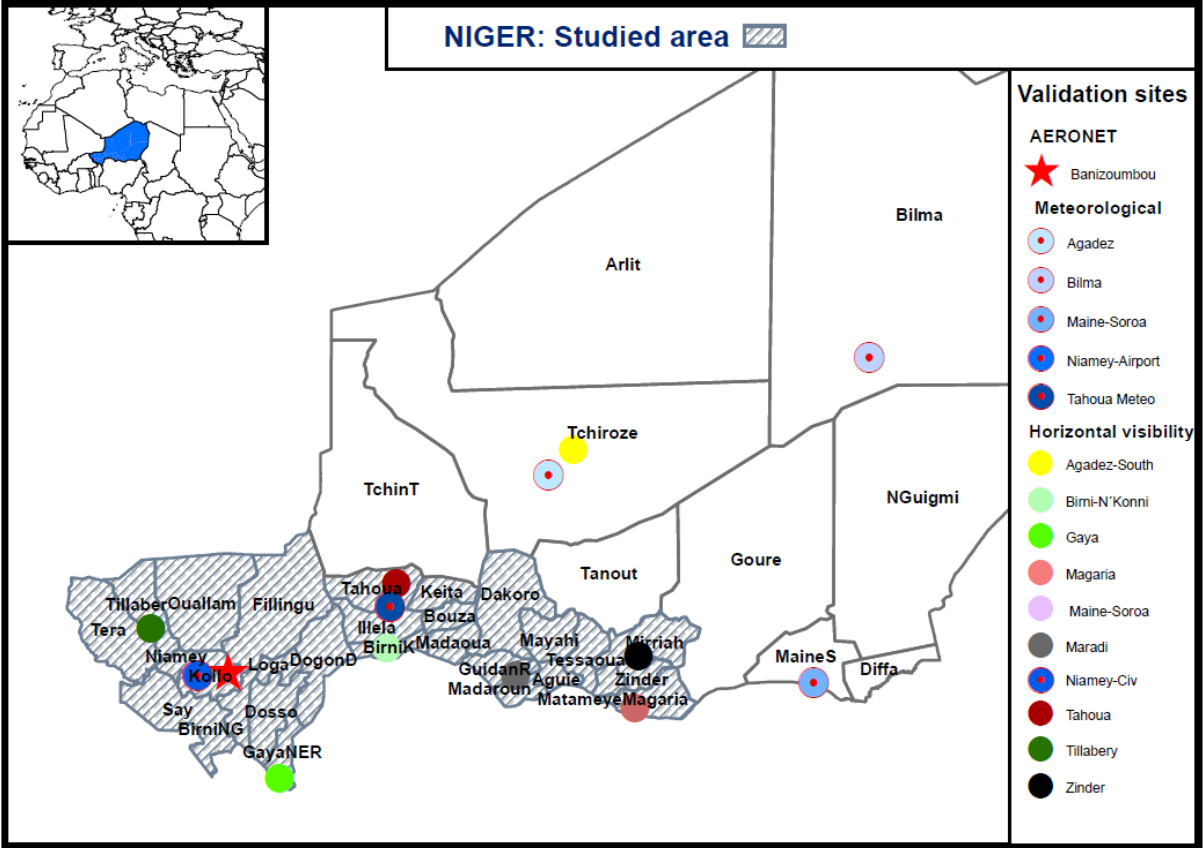


Figure 3.2.; Map of Niger with shadowed districts and validation sites used in this work.

We have used a 30 year simulation (February 1979- March 2010) of the NMMB/BSC-Dust (Pérez et al., 2009), a new dust aerosol cycle model embedded online within the NCEP Non-hydrostatic Multiscale Model (NMMB), within a domain that covers Northern Africa, Middle East and Europe (Figure 3.3.). A detailed description of the model is provided in the forthcoming paper Pérez et al., (2011). The resolution of the model was set to  $0.5^\circ \times 0.5^\circ$  and 40 hybrid sigma-pressure model layers. The simulation was reinitialized every 24 hours with Reanalysis-2 pressure level data and GLDAS for soil moisture and temperature with a spin-up of 12 hours (i.e, a 36-hours simulation for every simulated day has been performed and kept the last 24 hours). The initial state of dust concentration in the model is defined by 24-hour forecast from the previous-day model run. The reanalysis has been run at the Barcelona Supercomputing Center (BSC-CNS), partner of AEMET in this O-INT Working Package. In the present study the reanalysis corresponding to the period ranging from middle 1995 to 1997 has been rejected because some wrong data found in GLDAS database used for the reanalysis. The NMMB/BSC-Dust model will be implemented in a near future at the BSC-CNS as an operational model for dust forecasting. It will contribute to the World Meteorological Organization Sand and Dust Storm Warning Advisory and Assessment System (SDS WAS) Regional Center for Northern Africa, Middle East and Europe. This Regional Center is hosted by the consortium formed by AEMET and BSC-CNS.

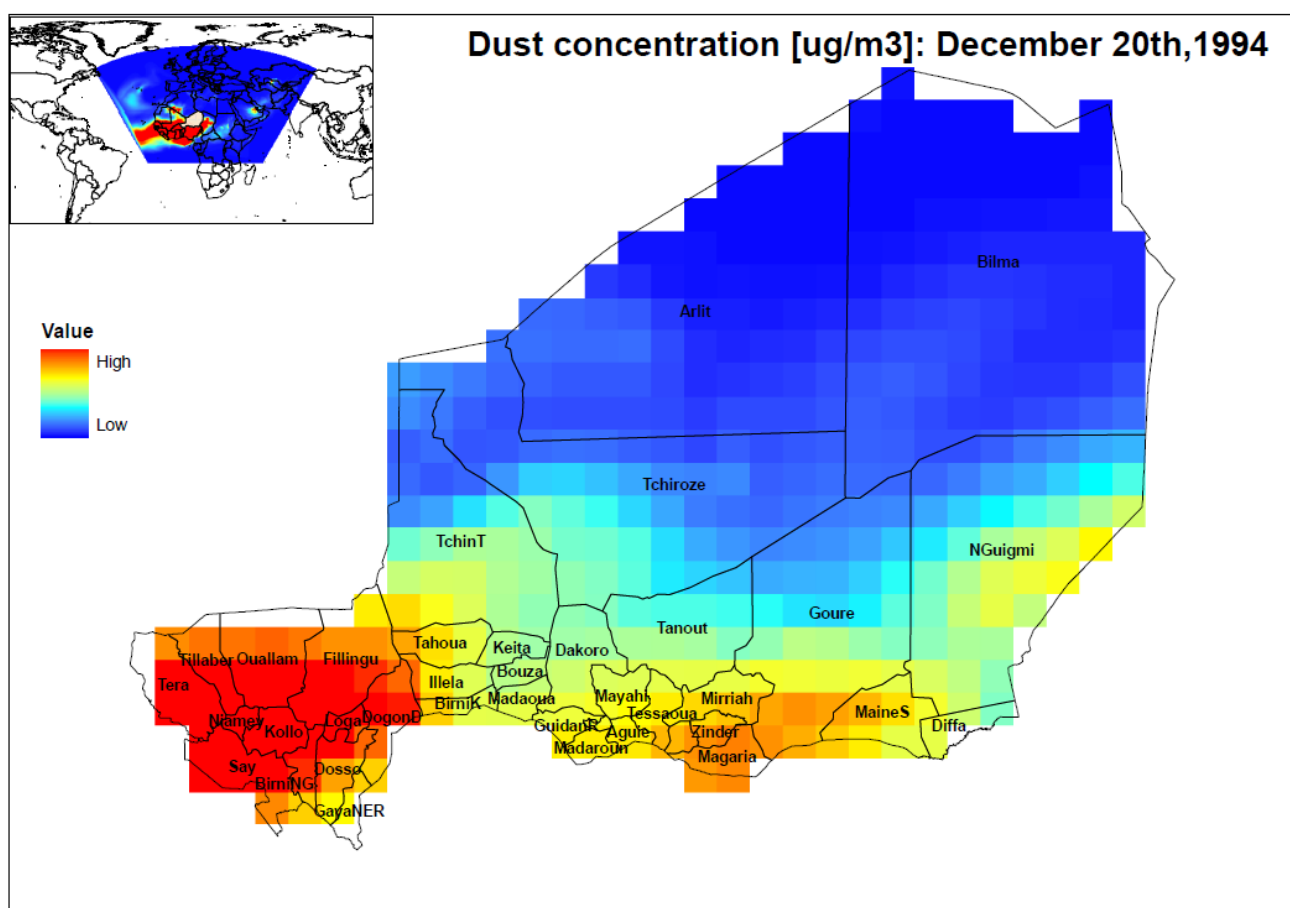


Figure 3.3.; NMMb/BSC-Dust Regional domain used (left upper corner) depicting the simulated surface dust concentration over Niger on December 20th, 1994 with maxima dust concentrations in the southern districts of Niger.

Data from the NMMB/BSC-Dust reanalysis (surface dust concentration, AOD, temperature, absolute humidity, relative humidity, meridional wind) have been weekly averaged for the test case geographical domain of southern Niger.

The AERONET (Aerosol Robotic Network; Holben et al., 1998; <http://aeronet.gsfc.nasa.gov>) station of Banizombou (13.54° N, 2.66° E, 250 m a.s.l.) (see Figure 3.2), within the test case geographical domain, have been compared against AOD obtained from NMMb/BSC-Dust model reanalysis.

The following in-situ meteorological stations (see Figure 3.2) within the test case geographical domain have been used for long-term validation of NMMb/BSC-Dust basic meteorological variables: Agadez (WMO 61024), Bilma (WMO 61017), Maine-Soroa (WMO 61096), Tahoua (WMO 61043) and Niamey-Aero (WMO 61052) This dataset has been downloaded from NNDC Climate data Online (<http://cdo.ncdc.noaa.gov>).

Horizontal visibility records from Agadez-South, Tillabery, Tahoua, Niamey, Birni N’Konni, Maradi, Zinder, Magaria, and Gaya meteorological stations (see Figure 3.2) in Niger have been used for NMMb/BSC-Dust surface dust concentration verification for the period 1994-1999. This data set has been obtained from IRI database (<http://iridl.ldeo.columbia.edu>).

ECMWF ERA-INTERIM and NCEP reanalysis have been used for comparing temperature and wind against NMMb/BSC-Dust model (over Niamey), and for analysed epidemic and non-epidemic episodes assessment.

Long-term series of AAI from Total Ozone Mapping Spectrometer (TOMS; December 1978-April 1993 and August 1996-December 2005) and Ozone Monitoring Instrument (OMI; October 2004-March 2010), and AOD from the MODIS/Aqua using Deep Blue algorithm (July 2002- March 2010) have been used to validate AOD values derived from NMMb/BSC-Dust reanalysis. In the pre-processing stage, TOMS, OMI, MODIS satellite images and the NMMb/BSC-Dust model of the same area were geometrically co-registered with the MODIS grid map and geodetically transformed into the World Geodetic System (WGS84).

#### 4. **Background: meteorological conditions**

Niger extends southward from the tropic of Cancer. The country can be roughly divided into three zones: the north, center, and the south. The northern zone, covering about two-thirds of the surface area, is located within the Sahara. In the southern part of the country the climate is of the type known as Sahelian, which is characterized by a single, short rainy season (from May to October). Figure 4.1 shows the annual course of precipitation (mm), wind speed ( $\text{ms}^{-1}$ ), vapour pressure (hPa) and minimum-temperature ( $^{\circ}\text{C}$ ), corresponding to the climatological period 1961-1990, for seven meteorological stations of Niger ranging from northern to southern latitudes. The rains last from one to four months, according to the latitude. The precipitation in Northern Niger (records in red) is very poor, and all meteorological stations in Niger show a dry season from October to April (Figure 4.1a). In late December, January and February the continental equivalent of the northeast trade winds, the Harmattan, blows southwestward from the Sahara toward the equator.



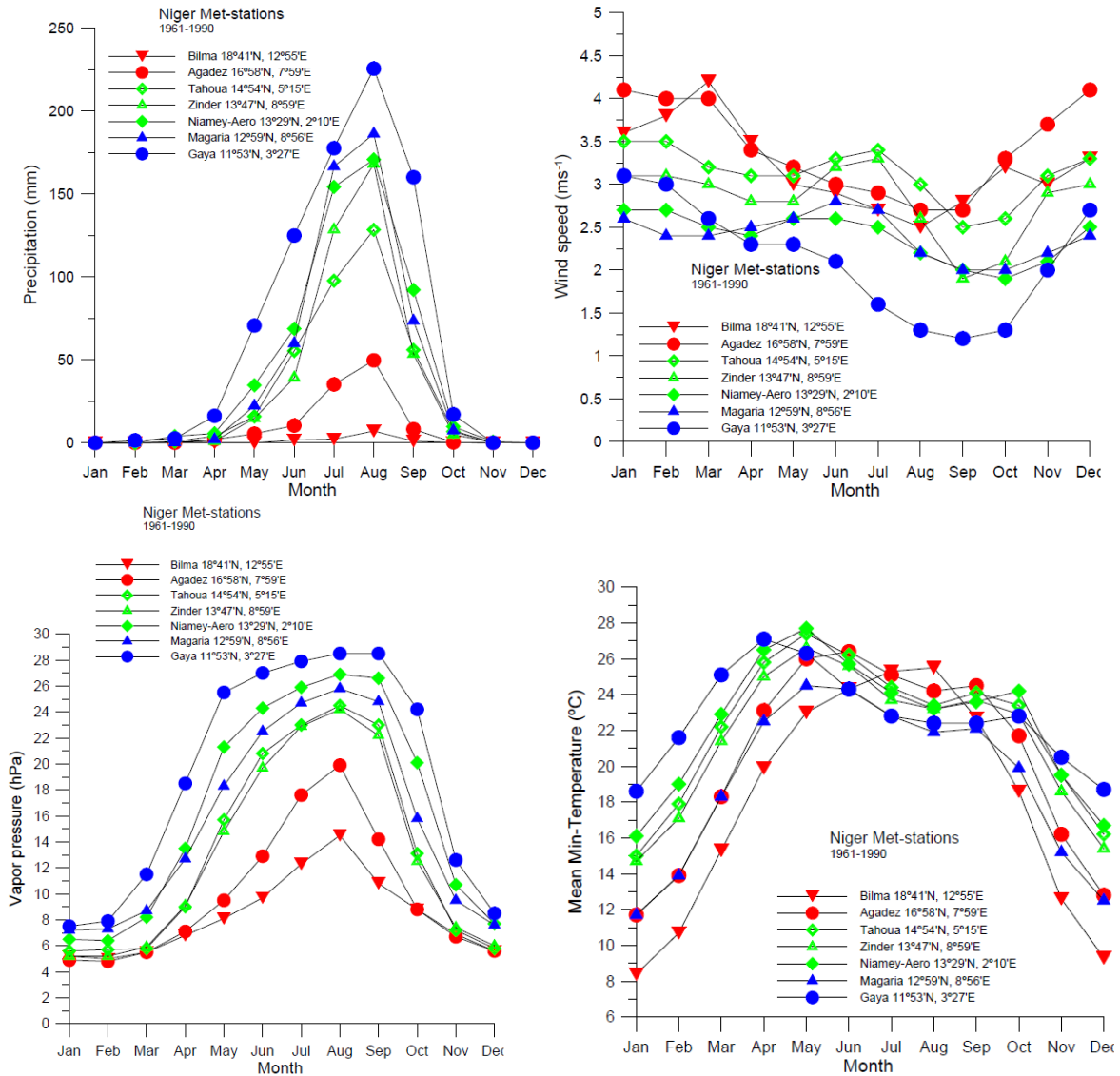


Figure 4.1; Monthly mean values of precipitation (mm) (a), wind speed (ms<sup>-1</sup>) (b), vapour pressure (hPa) (c), and mean minimum-temperature(°C) (d), corresponding to the climatological period 1961-1990, for seven meteorological stations of Niger ranging from 18°41'N to 11°53'N.

The Harmattan is a dust-laden and very dry wind hindering normal living conditions on the southern fringe of the desert. Stronger winds coincide with the dry season (from October to April), being the Harmattan more active in northern Niger (see red wind speed records in Figure 4.1b). Very dry air is present during the dry season (Figure 4.1c), being then recorded the lower minimum temperatures (Figure 4.1d). From April to May the southern trade winds blowing from the Atlantic reach the equator and are diverted toward the Sahara where they meet with the Harmattan resulting in violent convective storms and the beginning of the rainy season.

The seasonal cycle of the Harmattan front can be approximated as a northward progression of the system between February and August, followed by southward retreat from September to January (Haywood et al., 2008), as it is indicated in the scheme (Figure 4.2). In winter time (from December to March) our geographical domain in Niger is in the position marked by line "1". In this position a transport of Saharan dust to Niger within the surface layer takes place. High surface dust concentrations are not necessary recorded together with high AOD values under this scenario.

However, by the end of the Saharan dust period, after April-May, the “Harmattan Front” (Haywood et al., 2008) favours convective activity (scenario marked by line “2”) favouring the local dust emissions in southern Niger (Marticorena et al., 2010).

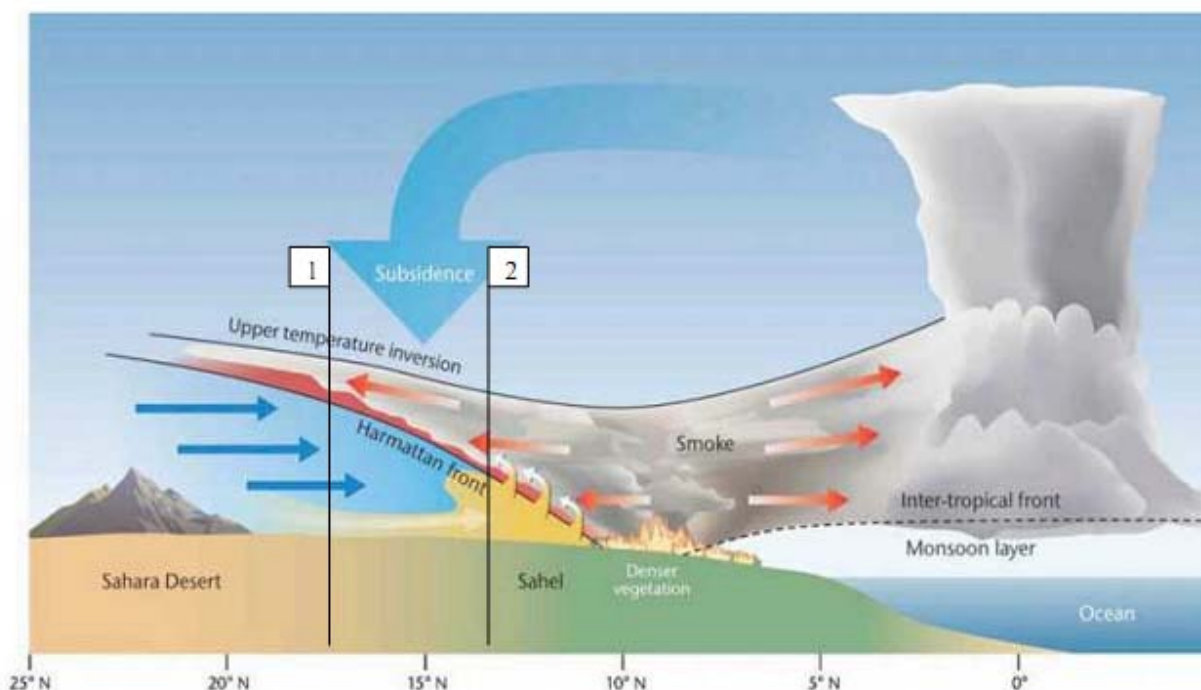


Figure 4.2; Schematic meridional cross section of atmospheric circulations over West Africa showing the northward transport of biomass burning aerosol in warm, ascending air (red arrows) and the westward/southward transport of mineral dust in a cooler airflow (blue arrows). The “Harmattan front” is shown by the solid line which marks the boundary between the two air masses with arrows representing mixing of the dust with the biomass burning smoke (Haywood et al., 2008).

## 5. NMMb/BSC-Dust model verification over Niger

The first activities of this study have consisted of carrying out a validation/verification of different variables obtained from the long-term NMMb/BSC-Dust reanalysis over Niger, as complete as possible. This has not been an easy task since the shortage of existing observations in this region.

### 5.1. Temperature validation

Here an example of mean temperature validation is presented (Figure 5.1). In this case NMMb/BSC-Dust, ERA-Interim and NCEP reanalysis over Niamey airport (13.483N, 2.166E) were compared against monthly temperature recorded at the Niamey airport station (only available in the period 1981-1991). The agreement is fairly good. The three reanalysis capture similarly the year-to-year seasonal variations. However the NMMb/BSC-Dust reanalysis tend to underestimate temperatures.

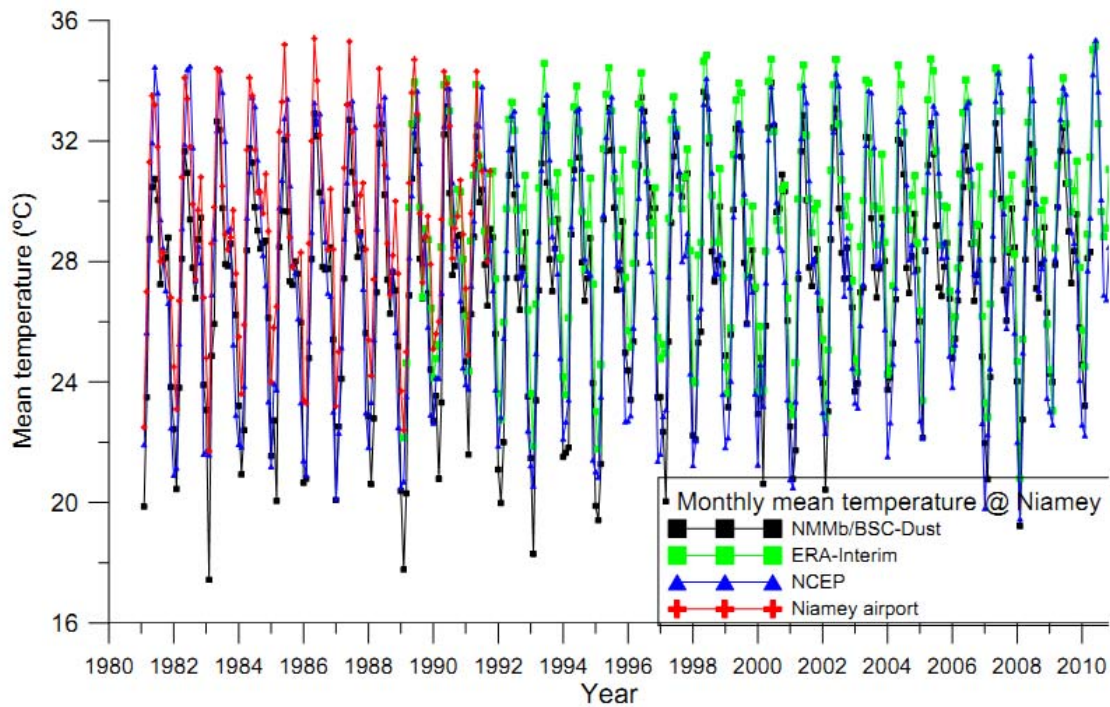


Figure 5.1.; Monthly mean temperature at Niamey airport (13.483N, 2.166E) in the period 1981-2011. In-situ observations (in red), NMMb/BSC-Dust reanalysis (in black), ERA-Interim reanalysis (in green) and NCEP reanalysis (in blue).

ERA-Interim shows better results when compared with in-situ records, although only two years are available for comparison. NMMb/BSC-Dust shows colder temperatures when compared with in-situ observations. The correlation is fairly good ( $r^2= 0.84$ ). NMMb/BSC-Dust tracks well the inter-annual variations. The correlation is lower between NMMb/BSC-Dust and NCEP ( $r^2= 0.79$ ). The correlation between NMMb/BSC-Dust and ERA-Interim is good ( $r^2= 0.91$ ). While the correlation is very good for hot months (in summer), a higher scatter is observed in winter months. NMMb/BSC-Dust clearly shows lower temperatures than in-situ and ERA-Interim reanalysis, especially in winter.

## 5.2. Meridional wind comparison

The seasonal climate cycle in West Africa, in general, and in southern Niger, in particular, is dominated by the switch between the two climatic regimes driven by trade winds: the dry Harmattan northeasterly winds from the Sahara, and moist southwesterlies from the Gulf of Guinea. So, meridional wind is an important variable since this variable marks very well the onset of the dry season.

We have performed a comparison of meridional wind (monthly means) from three reanalysis: NMMb/BSC-Dust, ERA-Interim and NCEP. Monthly mean meridional winds computed over Niamey airport (13.483N, 2.166E) with the three reanalysis are shown in Figure 5.3.

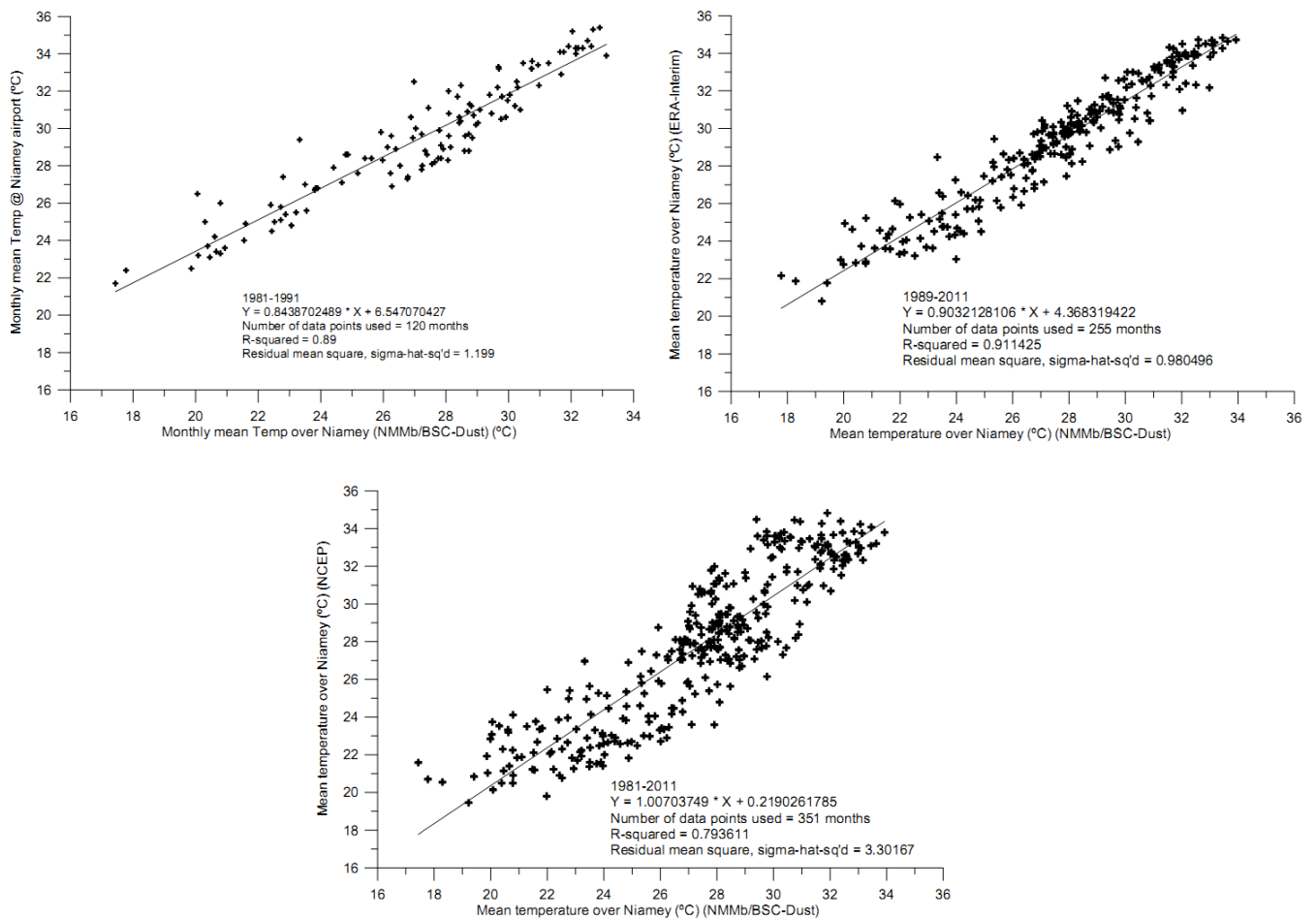


Figure 5.2.; Monthly mean temperature over Niamey airport (13.483N, 2.166E) from NMMb/BSC-Dust reanalysis vs in-situ monthly mean records for the period 1981-1991 (a) ERA-Interim reanalysis for the period 1989-2011 (b), and NCEP reanalysis for the period 1981-2011 (c).

The general agreement is fairly good. The seasonal and interannual variations are captured in the same way by the three reanalysis. NMMb/BSc-Dust shows a fairly good correlation with NCEP (for the period 1981-2011) ( $r^2=0.84$ ) and a higher correlation ( $r^2=0.91$ ) with ERA-Interim (for the period 1989-2011). It is worth to highlight that the correlation during Harmattan regime (negative meridional winds) is very good with both ERA-Interim and NCEP. Higher discrepancies are observed during Monsoon season (positive meridional winds) and during the transition period from Harmattan to Monsoon. NMMb/BSC-Dust tends to underestimate lightly the wind speed during the Harmattan regime compared to ERA-Interim.

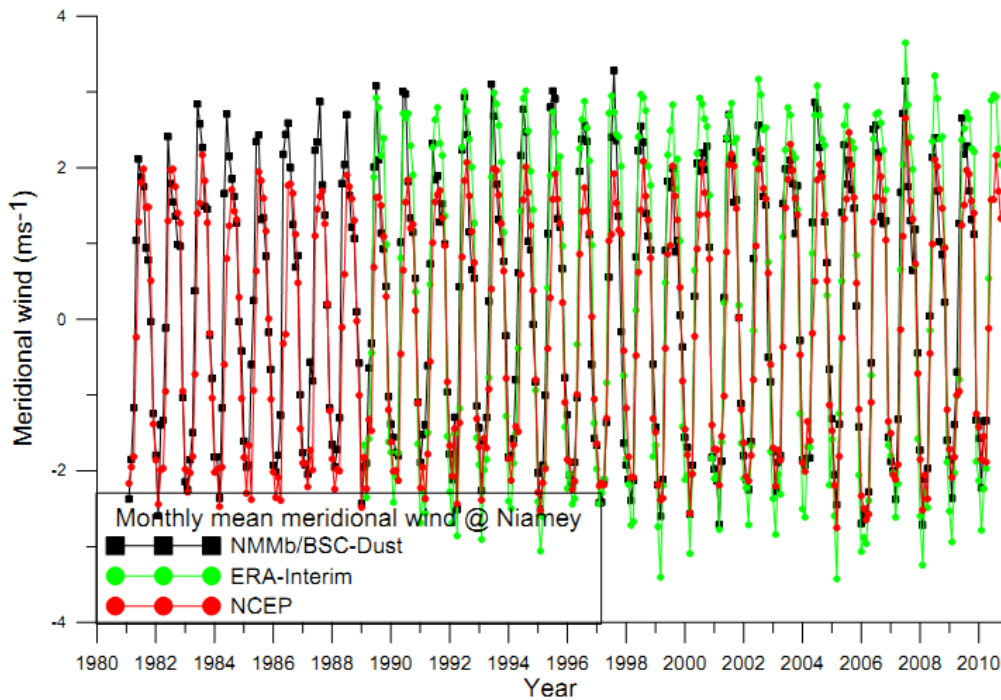


Figure 5.3.; Monthly mean meridional wind over Niamey airport (13.483N, 2.166E) in the period 1981-2011. NMMb/BSC-Dust reanalysis (in black), ERA-Interim reanalysis (in green) and NCEP reanalysis (in red).

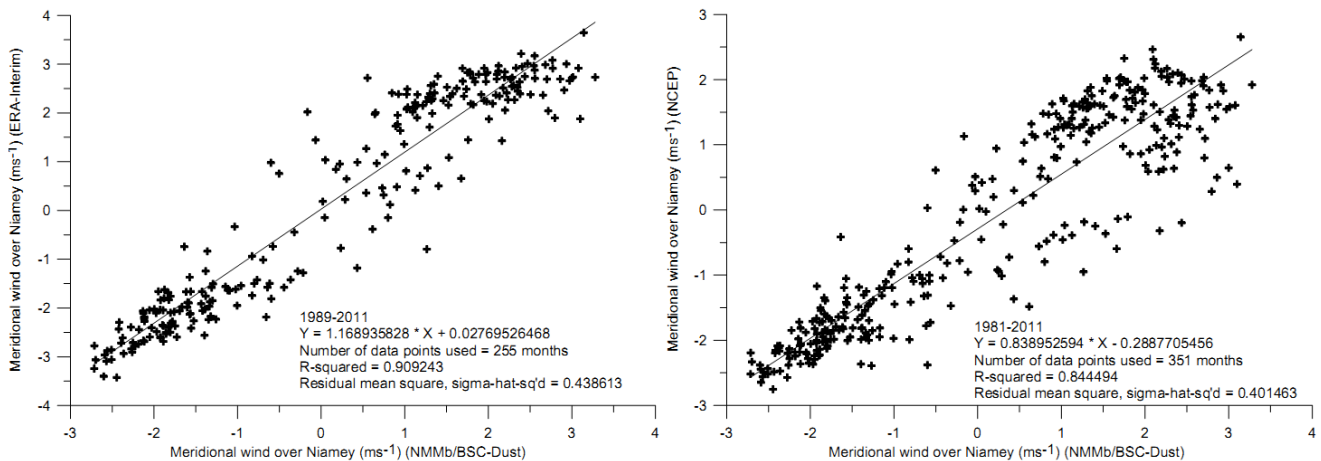


Figure 5.4.; Monthly mean meridional wind over Niamey airport (13.483N, 2.166E) from NMMb/BSC-Dust reanalysis vs ERA-Interim reanalysis for the period 1989-2011 (a), and NCEP reanalysis for the period 1981-2011.

### 5.3. Aerosol optical depth (AOD) validation against Banizoumbou-AERONET station

Daily AOD at the AERONET Banizoumbou station has been compared with AOD from NMMb/BSC-Dust reanalysis. We have performed a full verification using the whole period of available observations (1995-2010) in AERONET (<http://aeronet.gsfc.nasa.gov>). We present here the comparison of two years (2007 and 2008) as an example (Figure 5.5).

The day-to-day variations are well captured by NMMb/BSC-Dust, although differences in peak magnitude can be significant for some days. In winter (dry season) when the Harmattan regimen is well established we find some overestimation of AOD from NMMb/BSC-Dust reanalysis. This might be due to the fact that Saharan dust travels in relatively thin layers near ground in this season



resulting in actual relatively low AOD. We have observed a very good correlation between AOD and surface dust concentration from NMMb/BSC-Dust reanalysis ( $r^2=0.91$ ). However, in winter, high surface dust concentrations do not correspond necessarily with high content of aerosols in the total column (AOD) as it has been experimentally observed (Marticorena et al., 2010).

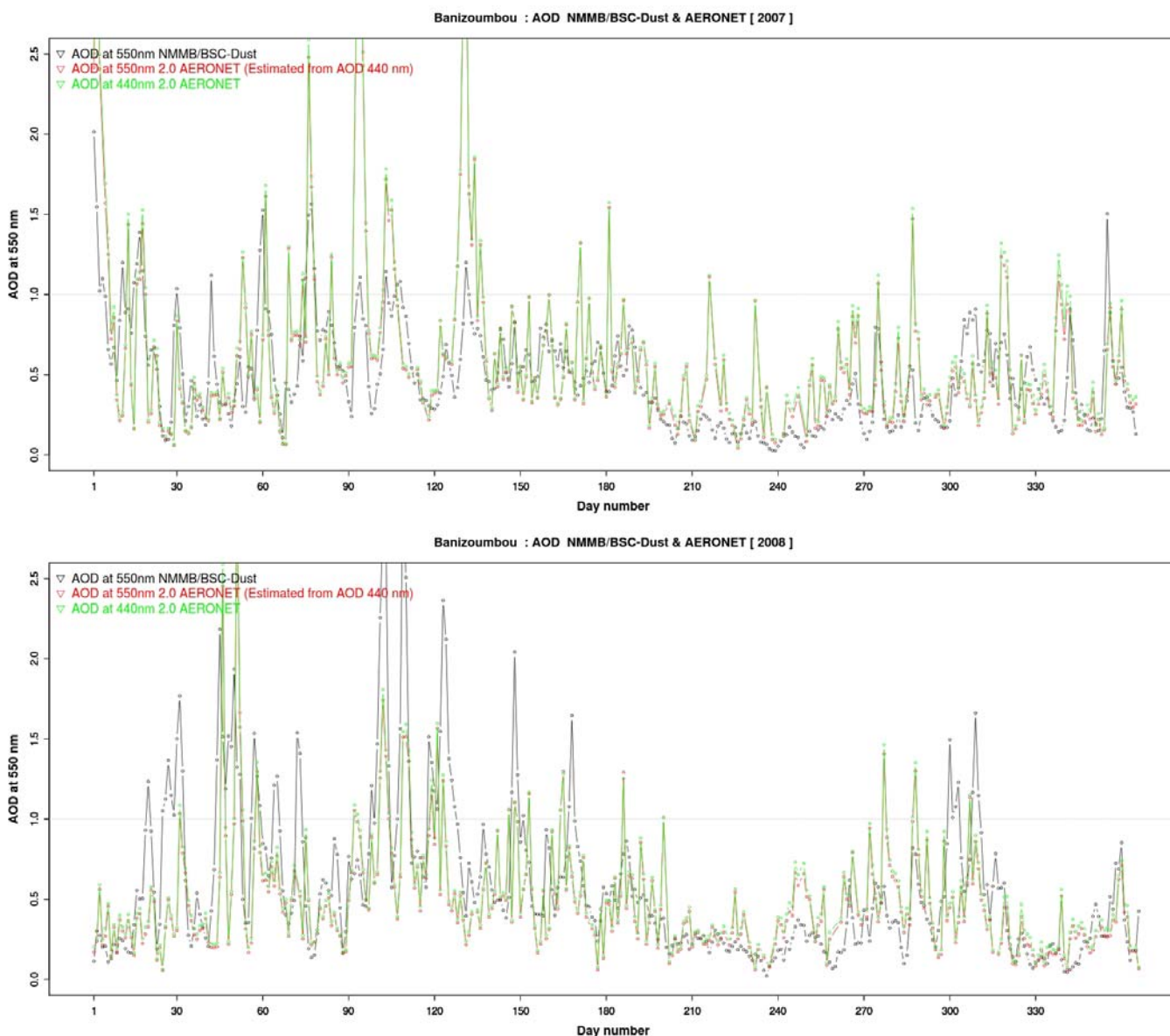


Figure 5.5; Daily Aerosol Optical Depth (AOD; Version 2.0) at Banizoumbou-AERONET station and AOD from NMMb/BSC-Dust reanalysis for the same station (in black) for 2007 and 2008.

On the other hand in the wet season (summer) the NMMB/BSC-Dust reanalysis seems to underestimate the AOD. In this case the explanation is simple. As it has been stated in section 4, in summer the Harmattan front is in its northernmost position increasing convective activity in southern Niger and so favouring the local dust emissions. These mesoscale storms are not captured by the NMMb/BSC-Dust reanalysis. Anyway, the results are not bad and rely strongly on comparing year. Notice that in the case of AOD AERONET data are not selected (biomass burning aerosols contribution has not been removed) and they might be affected by biomass burning. Furthermore, in the wet season an incorrect simulation of rainfall in NMMb / BSC-Dust can also induce errors.

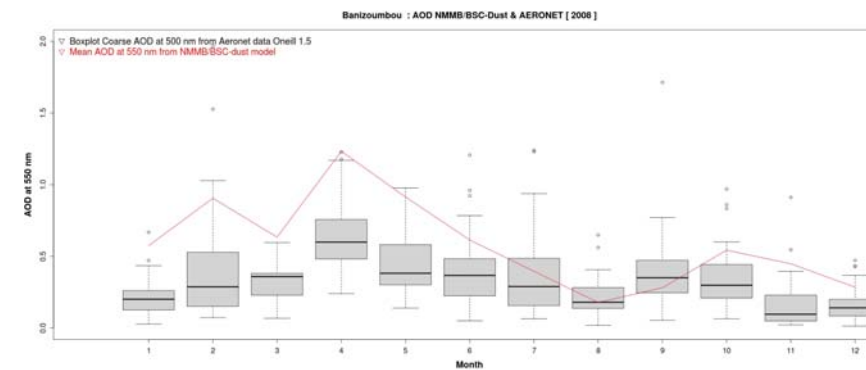
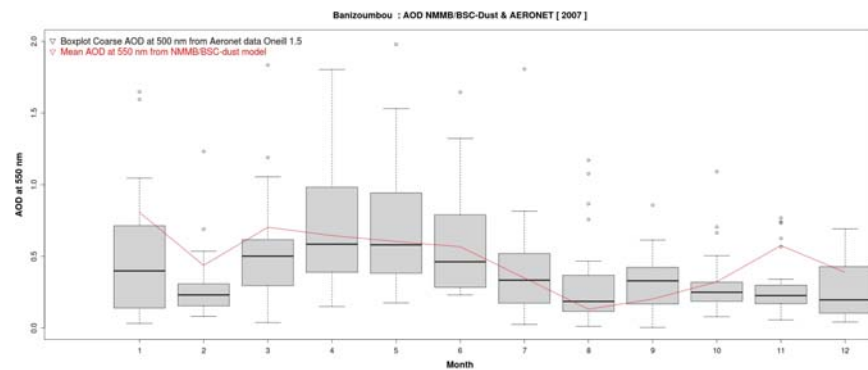
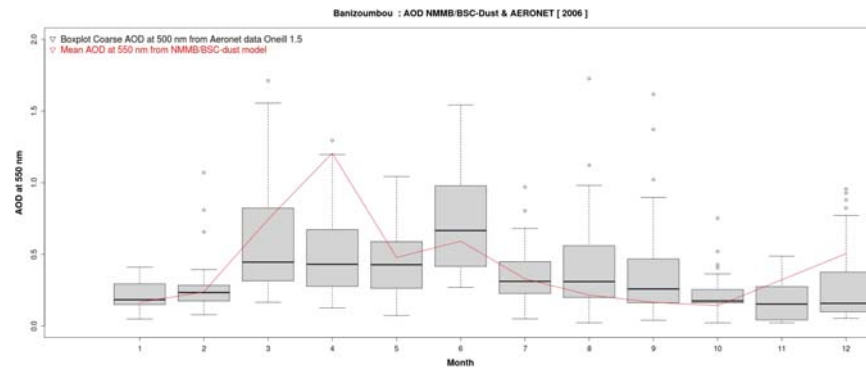
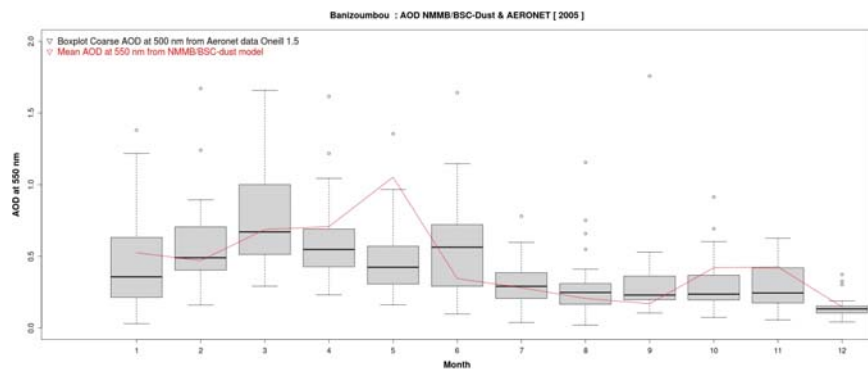
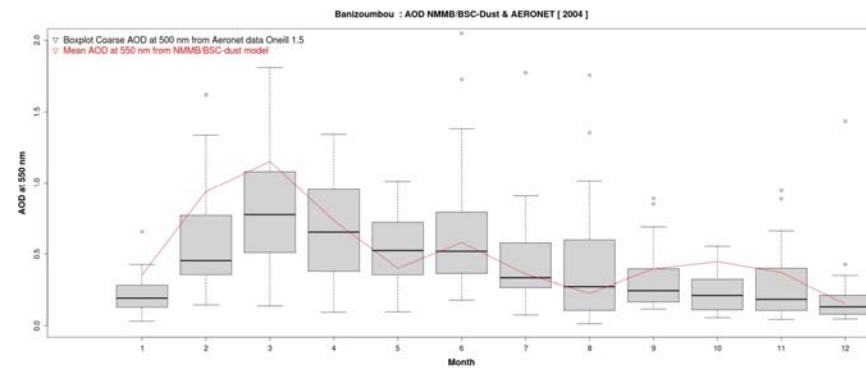
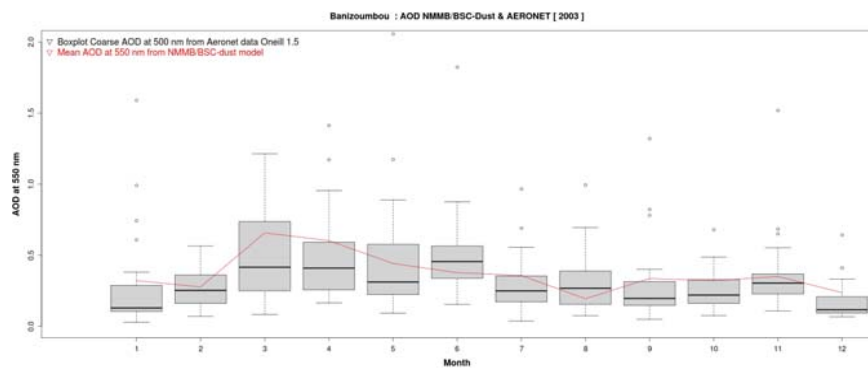


Figure 5.6; Monthly Aerosol Optical Depth box plot for coarse fraction (AOD Version 1.5 O'Neill algorithm) at Banizoumbou-AERONET station and monthly AOD from NMMb/BSC-Dust reanalysis for the same station (red line) for 2003, 2004, 2005, 2006, 2007 and 2008, respectively.

Monthly AOD box plots for coarse mode particle size (coarse fraction) (AOD Version 1.5) using the Spectral Deconvolution Algorithm (SDA; O'Neill et al., 2003) at Banizoumbou-AERONET station and monthly AOD from NMMb/BSC-Dust reanalysis for the same station (red line) for 2003, 2004, 2005, 2006, 2007 and 2008, respectively are shown in Figure 5.6. Monthly data have been averaged using coincident NMMb/BSC-Dust and AERONET daily mean data. Box-plots of AOD-Coarse indicate the natural variability for each month and year. It can be seen a high year-to year variability, especially in dry season. The interannual variations and the seasonal course every year in AOD are fairly well captured by NMMb/BSC-Dust reanalysis.

#### 5.4. AOD from NMMb/BSC-Dust verification against AAI from TOMS-OMI and AOD from MODIS-Aqua/Deep Blue

Long-term series of AAI from TOMS and OMI, as well AOD from MODIS-Aqua/Deep Blue have been used to verify monthly AOD values derived from NMMb/BSC-Dust reanalysis in this region. The monthly mean data used in each series have been calculated from daily mean data matching between NMMb / BSC-Dust and the corresponding satellite sensor.

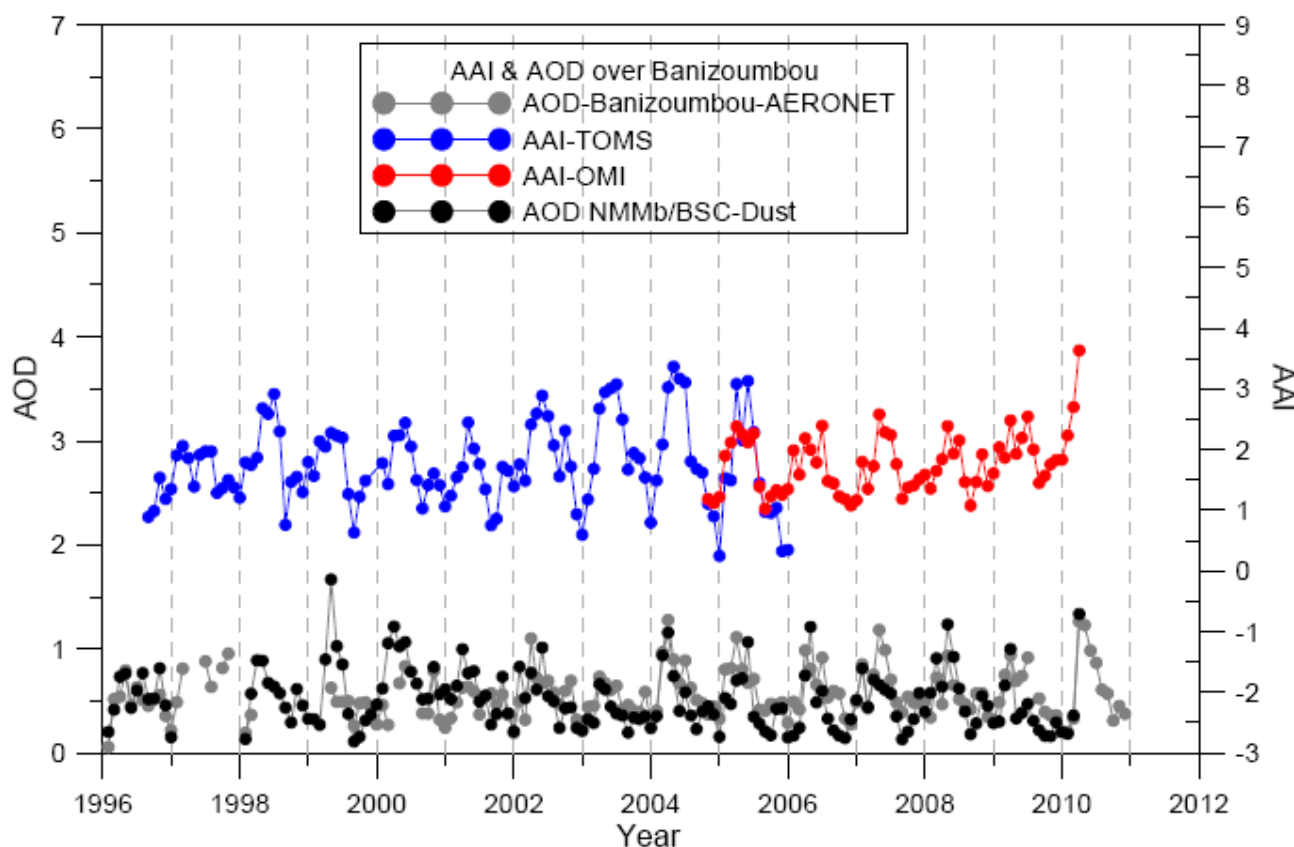


Figure 5.7; Monthly averages of Aerosol Optical Depth (AOD; Version 2.0) at Banizoumbou-AERONET station (grey), AOD from NMMb/BSC-Dust reanalysis (black), AAI from TOMS (blue) and AAI from OMI over Banizoumbou station.

The series of AAI shows a major discontinuity between TOMS and OMI. Furthermore the TOMS series shows a clear an instrumental drift at the end of the record. AAI from TOMS shows larger annual amplitude than AAI from OMI. According to the OMI Quality Assurance Team warning, the present version of OMTO3 data are not suitable for trend studies (<http://toms.gsfc.nasa.gov/omi/OMTO3Readme.html>). Furthermore, it is known that TOMS and OMI underestimates dust under heights less than 1.5 km (Torres et al., 2002; Ginoux and Torres,



2003). Since large scale subsidence is likely to ensure that dust transport occurs in the lowest layers during winter in this region whereas deep convection during summer may lift dust to high altitudes (Mahowald and Dufresne, 2004), we understand the phase shift in the annual cycle of the TOMS AAI data towards the summer months (Washington and Martin, 2005), when the boundary layer deepens considerably, compared with the AERONET AOD. All these circumstances, together with the non-optimal spatial resolution of satellite data, introduce difficulties and uncertainties when we use long-term AAI series to cross with others such as the number of cases of meningitis. Considering this aspect the AOD NMMb/BSC-Dust tracks better than TOMS the seasonal variation and behaviour of dust in our region of study.

The correlations between AOD-Banizoumbou/AERONET and AAI-TOMS and AAI-OMI ( $r^2=0.39$  and  $r^2=0.49$ , respectively) are similar to the correlation found between AOD-Banizoumbou/AERONET and AOD-NMMb/BSC-Dust ( $r^2=0.38$ ) (see Figure 5.8.).

The correlations between AOD-NMMb/BSC-Dust and AAI-TOMS and AAI-OMI are  $r^2=0.27$  and  $r^2=0.35$ , respectively. So the agreement of AOD derived from NMMb/BSC-Dust reanalysis with both satellite and ground based AOD is similar to that found between AERONET and satellite observations.

Concerning the spatial agreement, we have computed the monthly anomalies of each “pixel” for each month and year within  $0^\circ\text{N}-30^\circ\text{N}/25^\circ\text{W}-25^\circ\text{E}$ . As an example in Figures 5.10 and 5.11 the anomalies of AAI-TOMS and AOD-NMMb/BSC-Dust for January 2000 and January 2004 are shown. The pixel anomalies have been calculated for coincident days. The spatial patterns observed in NMMb/BSC-Dust anomalies are rather similar to those of AAI-TOMS. In January 2000 three bands of high (in red) and moderate (in yellow) anomalies are observed in a NE-SW axis in both patterns. One of these high-dust bands covers some of the Sahel countries and specifically Niger. On the contrary, in January 2004 high anomalies (high dust) are confined in the tropical-equatorial band and the eastern part of the geographical domain, showing negative or relatively lower positive anomalies in the Sahel countries.

The longest record available of aerosol content from satellite-based sensors is AAI. Nevertheless it would be desirable to compare directly with AOD from satellites. In deserts and dry regions, as Niger, there is a serious difficulty in separating the signals of aerosols from those of highly reflective surfaces. In order to avoid this problem MODIS Deep Blue aerosol retrieval algorithm uses the blue channels, where the surface contribution is relatively low, to retrieve aerosol properties over such regions (Hsu et al., 2004; 2006). We have compared the AOD Deep Blue anomalies with NMMb/BSC-Dust AOD anomalies from 2003 to 2010. An example is shown in Figure 5.12 where AOD anomalies from Deep Blue-MODIS and NMMb/BSC-Dust for January 2004 are depicted. Positive anomalies are observed over Niger while positive anomalies are confined within the tropics and the eastern regions. Further detailed analysis of AOD-Modis and AOD-MISR will be performed in a near future in order to perform spatial validations of NMMb/BSC-Dust reanalysis.

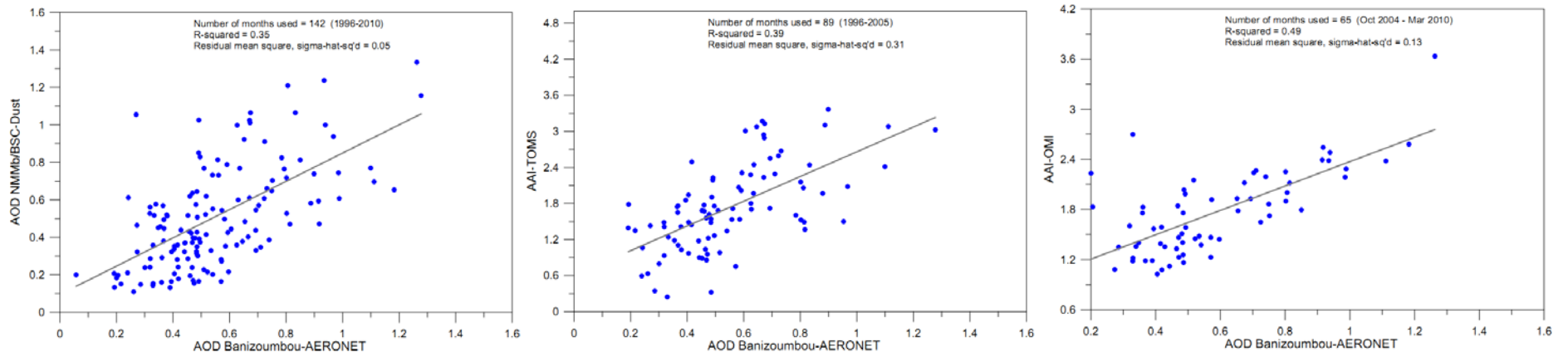


Figure 5.8; Monthly averages of Aerosol Optical Depth (AOD; Version 2.0) at Banizoumbou-AERONET station versus AOD NMMb/BSC-Dust, AAI/TOMS and AAI/OMI over Banizoumbou station (from left to right).

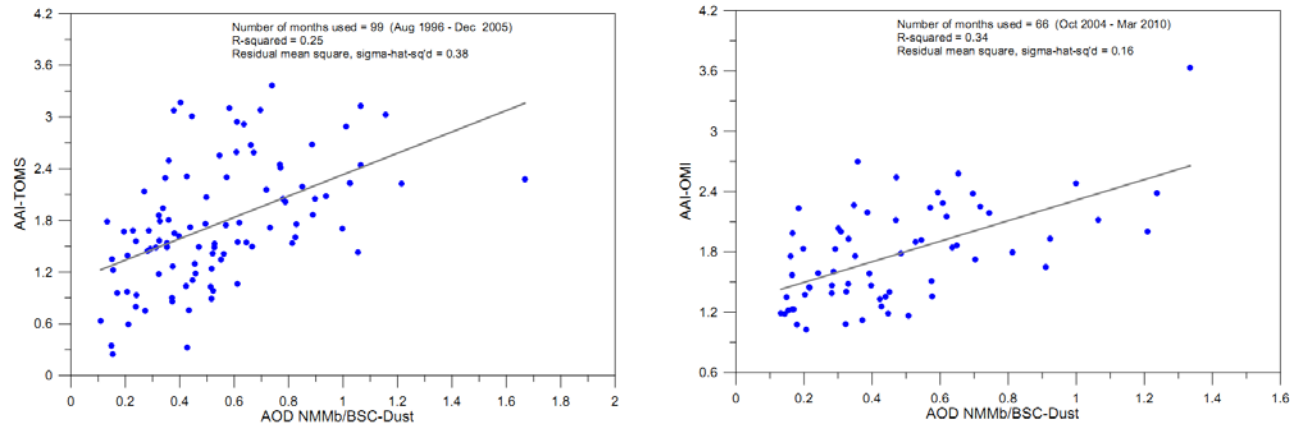
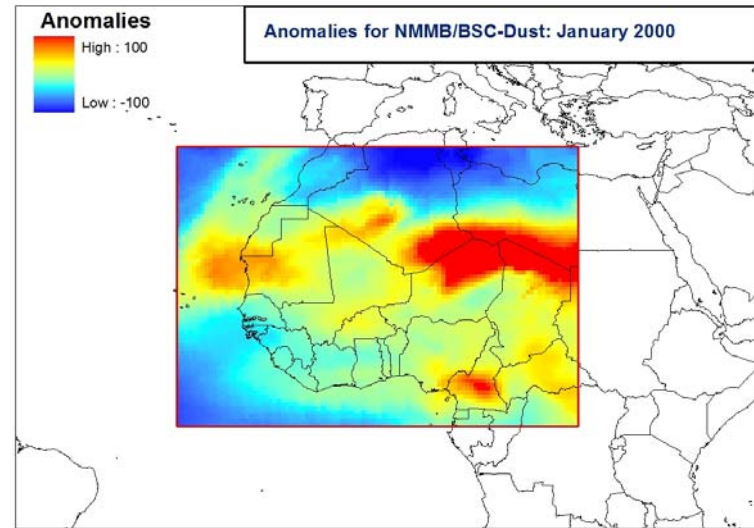
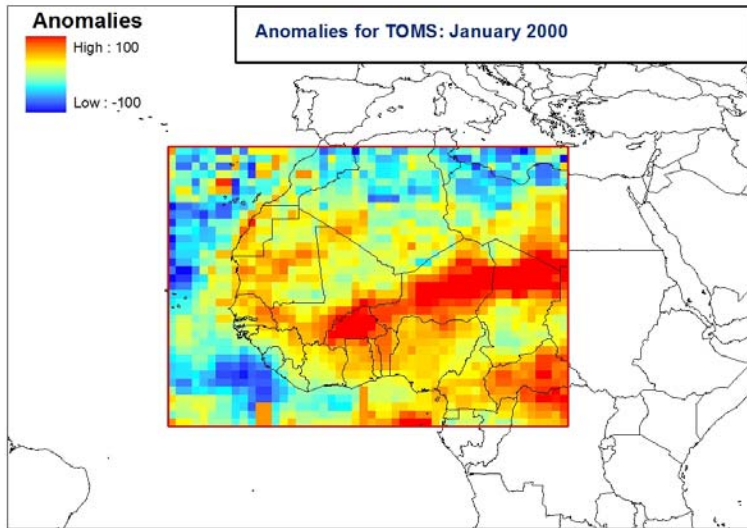
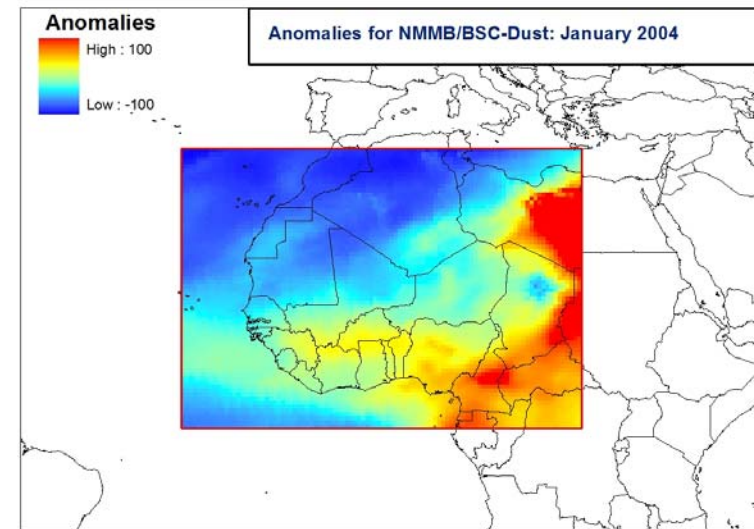
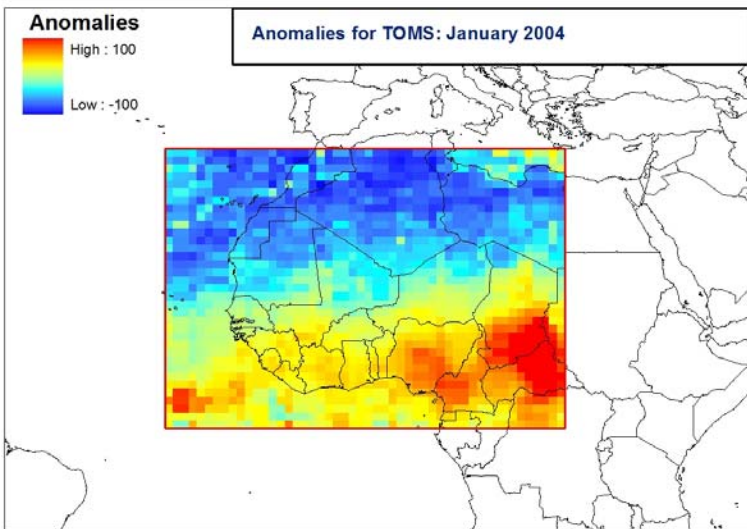


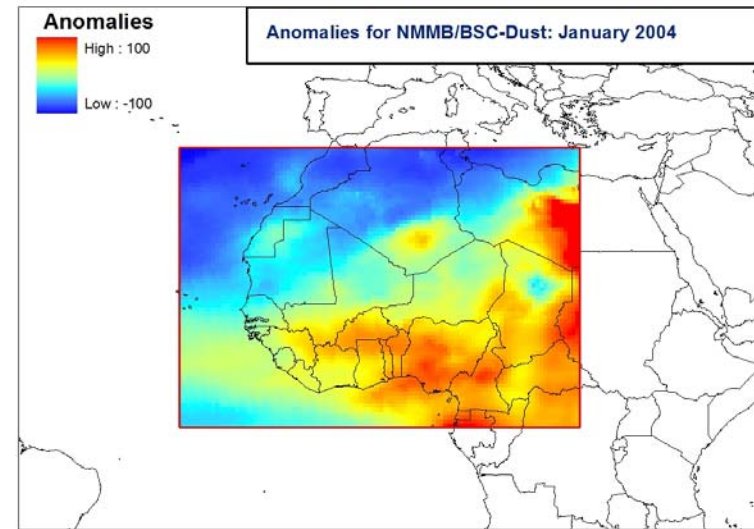
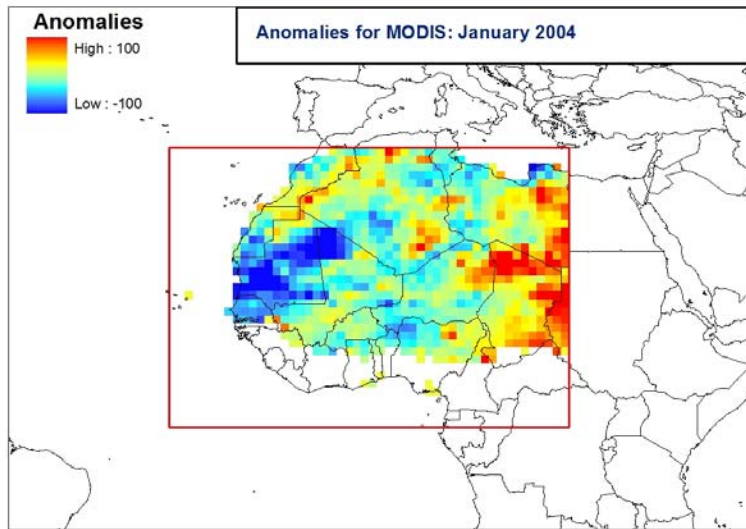
Figure 5.9; Monthly averages of AOD-NMMb/BSC-Dust versus AAI/TOMS and AAI/OMI over Banizoumbou station (from left to right).



5.10; Monthly anomalies for January 2000 of AAI/TOMS (left) and AOD-NMMb/BSC-Dust (right).



5.11; Monthly anomalies for January 2004 of AAI/TOMS (left) and AOD-NMMb/BSC-Dust (right).



5.12; Monthly anomalies for January 2004 of AOD/Deep-Blue Modis (left) and AOD-NMMb/BSC-Dust (right).

## 5.5. Surface dust concentration

The most important verification for NMMb/BSC-Dust is related to the surface dust concentration. However in the Sahel region there is a lack of meteorological observations, in general, and almost nothing of in-situ surface dust concentration.

As a first step we have compared the surface dust concentration from NMMb/BSC-Dust reanalysis with estimated PM10 from horizontal visibility obtained at several meteorological stations of Niger.

The World Meteorological Organization's definition of daytime visibility is as follows: "Meteorological visibility by day is defined as the greatest distance at which a black object of suitable dimensions, situated near the ground, can be seen and recognized when observed against a background fog or sky" (WMO, 1971).

The relationship between horizontal visibility and PM10 is based on the D'Almeida's (1986) work. He carried out a detailed study on the relationship between horizontal visibility and PM10 levels of mineral dust mass concentration using 11 stations in the Sahara and the Sahelian belt. D'Almeida found a very good correlation ( $r^2 = 0.95$ ) between horizontal visibility (within the range 200m-40km) and PM10 in the following relation:

$$PM10 = 914.06 VV^{-0.73} + 19.03$$

where PM10 is in  $\mu\text{g m}^{-3}$  and VV is the horizontal visibility in km.

We have used the D'Almeida's equation to convert the visibility range into "simulated" PM10 ( $\mu\text{g m}^{-3}$ ) concentrations of the following stations in Niger for the period January 1994-December 1999: , Agadez-South, Tillabery, Tahoua, Niamey-Civ, Birni-N'konni, Maradi, Zinder, Magalia and Gaya. Data has been obtained from IRI database.

In Figure 5.13 we can see some examples of comparisons between PM10 ( $\mu\text{g m}^{-3}$ ) daily means estimated from horizontal visibility (in black) and surface dust concentration from NMMb/BSC-Dust reanalysis (in red) calculated over Birni N'Konni station (WMO 610750; 13.9°N, 5.3°E), Niamey station (WMO 610520; 13.5°N, 2.2°E) and Gaya station (WMO 610990; 11.9°N, 3.5°E) for 1994, 1995 and 1998, respectively, using the average of the 4 nearest pixels (NMMb/BSC-Dust reanalysis) to the coordinates of each station. For example, we can detect from in-situ observations a dusty atmosphere from January to April 1994 and a high dust event in December this year in the three stations. In January they take place two followed episodes of high dust content in January and February, respectively. Between March and April it is identified a third one. Late year, again in the dry season, it is observed an important dust event in November and another one of smaller intensity in December. In 1998, the very beginning of the year, there is a pronounced dust peak, and after an episode of longer duration between mid-February, and well into April. In winter we can see very well two episodes, one in November and a second one peaking in mid-December.

According to Lerner et al. (2004), there are several shortcomings in using visibility observations that must be considered. Estimation of the horizontal visibility range is inherently subjective as visibility can be defined as a minimum detectable contrast by an observer's eyes. On the other hand reported visibilities suffer from errors due to coarse reporting bins, difficulties in judgment beyond 10 km (when the horizon is unobscured). To this respect, some stations do not report reduction in

visibility if it is higher than 10 km. This could be one reason (besides the inherent uncertainties in the D'Almeida's experimental formula) explaining that the PM<sub>10</sub> estimated from the visibility is never less than 150  $\mu\text{g m}^{-3}$ . On the other hand, reduced visibility range can be also due to biomass burning aerosols and fog, not only to Saharan dust. In the dry season may occur occasionally monsoon incursions northward transporting biomass burning aerosol from southern sources down to the ground level (Marticorena et al., 2010). We have also to consider that the Almeida's formula is valid, with significant uncertainties, for the horizontal 200m-40km range. Some severe dust storms in the Sahel can reduce visibility to only some tenths of meters. Taking into account all these constraints the results of the comparison between PM<sub>10</sub> estimated from horizontal visibility and surface dust concentration from NMMb/BSC-Dust reanalysis are very satisfactory. Our results demonstrate that NMMb/BSC-Dust catches the severe dust events every year, as well as the year-to-year variations, and the surface dust concentrations from NMMb/BSC-Dust reanalysis are of the same magnitude of those estimated from visual observations.

Any way we have tried to compare surface dust concentration with some in-situ actual PM<sub>10</sub> data to confirm the good behaviour of the reanalysis. So, we have visually compared the daily PM<sub>10</sub> data series at Banizoumbou (60 km East of Niamey) from January 2006 to December 2008 (published by Marticorena et al., (2010)) with daily surface dust concentrations from the NMMb/BSC-Dust reanalysis over Banizoumbou (average of the four nearest 0.5° pixels to the station). The sampling method used at Banizoumbou (discarding south wind sector) assures that PM<sub>10</sub> concentrations correspond mostly to mineral dust and not to biomass burning (Marticorena et al., 2010), so data can be directly compared with dust reanalysis. As it can be seen in Figure 5.14, the agreement is really good. Unfortunately we could not perform a quantitative comparison between observations and reanalysis because data are not accessible. By visual inspection we can see that the seasonal pattern is well captured by the reanalysis as well as the year-to-year variations. For example, notice the longer dust maximum plateau in winters 2007 and 2008 compared to winter 2006 (including the secondary minima observed in winters), the minimum around August 2007, or the singular behaviour at the end of 2008. All these features are well simulated with the NMMb/BSC-Dust reanalysis. The reanalysis underestimates surface dust concentration during the rainy season (from June to September, see Figure 5.14). Notice that in-situ PM<sub>10</sub> daily medians are well fitted by daily means of NMMb/BSC-Dust in summer. Some sporadic high dust events make the difference between observed and simulated data. Why? The reason for this difference during the rainy season is that during this period, the northeasterly advancement of the monsoon creates unstable atmospheric conditions and the formation of thunder cells and squall lines may lead to the development of strong downdrafts generating spectacular dust walls (Gillies et al., 1996; Knippertz et al., 2009). The dust raised by a haboob may persist several days after the storm winds have abated (Jaenicke, 1985). The Arabic word "haboob," meaning "strong wind," describes a weather phenomenon characterized by immense walls of blowing sand and dust. The NMMb/BSC-Dust reanalysis cannot capture these mesoscale structures because this model uses a convective parameterization that does not simulate the downdrafts.

In any case, we focus in the dry season when we try to find a relationship between dust and meningitis. During this period (from November to April), **the verification of daily surface dust concentration from NMMb/BSC-Dust reanalysis shows very satisfactory agreement with direct or indirect in-situ observations.** Therefore we conclude that we can confidently use NMMb/BSC-Dust reanalysis to relate long-term number of meningitis cases to dust in our geographical domain (southern Niger).



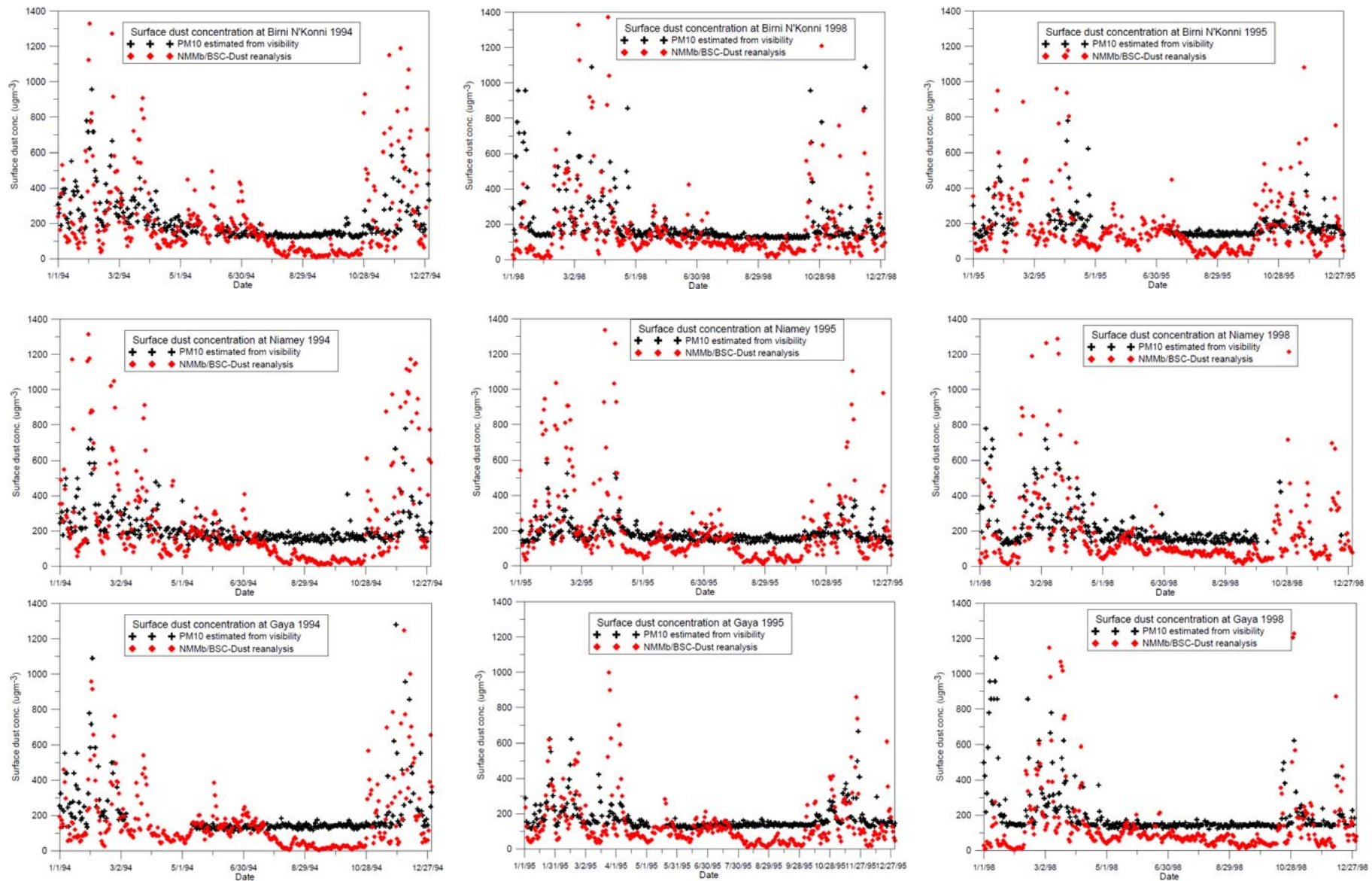


Figure 5.13.; PM10 ( $\mu\text{g m}^{-3}$ ) daily means estimated from horizontal visibility (in black) and surface dust concentration from NMMb/BSC-Dust reanalysis (in red) for Birni N'Konni station (WMO 610750; 13.9°N, 5.3°E) (upper panel), Niamey station (WMO 610520; 13.5°N, 2.2°E) and Gaya station (WMO 610990; 11.9°N, 3.5°E) for 1994, 1995 and 1998 (from left to right), respectively.

We have tried to remove biomass burning aerosol contribution in visibility records, using the relative humidity as a filter. PM10 values estimated from horizontal visibility data and NMMb/BSC-Dust surface dust concentration for Niamey station for January-May 1995 (dry season) are shown in Figure 5.14. We have compared only days in which relative humidity is lower than 40%. A better agreement is found, but it is not entirely satisfactory. The task of separating the contribution of biomass burning of mineral dust is not simple in this region in which the mixture of both aerosols is produced in a very dry atmosphere. The relative humidity in our study region is usually found between 20% and 40% in the dry season (Harmattan regime). If we used a relative humidity threshold lower than 40% to filter data, much of the data series would be eliminated. This subject requires further analysis.

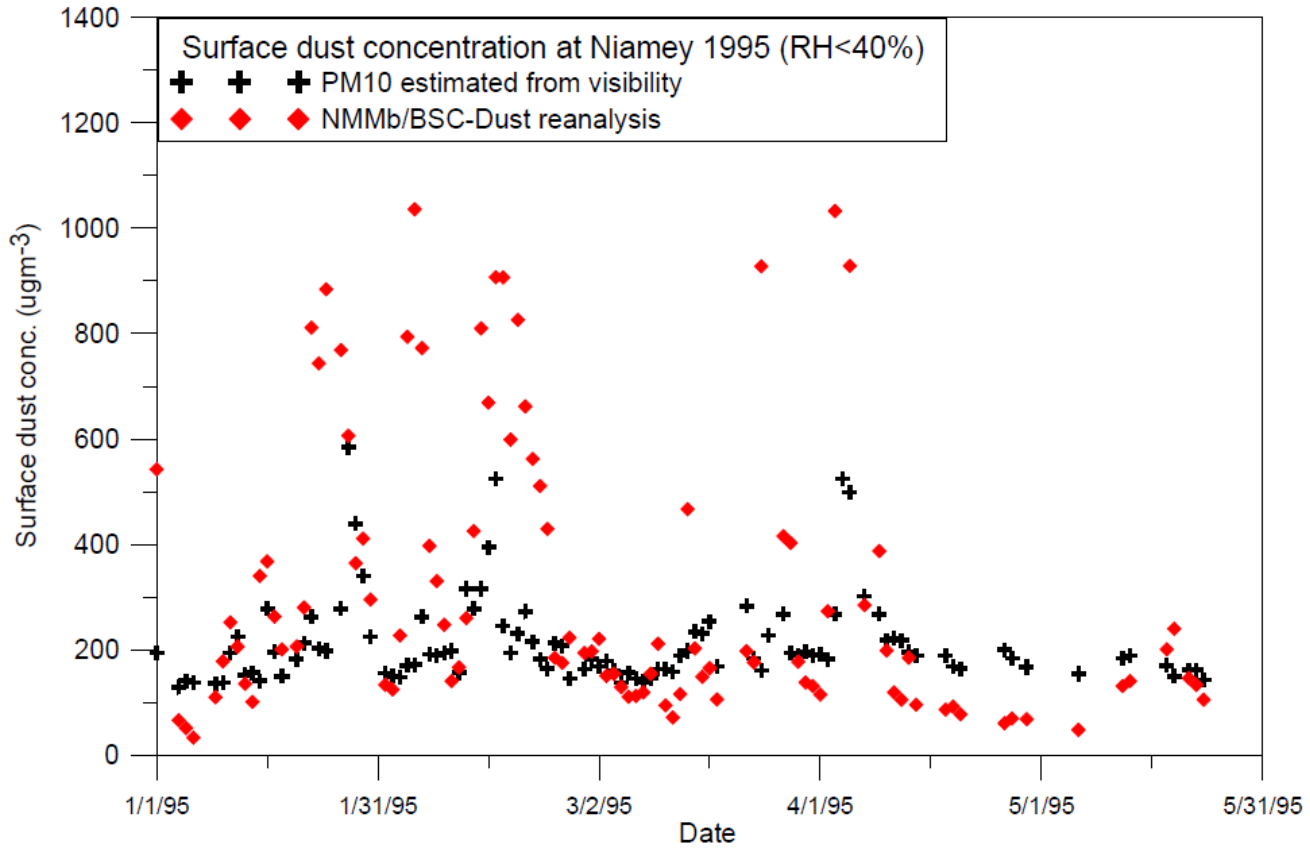


Figure 5.14.; PM10 (ugm<sup>-3</sup>) daily means estimated from horizontal visibility (in black) and surface dust concentration from NMMb/BSC-Dust reanalysis (in red) for Niamey station (WMO 610520; 13.5°N, 2.2°E) for January-May 1995. Only days with daily relative humidity less than 40% are depicted.



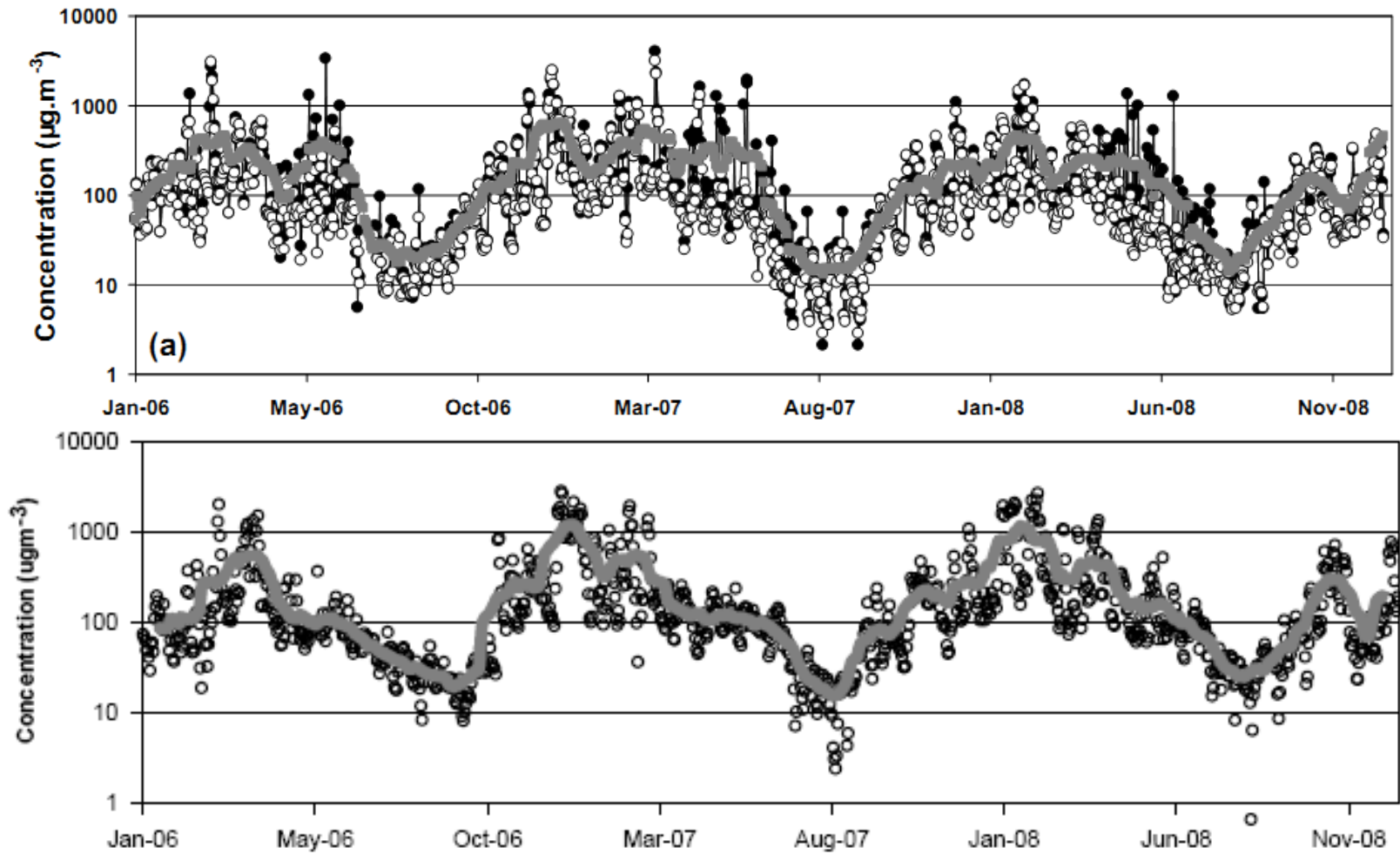


Figure 5.15.; PM10 Daily means (black circles) and medians (open circles) at Banizoumbou, from AMMA project (Marticorena et al., 2010) in upper panel, and surface dust concentration over Banizoumbou from NMMb/BSC-Dust reanalysis (daily averages of the 4 nearest  $0.5^\circ$  pixels to the station) in lower panel. The grey line is the 30-day running average in both graphics.

## 6. Results and discussion

### 6.1. Meningitis records

MM outbreaks show a high temporal and spatial variability. As it can be seen in Figure 6.1., where meningitis records in Niger, Mali and Burkina Faso are depicted, there is a great year-to-year variability in the number of meningitis cases, and the disease affect heterogeneously the three countries in the same years (Djingarey et al., 2008).

In our test case geographical domain the record of weekly number of meningitis cases from 1986 to 2008 is shown in Figure 6.2. According to this record we have considered [1987-1991], [1998-1999], 2001 and [2004-2008] as years with low incidence of meningitis ("**Non-epidemic years**" (NEY)), and [1993-1996] and 2000 as years with high incidence of meningitis ("**Epidemic years**" (EY)). The previous definition is subjective and arbitrary. However it allows us to perform a first exploratory analysis.

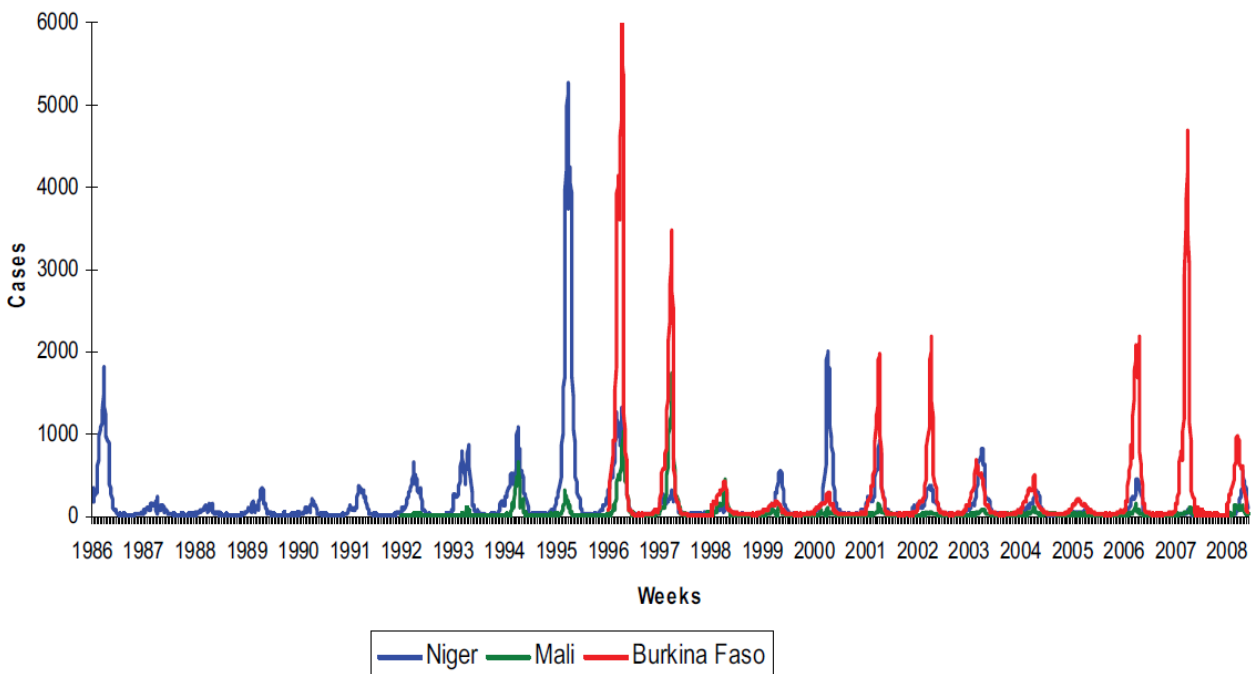


Figure 6.1; Meningitis epidemic weekly evolution over the years in Burkina Faso (1997–2008), Mali (1992–2008), and Niger (1986–2008) (Djingarey et al., 2008).

Figure 6.3 shows the annual distribution of number of meningitis cases averaged at weekly scale in the period 1986-2008 for our test case geographical domain. Please, note that the average is not normalized with the population amount in each district. According to these results, the "upward phase" (as it is denominated by Sultan et al., 2005) starts in the weeks 4-5, achieving the maximum number of meningitis cases between the week 12 and 16, following a decrease in the number of meningitis cases ("downward phase" according to Sultan et al., (2008)) between the week 17 and 22. The number of meningitis cases remains close to zero between the week 23 and 52.

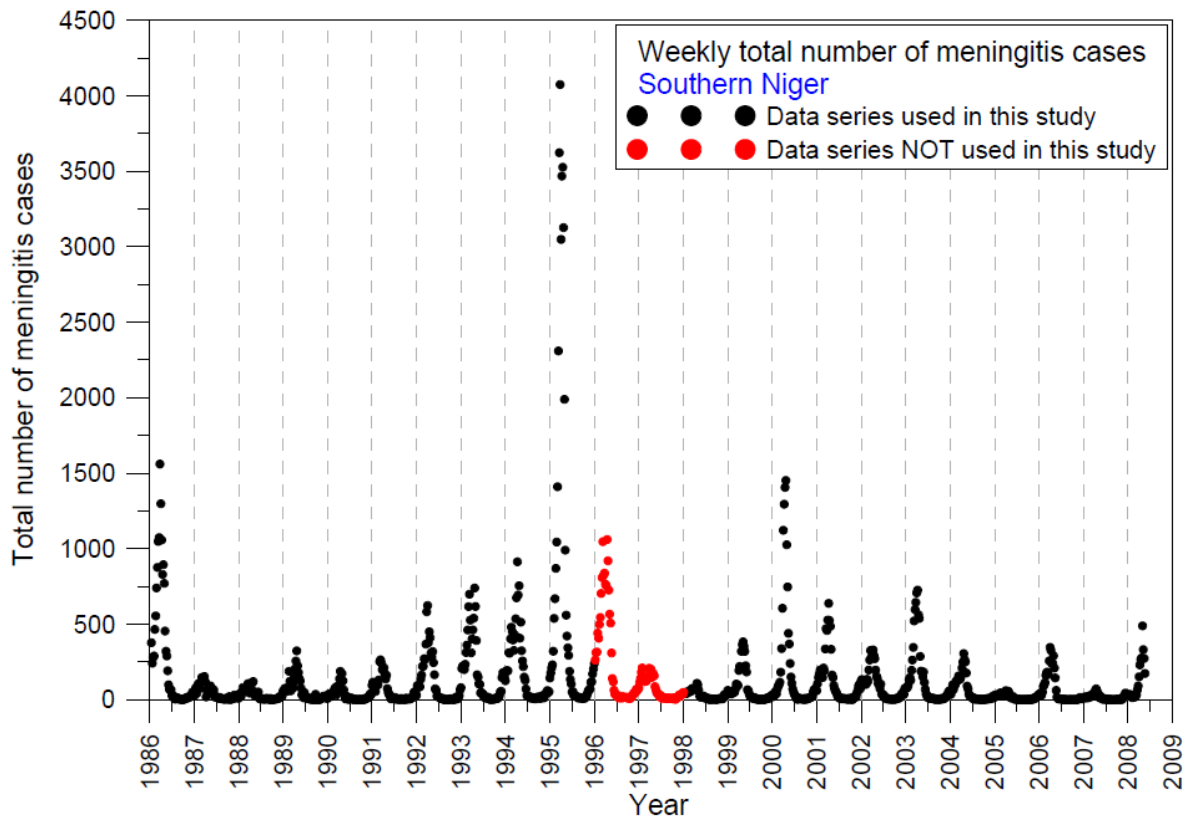


Figure 6.2; Weekly total number of meningitis cases in the districts of southern Niger used in this study (black dots): AGUIE, BIRNI-N'KONNI, BOUZA, DAKORO, DOGON-DOUTCHI, DOSSO, FILINGUE, GAYA, GUIDAN-ROUMDJI, ILLELA, KEITA, KOLLO, LOGA, MADAOUA, MADAROUNFA, MAGARIA, MATAMEYE, MAYAHI, MIRRIAH, OUALLAM, SAY, TAHOUA, TESSAOUA, TILLABERI, and ZINDER.

NMMb/BSC-Dust Reanalysis [Southern Niger] [1987-2008]

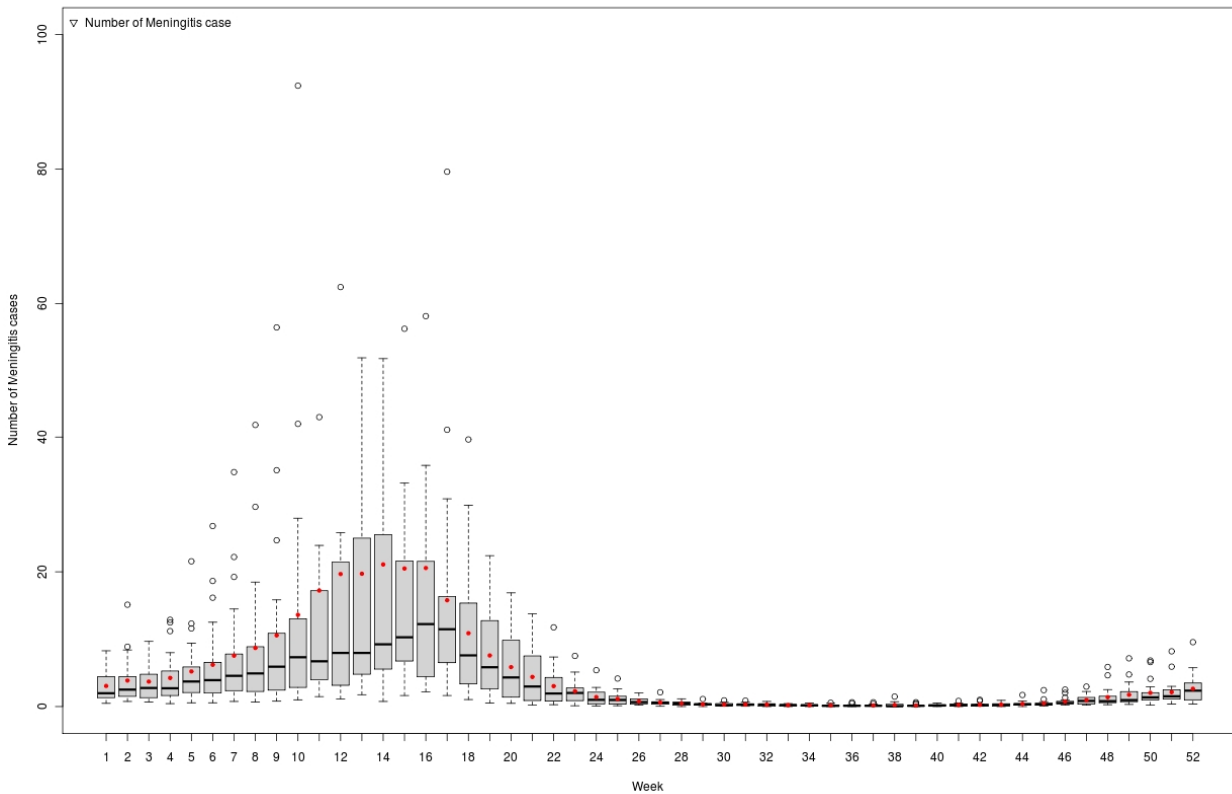


Figure 6.3; Annual distribution of number of meningitis cases averaged at weekly scale in the period 1986-2008 for our test case geographical domain (Southern Niger districts).

## 6.2. Relationship between meningitis and atmospheric conditions

Thompson et al. (2006) suggest that a dusty late autumn and early winter might increase the incidence of meningitis cases. Some previous works have tried to estimate the temporal and spatial variation of Saharan dust in the Sahel region using indirect observations, such as long-term horizontal visibility series (Goudie and Middleton, 1992; N'Tchayi et al., 1994). However, visibility range is not a confident parameter. Most of the synoptic and airport meteorological stations (Metar reports) only report reduction in visibility when the horizontal visibility is less than 10 km. On the other hand remote sensing techniques, based on ground stations (Aerosol RObotic NETwork; - AERONET-; [www.aeronet.gasfc.nasa.gov](http://www.aeronet.gasfc.nasa.gov)) or on satellite (AAI from TOMS-OMI, AOD from Deep Blue and MISR), have been used to estimate dust on ground. However total column aerosol not always reflect the dust conditions near the surface, and especially in the Sahel region during the dry season in winter. Chiapello et al. (1995) had also reported this disconnection between the AOD and the surface dust concentration for low layer transport of Sahelian/Saharan dust over the North-Eastern Tropical Atlantic. Micropulse lidar (MPL) extinction profiles obtained in Niamey (Niger) show large dust storms occurred in dry periods. Aerosol extinction profiles peaked near 500 nm during the January–April period and near 100 m during the October–December period (McFarlane et al., 2009; Cavalieri et al., 2010), confirming the conceptual model explained by the Schematic meridional cross section of atmospheric circulations over West Africa (Figure 4.2.). Saharan dust intrusions take place in thin layers near ground in late autumn and early winter.

On the other hand, there is a clear lack of in-situ measurements of surface dust concentration. The unique information from in-situ mineral dust content in this region comes from the three ground based stations forming the “Sahelian Dust Transect” of the AMMA (African Monsoon Multidisciplinary Analysis) International Program (Marticorena et al., 2010). One of the stations, Banizoumbou (13.54°N, 2°66'E) is in Niger. However the PM<sub>10</sub> record (atmospheric concentration of particulate matter smaller than 10 µm) is quite short (since January 2006) for our purposes. PM<sub>10</sub> data from this station has been used to verify the simulated surface dust concentration from the NMMb/BSC-Dust reanalysis in the period 2006-2008.

All the mentioned observational limitations encouraged us to use long-term reanalysis in order to cross this information with long-term meningitis records and perform a joint analysis.

We have grouped atmospheric data derived from the long-term NMMb/BSC-Dust reanalysis, (1986-2008) in two datasets, corresponding to “**Epidemic years**” (E-yrs) and “**Non-epidemic years**” (NE-yrs) (see section 6.1.), respectively, obtaining the annual course of some atmospheric variables from weekly means for both scenarios.

NE-yrs show a flat record. Climatologically 10 cases per week of meningitis (averaged value for all the districts of our study area) are not surpassed until week 10, which exceeds the average of 5 cases per week (Figure 6.4, upper panel). Note that this is the average number of cases and not the incidence. The weekly maximum values are observed at weeks 16 and 17, decreasing rapidly beyond this week, and returning to background values of less than 5 cases per week from week 21 until the end of the year. In the months of November and December of years before non-epidemic years weekly averaged values do not exceed five cases per week (Figure 6.4, upper panel). However in E-yrs 5 cases per week is exceeded as early as week 48 of the previous year (Figure 6.4), reaching more than 10 cases per week at week 4, when the epidemic of meningitis begins to activate rapidly. Weekly average values are observed between weeks 11 and 16, with more than 40 cases per week. This 5-week period is the active period of the epidemic. At week 17 begins a rapid decline,

coinciding with the onset of the rainy season, reaching background conditions at week 24. A typical non-epidemic year was 2004 (Figure 6.5, upper panel). This year repeats exactly the behaviour of the average non-epidemic years. The maximum average of all districts (more than 10 cases per week) is achieved at week 16 with a total of 306 cases for all districts.

1995 was a strong epidemic year (see Figure 6.2.). This year 5 cases per week (average of all districts not taking into account population in each district) was surpassed already at week 52 of 1994 (Figure 6.5, lower panel), with a total of 144 cases in all our districts, surpassing the 10 cases per week in Week 3 (more than 230 cases as sum in all our districts), when starting the ascending branch of the meningitis cases graph reaching the highest values. 100 cases per week (averaged value for all districts) were exceeded between weeks 11 and 16, recording a maximum of 4075 total cases (sum of all districts) in week 12, a 1332% of the value reached in 2004 four weeks later. Within weeks 8-17 (March-April) the sum of cases in all districts exceeded 1000 cases of meningitis.

Concerning the surface dust concentration derived from NMMb/BSC-Dust reanalysis, we can observe that in NE-yrs (Figure 6.6.) the threshold of  $300 \text{ ug m}^{-3}$  (weekly average) is exceeded at week 52 of the previous year, exceeding the  $400 \text{ ug m}^{-3}$  in Week 2. Although standard deviations are relatively small in previous years, they can be high in the weeks that range from 2 to 16 (Figure 6.6.). However, in E-yrs surface dust concentrations in previous years are higher than in non-epidemic years, surpassing the threshold of  $300 \text{ ug m}^{-3}$  at week 46, and  $400 \text{ ug m}^{-3}$  at week 48. Another feature of the epidemic years is the great variability in surface dust concentration recorded in previous years. The surface dust concentrations are higher in E-yrs compared with NE-yrs, easily surpassing the  $500 \text{ ug m}^{-3}$  from week 2.

In November and December 2003, the year prior to 2004, chosen as representative of NE-yrs, weekly surface dust concentrations are usually below  $200 \text{ ug m}^{-3}$  (Figure 6.7, upper panel). However, in November and December 1994, before a year of peak incidence of meningitis in our study region (1995), the weekly average values of surface dust concentrations are usually above  $300 \text{ ug m}^{-3}$  (Figure 6.7, lower panel), being possible to record weekly average values exceeding  $600 \text{ ug m}^{-3}$ . In 2004 we can see a clear surface dust concentration maximum between weeks 10-11 (with average values exceeding  $600 \text{ ug m}^{-3}$  week), while in 1995 the weekly average values can be observed very high (above  $600 \text{ ug m}^{-3}$ ) in a wide band, between weeks 4 and 14.

The aerosol optical depth (AOD) for NE-yrs and E-yrs has been plotted in Figure 6.8.

Slightly higher values were observed in November and December in years prior to E-yrs compared with the same months in NE-yrs. The AOD values in NE-yrs show a clear maximum between weeks 16 and 20, and the AOD values are fairly constant between weeks 1 and 8. However, in E-yrs maximum AOD is blurred by relatively high values observed between weeks 11 and 28, with weekly average values higher than 0.75. However the most significant feature is the great variability from week to week in AOD in E-yrs. This variability is much lower in NE-yrs.

One possible explanation for this behavior could be that in the E-yrs some strong intrusions of Saharan dust could not be confined to layers near the ground, raising AOD substantially, and contributing to the enormous variability observed in AOD. In any case, this behaviour requires further analysis.

Meridional wind is represented in Figure 6.9. Negative values indicate northeasterly winds typical of Harmattan regime in winter, the dry season.

Differences in the meridional wind between NE-yrs and E-yrs are not important. In both cases Harmattan begins at week 43 (negative values). In 1995 (peak year of epidemic meningitis) the Harmattan begins at week 43, while in 2004 (taken as a non-epidemic reference) it begins at week 45 (Figure 6.10.).

The wind speed of the meridional component is slightly higher (more negative) in NE-yrs between weeks 49 and 52. In weeks 1-10 the Harmattan seems slightly more intense just in the NE-yrs. Harmattan strength is slightly stronger in 1995 (southern component with absolute values greater than  $2 \text{ ms}^{-1}$ ) than in 2004. This same pattern is repeated between weeks 1 and 7 but then the opposite occurs (Harmattan stronger in 2004) in weeks 9-12. However, this does not match the surface dust concentration simulated in NE-and E-yrs yrs. The explanation could be found in the fact that the concentration of dust in the Sahel during the dry season does not come from local sources but transported from the Sahara. The surface wind in the Saharan dust sources and subsequent transport from the Sahara to the Sahel, are the factors modulating the concentrations of dust in the Sahel and not local or regional wind in the Sahel. Once the Harmattan regime is established it is not necessary to have strong winds from the north in the Sahel for a greater transport of dust from the Sahara. In this sense, our results do not agree with Sultan et al. (2005) who found a clear relationship between the onset of the Harmattan and the meningitis epidemics. However, Sultan et al. (2005) used NCEP reanalysis, with a low resolution of  $2.5^\circ$  that can account for large scale transport. This could be the explanation for this discrepancy.

To confirm this hypothesis we calculated the meridional wind anomalies from NCEP reanalysis for March 2004, and March 1995 (Figure 6.11.). In 2004 there was a slightly positive anomaly (weaker Harmattan) in the Sahara and in our study area. This makes more difficult the arrival of dust-loaded air masses from the Sahara. On the contrary, in 1995 (peak year epidemic of meningitis) very negative anomalies (very strong Harmattan) are seen in the Sahara (northern Niger) where mineral dust sources are found favouring its transport to the Sahel. Anyway, a further analysis of backward trajectories at different points in Niger would be necessary.

Concerning the absolute humidity ( $\text{gm}^{-3}$ ) (Figure 6.12) the average weekly shows slightly lower values in December for the years prior to E-yrs. The  $5 \text{ gm}^{-3}$  threshold is reached at week 50 in E-yrs. This is confirmed by the simulations of 1995 (Figure 6.13.). In E-yrs absolute humidity values remain (weekly average) below  $5 \text{ gm}^{-3}$  at weeks 1-11, while in NE-yrs is below this threshold in weeks 6-11, and values with so low absolute humidity are not simulated in the preceding month of December.

In Figure 6.14 the specific humidity ( $\text{gkg}^{-1}$ ) anomalies from NCEP reanalysis for dry periods: December-2003/January-March 2004, and December 1994/January-March 1995 are depicted (Figure 6.14.). In NE-yrs abnormalities are not observed except in the southern Niger, in our study region, where a slight positive anomaly (wet conditions) is observed. By contrast, in E-yrs there are clear negative anomalies (drier conditions than normal), most important in the tropical belt, but also affecting our region of study. Related with humidity conditions is the soil moisture. NCEP anomalies of this parameter are shown for March 2004 and 1995 in Figure 6.15.. In 2004 a soil wetter than normal is found in much of the Sahel and in our study region. However in 1995 the opposite is observed, i.e. drier conditions than normal.

Regarding temperature there are significant differences between E-yrs-and NE-Yrs (Figure 6.16.). E-yrs weekly averaged temperatures observed in November and December of the previous years are clearly below  $20^\circ \text{C}$  from week 49 (December). No such low temperatures are observed in the NE-

ys. Temperatures continuously remain below this value during the first 7 weeks (January and much of February), while in NE-ys this only occurs in the first 3 weeks of January. Therefore the E-ys are characterized by long periods (11 weeks) that can be considered as "cold", while this period only lasts for 3-4 weeks for NE-ys. This is clearly confirmed by analyzing what happens in the two extreme years (Figure 6.17.). In 2004 (non-epidemic) weekly averaged temperatures below 20 ° C were only observed at week 5, while in 1995 (the very epidemic year) weekly averaged temperatures remain below 20 ° C from week 47 of the previous year to week 8, ie for a period of 14 weeks (more than 3 months). Clearly, it seems that temperature is an important factor in modulating the firing of meningitis epidemics together with surface dust concentration and absolute humidity.

It seems clear that atmospheric dust, low humidity and low temperatures in December, January and February play an important role in triggering the meningitis epidemics.

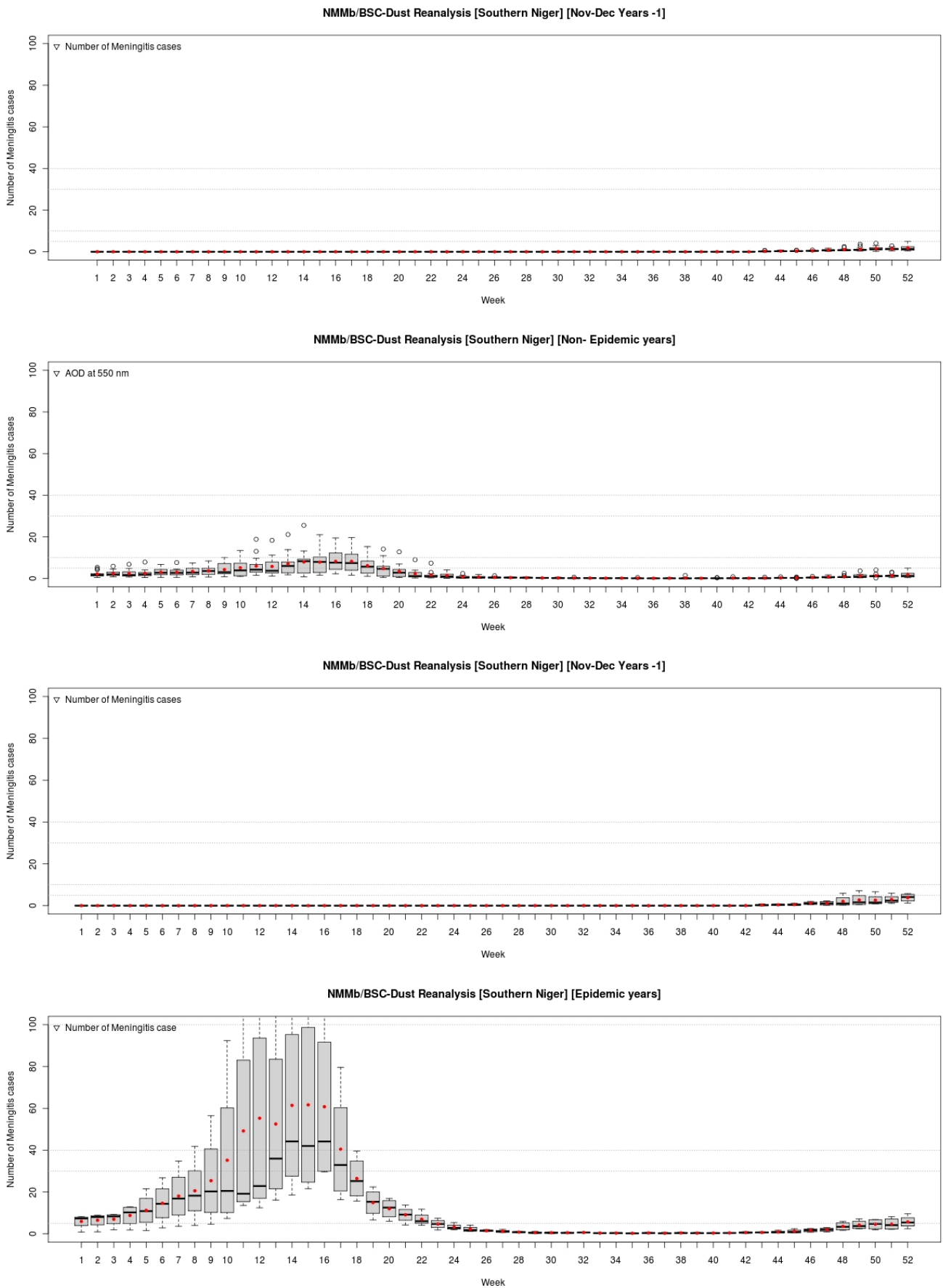
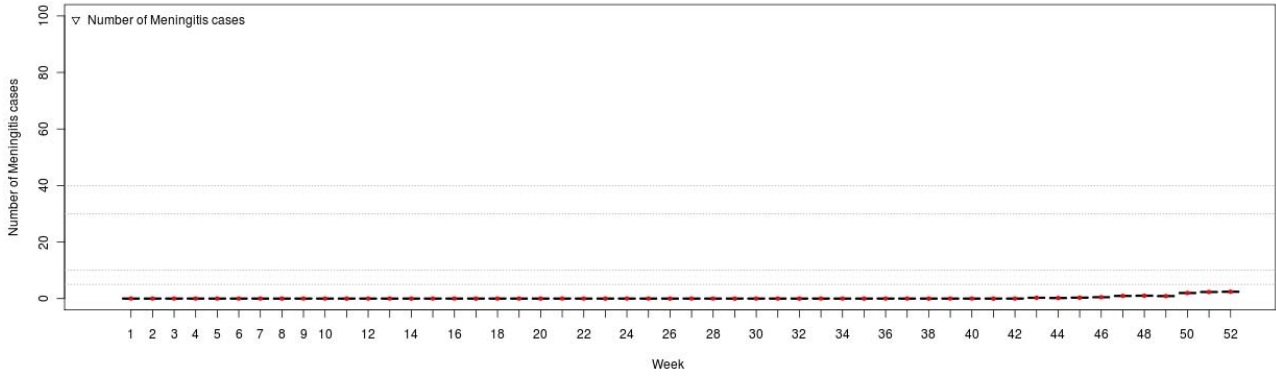


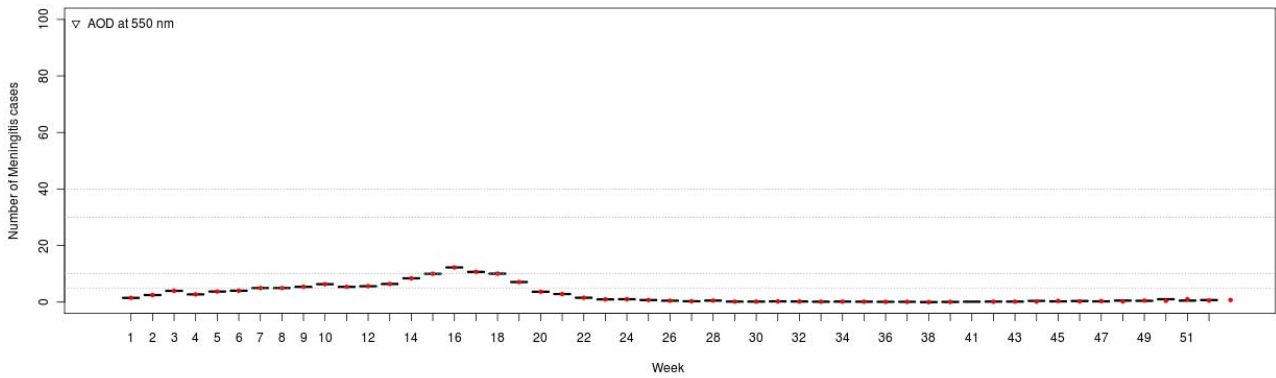
Figure 6.4; Weekly averages of **number of meningitis cases** for Non-epidemic years (upper panel) and for epidemic years (lower panel). Notice that weeks 43-52 (November +December) of the corresponding previous years have been depicted above the respective plots.



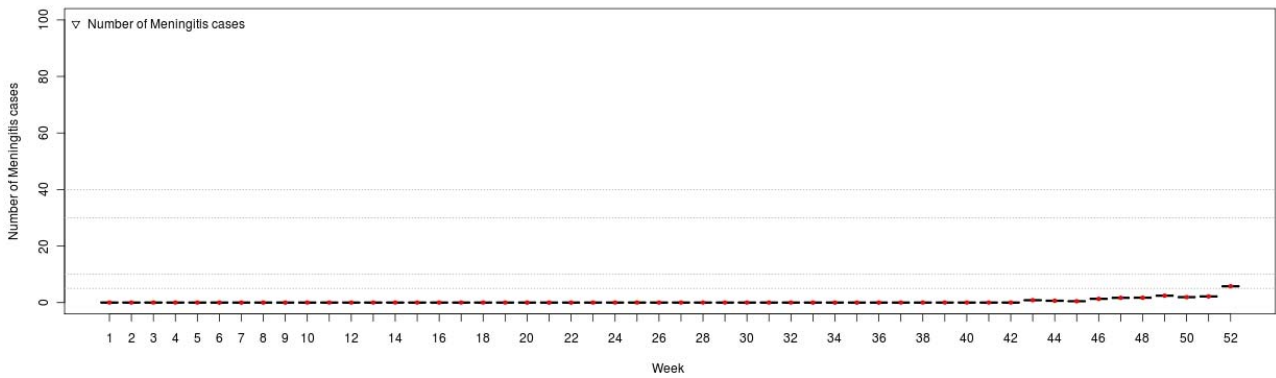
NMMb/BSC-Dust Reanalysis [Southern Niger] [Nov-Dec Years -1]



NMMb/BSC-Dust Reanalysis [Southern Niger] [Non- Epidemic years]



NMMb/BSC-Dust Reanalysis [Southern Niger] [Nov-Dec Years -1]



NMMb/BSC-Dust Reanalysis [Southern Niger] [Epidemic years]

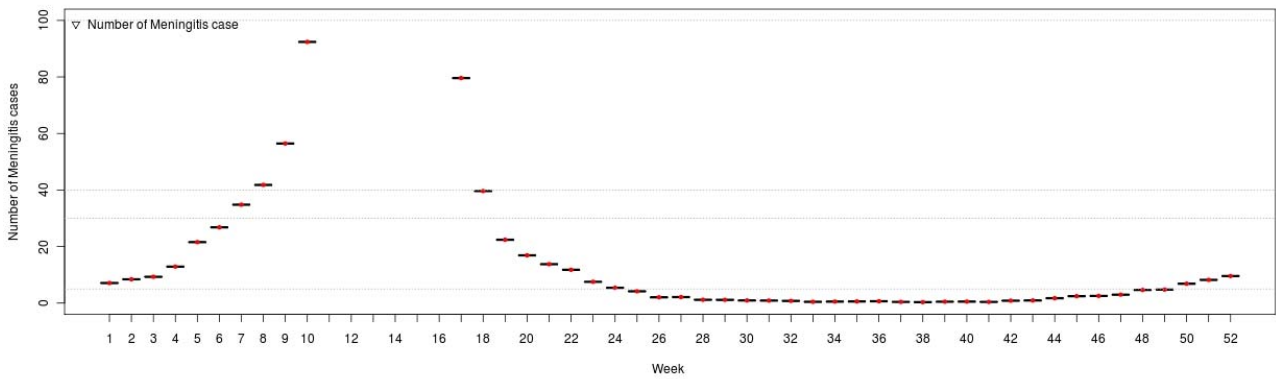
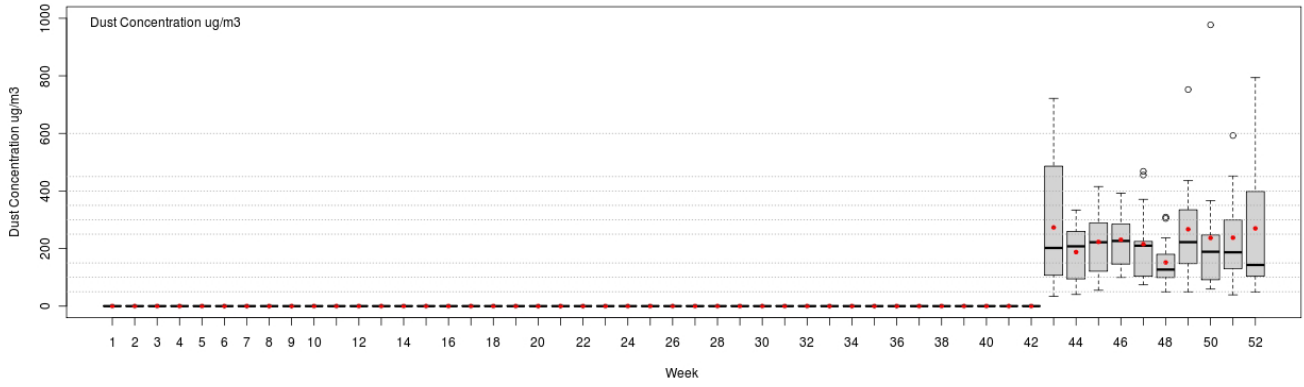
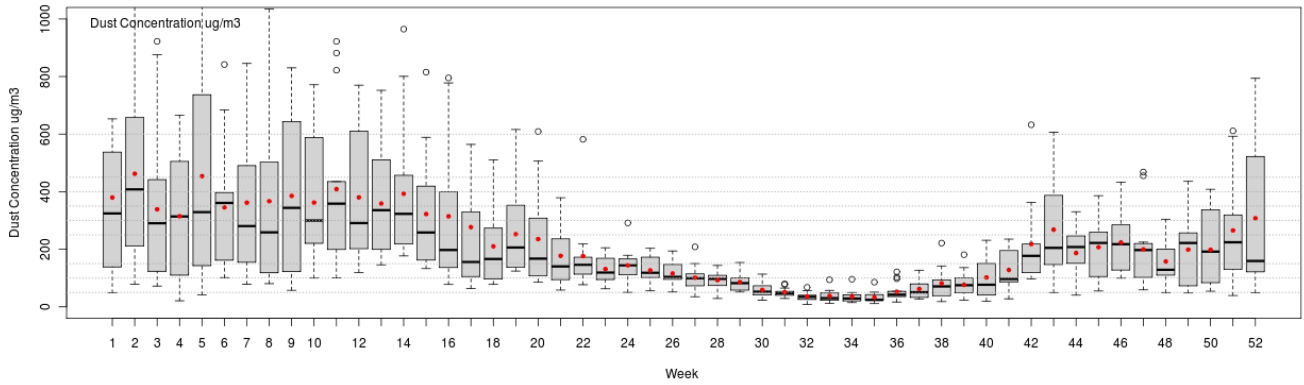


Figure 6.5.; Weekly averages of **number of meningitis cases** for 2004, a non-epidemic year (upper panel) and for 1995, an epidemic year (lower panel). Notice that weeks 43-52 (November +December) of the corresponding previous years, have been depicted above the respective plots.

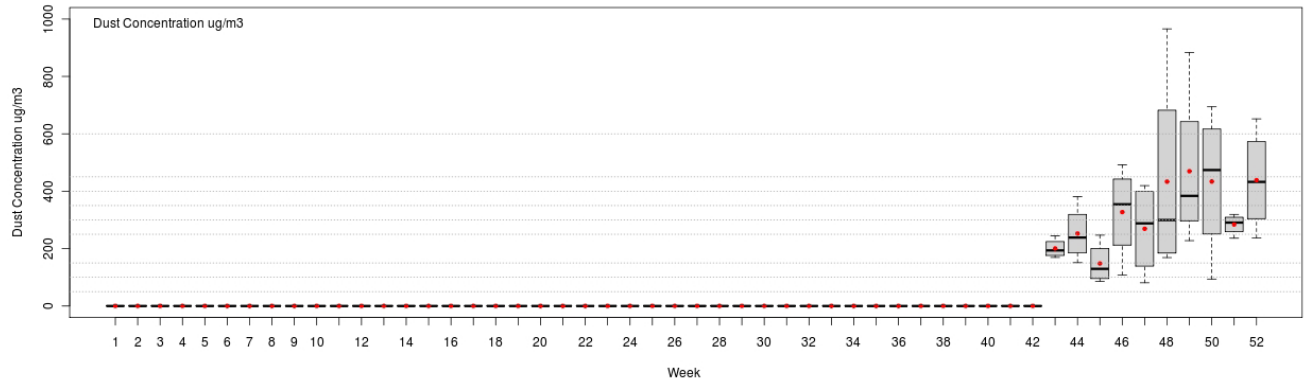
NMMb/BSC-Dust Reanalysis [Southern Niger] [Nov-Dec Years -1]



NMMb/BSC-Dust Reanalysis [Southern Niger] [Non- Epidemic years]



NMMb/BSC-Dust Reanalysis [Southern Niger] [Nov-Dec Years -1]



NMMb/BSC-Dust Reanalysis [Southern Niger] [Epidemic years]

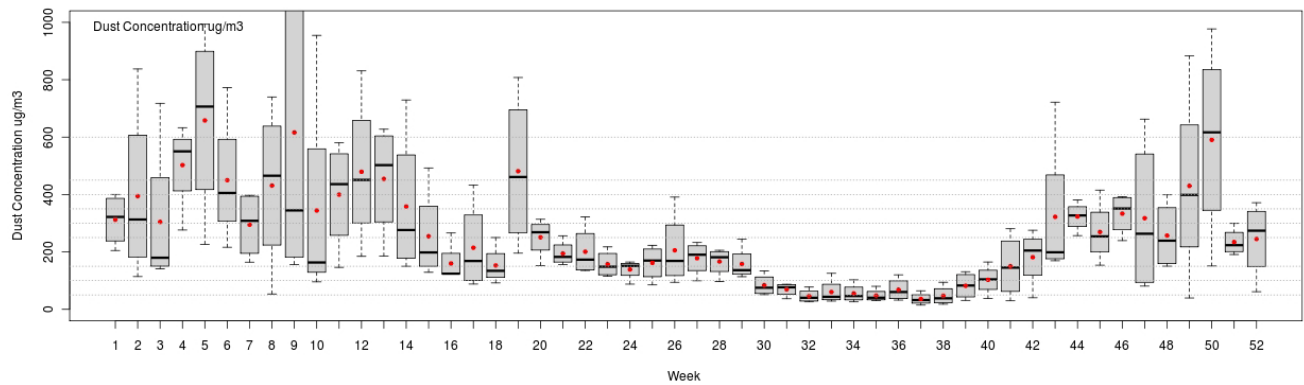


Figure 6.6; Weekly averages of **surface dust concentration ( $\mu\text{g}/\text{m}^3$ )** from NMMb/BSC-Dust reanalysis for non-epidemic years (upper panel) and for epidemic years (lower panel). Notice that weeks 43-52 (November +December) of the corresponding previous years, have been depicted above the respective plots.

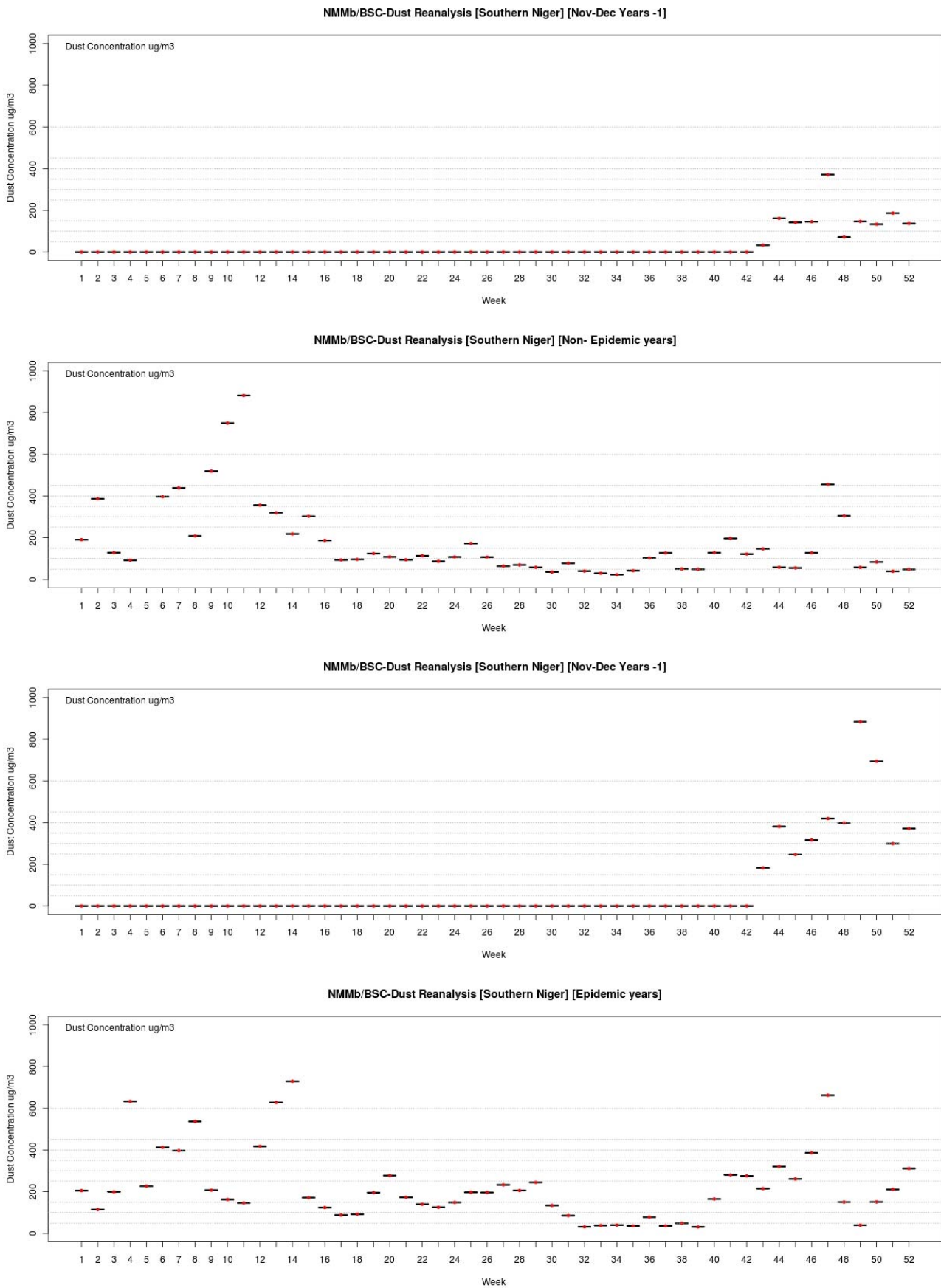


Figure 6.7.; Weekly averages of **surface dust concentration ( $\mu\text{g}/\text{m}^3$ )** from NMMB/BSC-Dust reanalysis for 2004, a non-Epidemic year (upper panel), and for 1995, a high epidemic year (lower panel). Notice that weeks 43-52 (November +December) of the corresponding previous years, have been depicted above the respective plots.

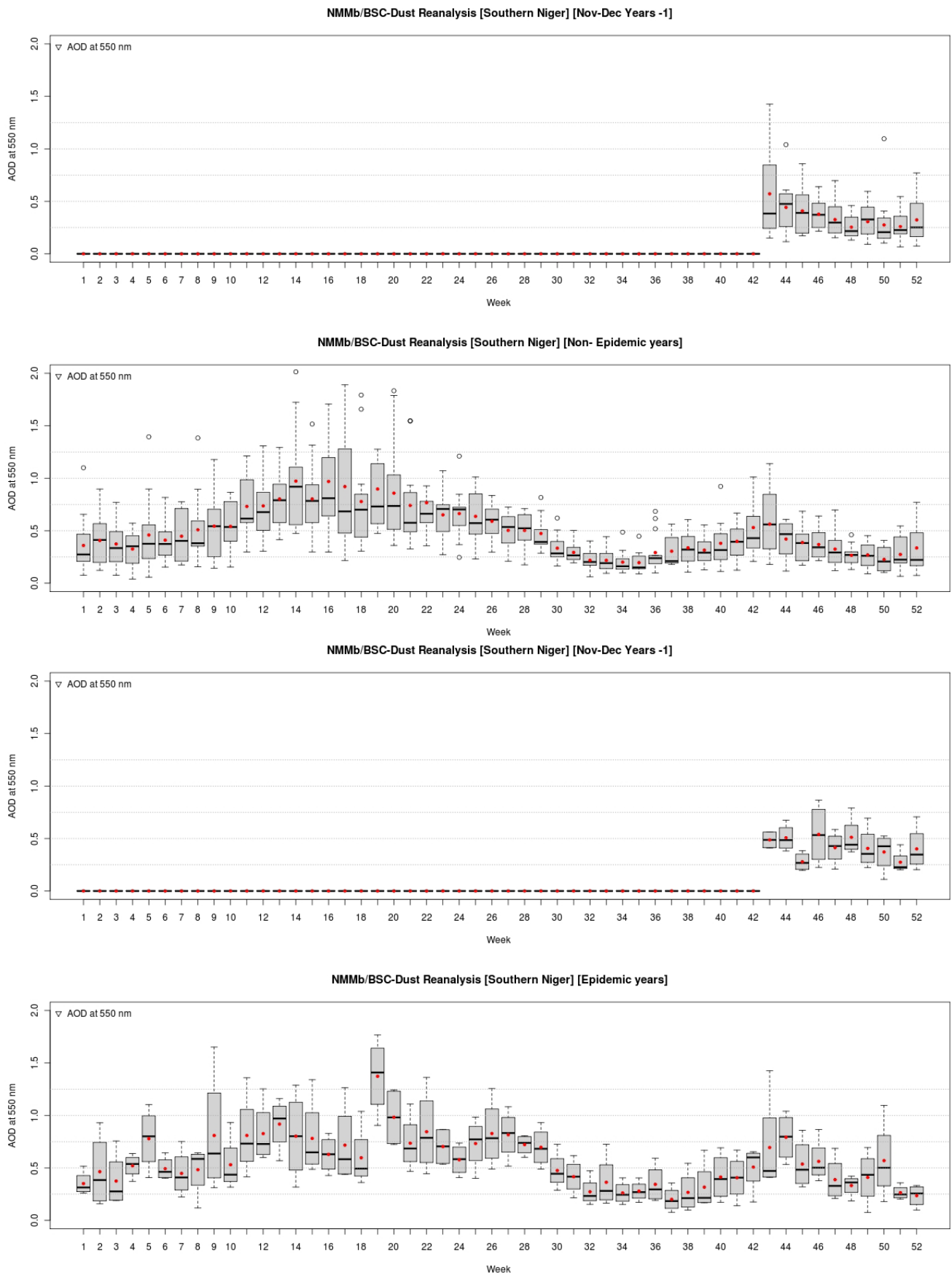
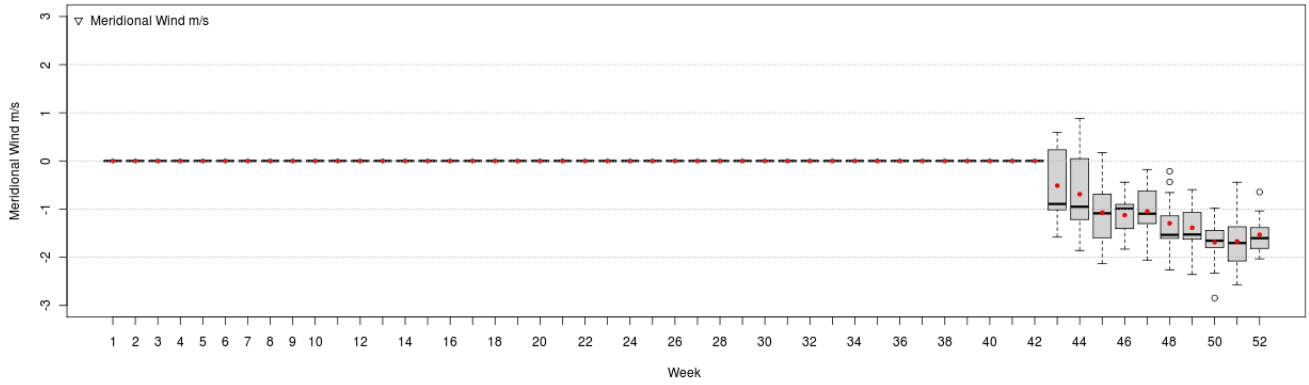
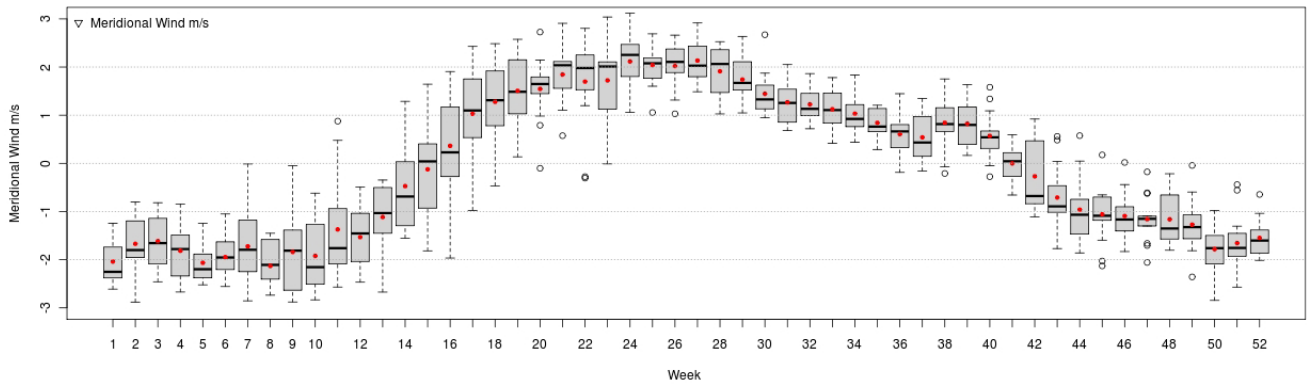


Figure 6.8; Weekly averages of **Aerosol Optical Depth (AOD)** from NMMb/BSC-Dust reanalysis for non-epidemic years (upper panel) and for epidemic years (lower panel). Notice that weeks 43-52 (November +December) of the corresponding previous years, have been depicted above the respective plots.

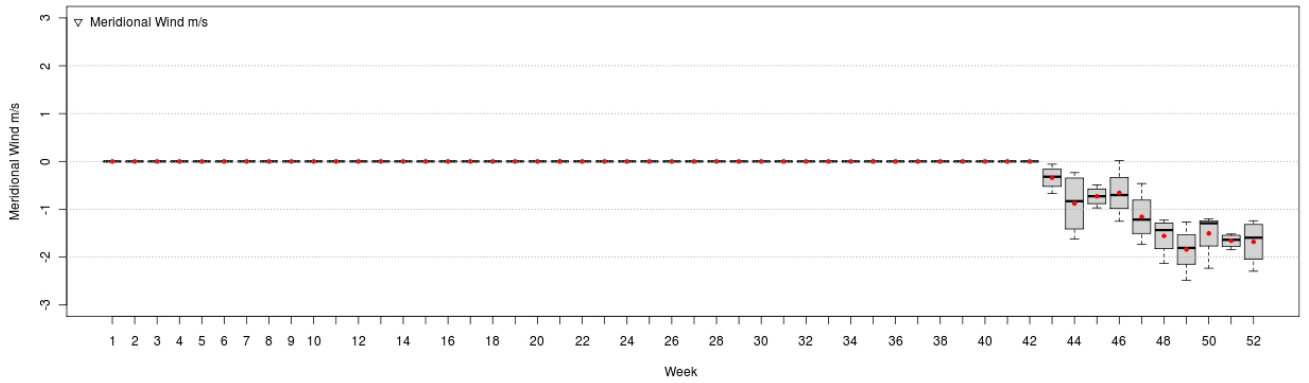
NMMb/BSC-Dust Reanalysis [Southern Niger] [Nov-Dec Years -1]



NMMb/BSC-Dust Reanalysis [Southern Niger] [Non- Epidemic years]



NMMb/BSC-Dust Reanalysis [Southern Niger] [Nov-Dec Years -1]



NMMb/BSC-Dust Reanalysis [Southern Niger] [Epidemic years]

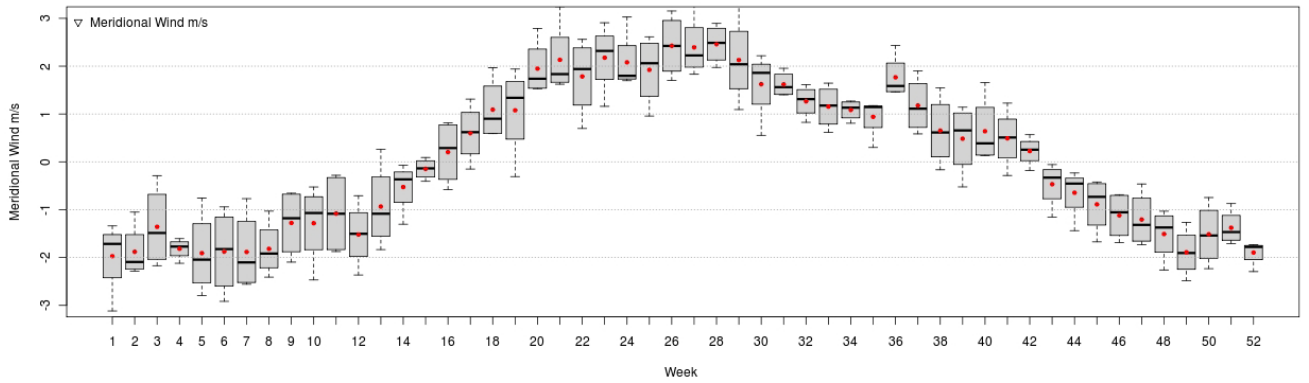


Figure 6.9.; Weekly averages of meridional wind ( $\text{ms}^{-1}$ ) from NMMb/BSC-Dust reanalysis for non-epidemic years (upper panel) and for epidemic years (lower panel). Notice that weeks 43-52 (November +December) of the corresponding previous years, have been depicted above the respective plots.

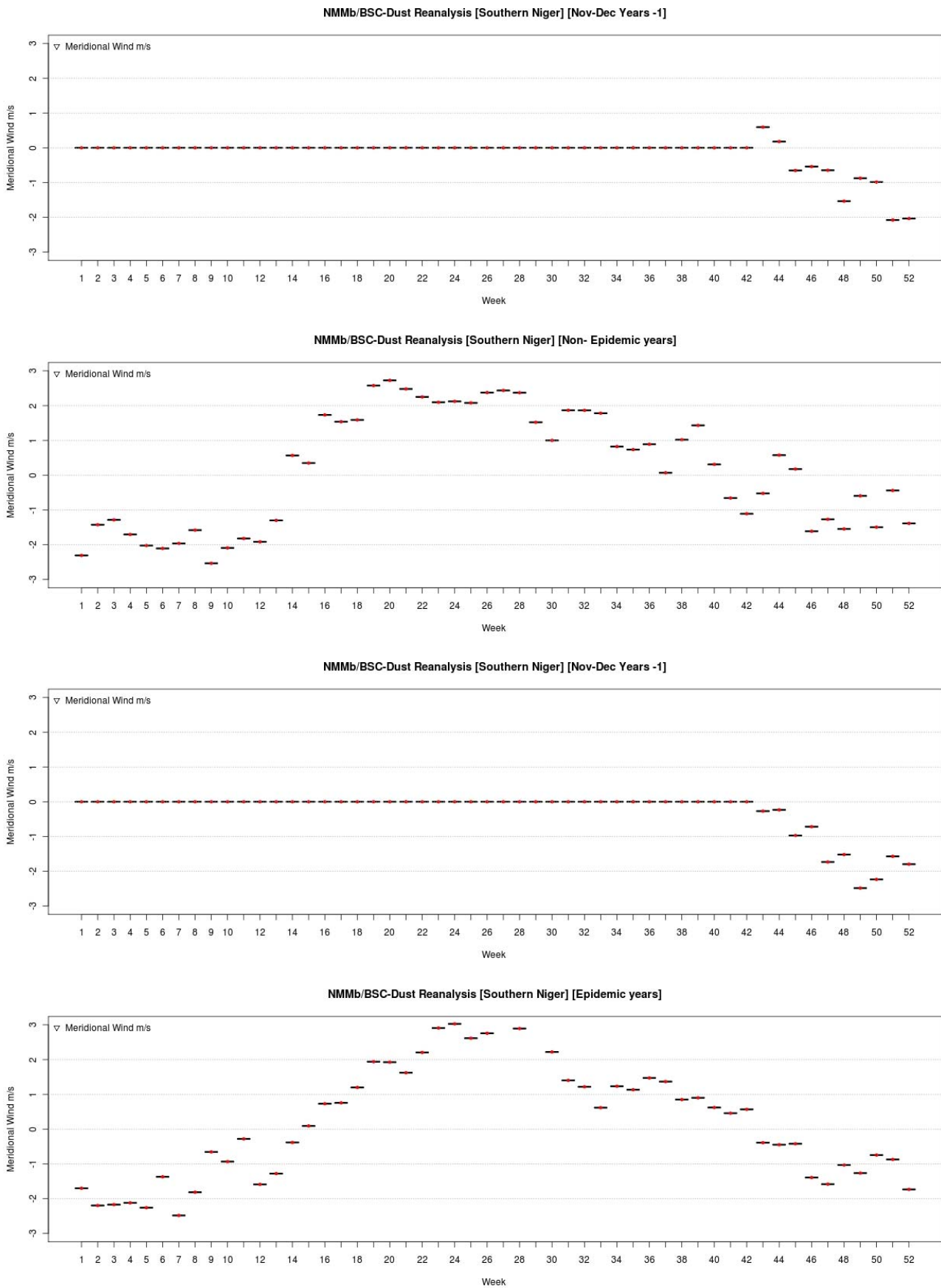


Figure 6.10.; Weekly averages of meridional wind ( $\text{ms}^{-1}$ ) from NMMb/BSC-Dust reanalysis for 2004, a non-Epidemic year (lower panel) and for 1995, a high epidemic year (upper panel). Notice that weeks 43-52 (November +December) of the corresponding previous years, have been depicted above the respective plots.

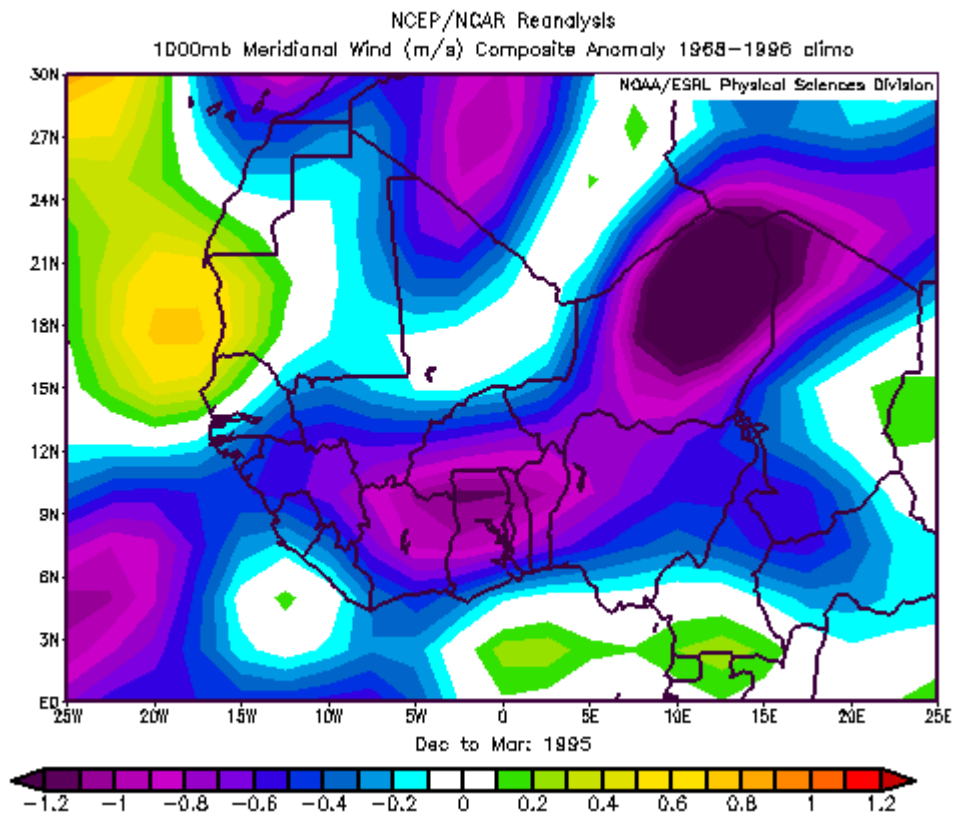
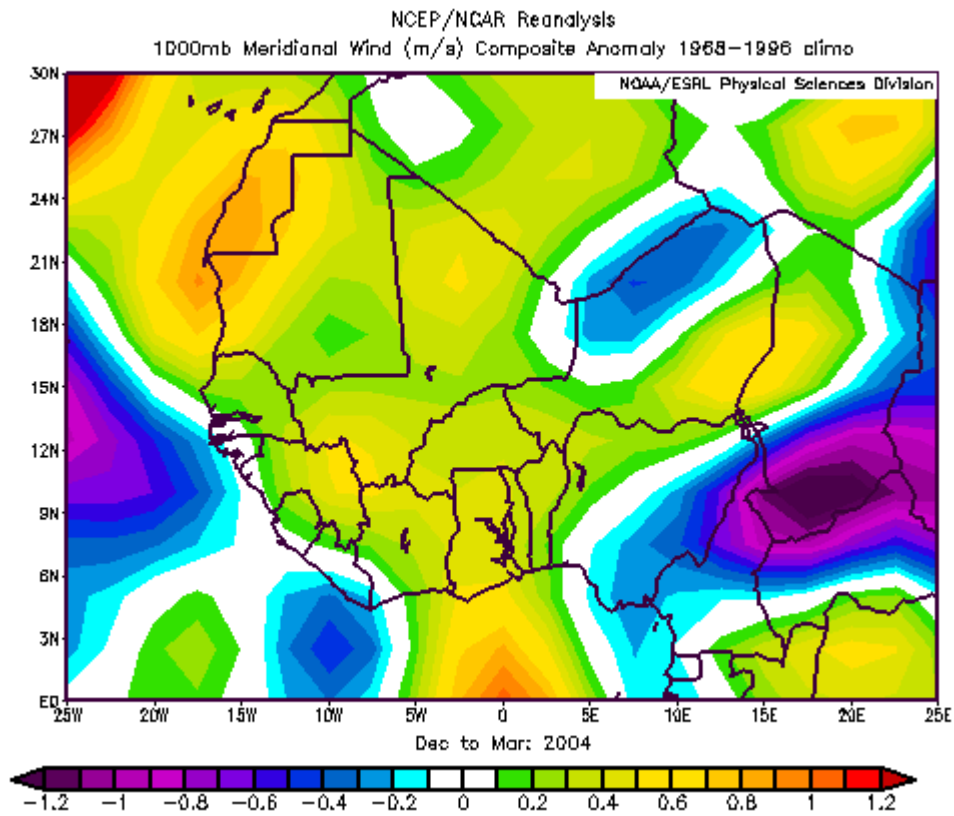
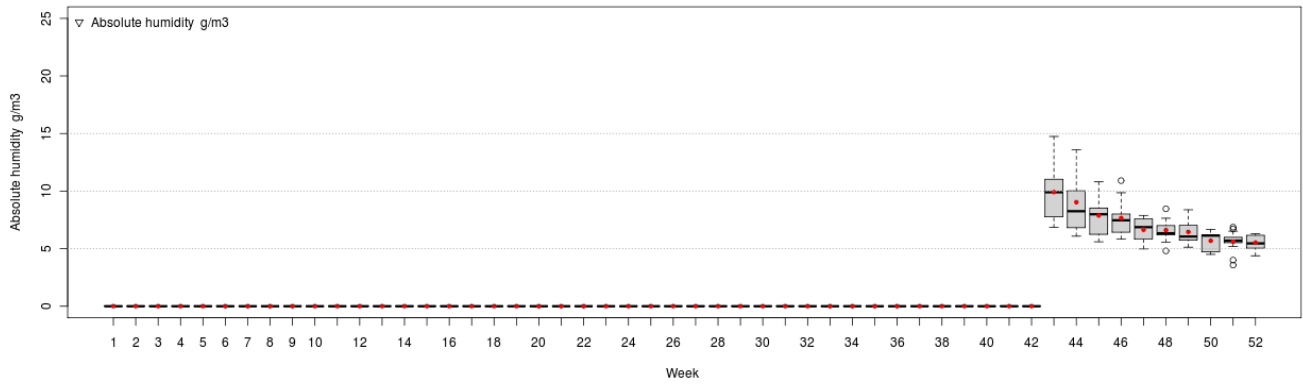


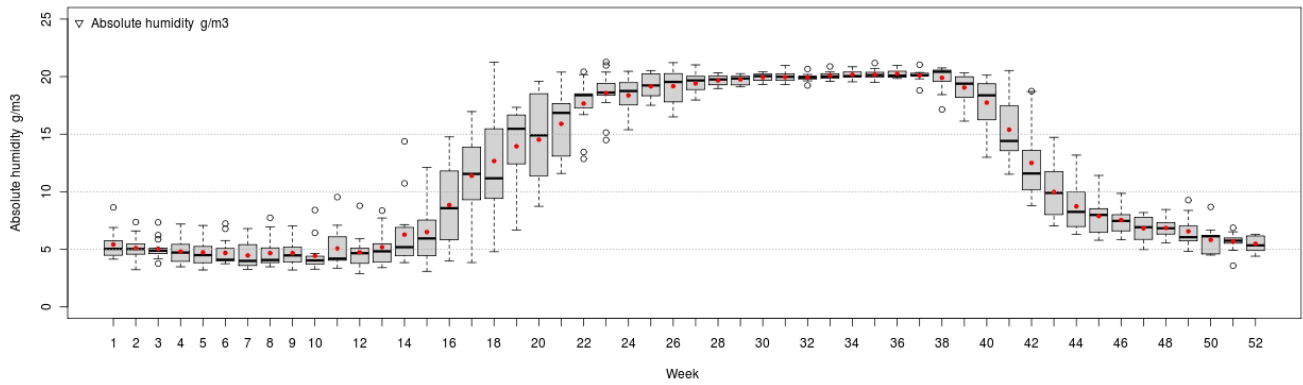
Figure 6.11.; NCEP Meridional wind ( $\text{ms}^{-1}$ ) anomalies for March 2004, a Non-epidemic year (up), and for March 1995, an epidemic year (down).



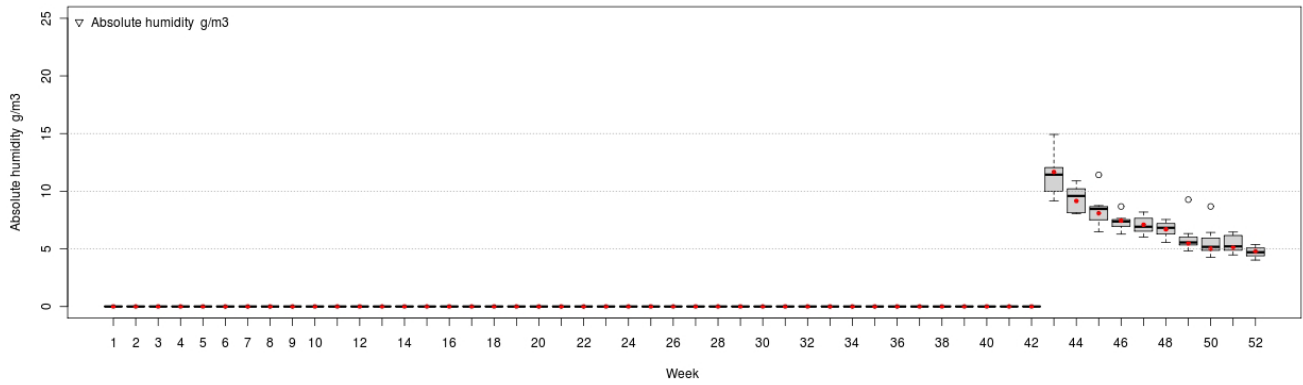
NMMb/BSC-Dust Reanalysis [Southern Niger] [Nov-Dec Years -1]



NMMb/BSC-Dust Reanalysis [Southern Niger] [Non- Epidemic years]



NMMb/BSC-Dust Reanalysis [Southern Niger] [Nov-Dec Years -1]



NMMb/BSC-Dust Reanalysis [Southern Niger] [Epidemic years]

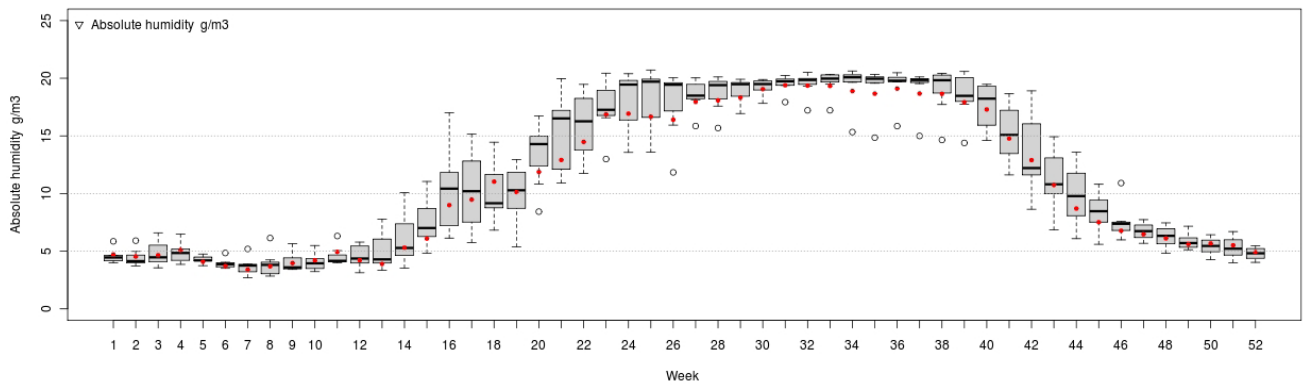
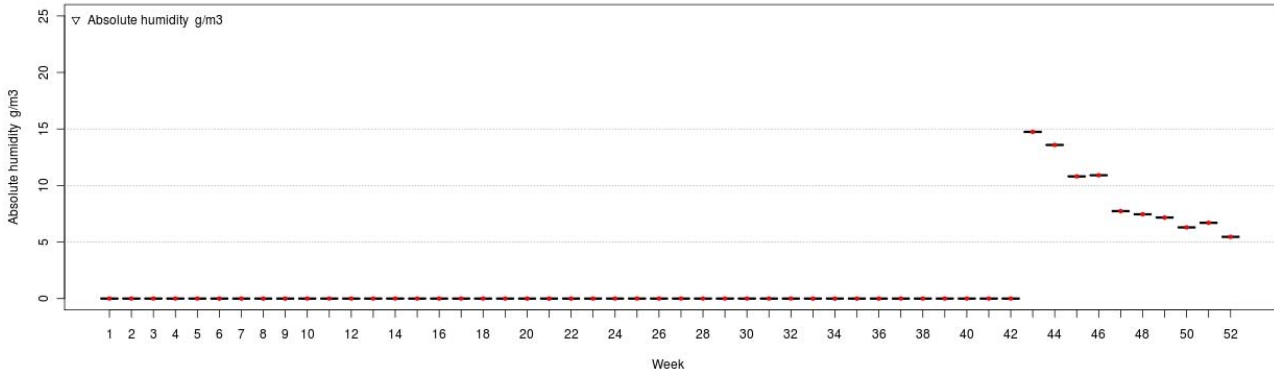


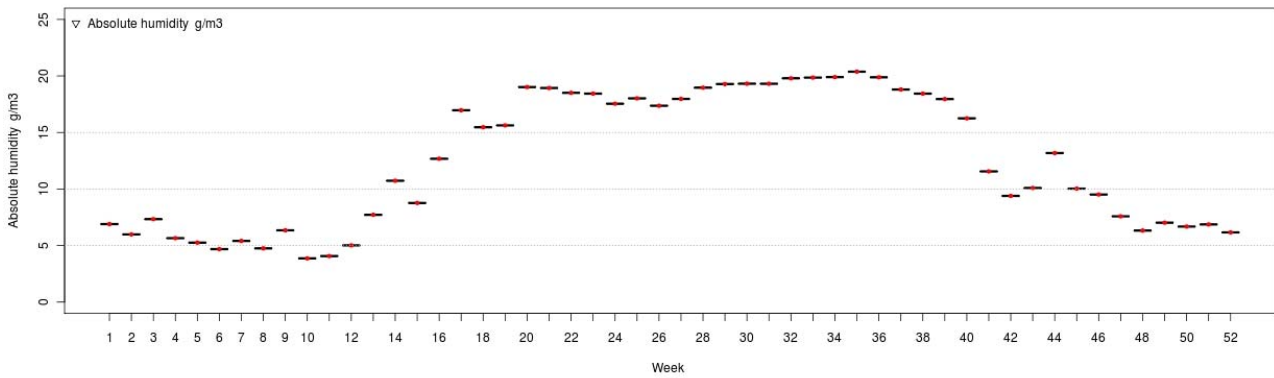
Figure 6.12.; Weekly averages of **absolute humidity ( $\text{gm}^{-3}$ )** from NMMb/BSC-Dust reanalysis for non-epidemic years (upper panel) and for epidemic years (lower panel). Notice that weeks 43-52 (November +December) of the corresponding previous years, have been depicted above the respective plots.



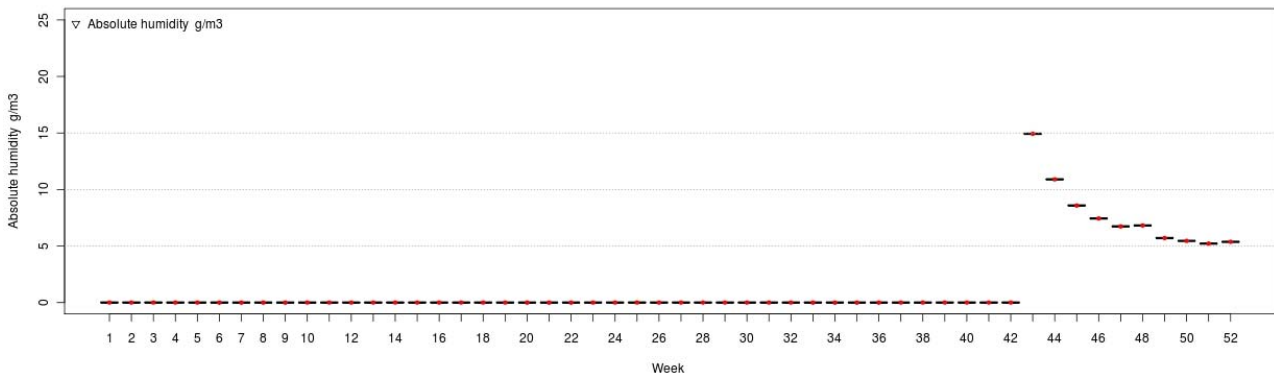
NMMb/BSC-Dust Reanalysis [Southern Niger] [Nov-Dec Years -1]



NMMb/BSC-Dust Reanalysis [Southern Niger] [Non- Epidemic years]



NMMb/BSC-Dust Reanalysis [Southern Niger] [Nov-Dec Years -1]



NMMb/BSC-Dust Reanalysis [Southern Niger] [Epidemic years]

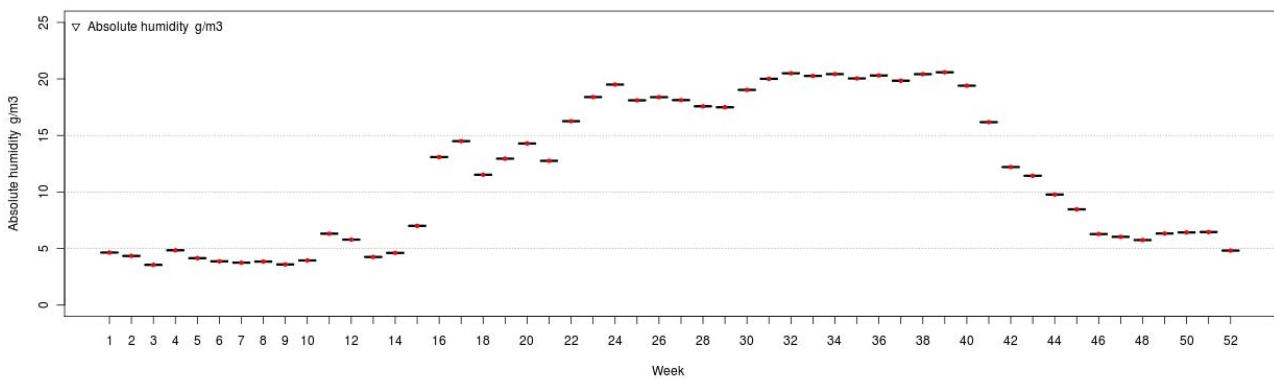


Figure 6.13.; Weekly averages of **absolute humidity ( $\text{gm}^{-3}$ )** from NMMb/BSC-Dust reanalysis for 2004, a non-Epidemic year (upper panel), and for 1995, a high epidemic year (lower panel). Notice that weeks 43-52 (November +December) of the corresponding previous years, have been depicted above the respective plots.

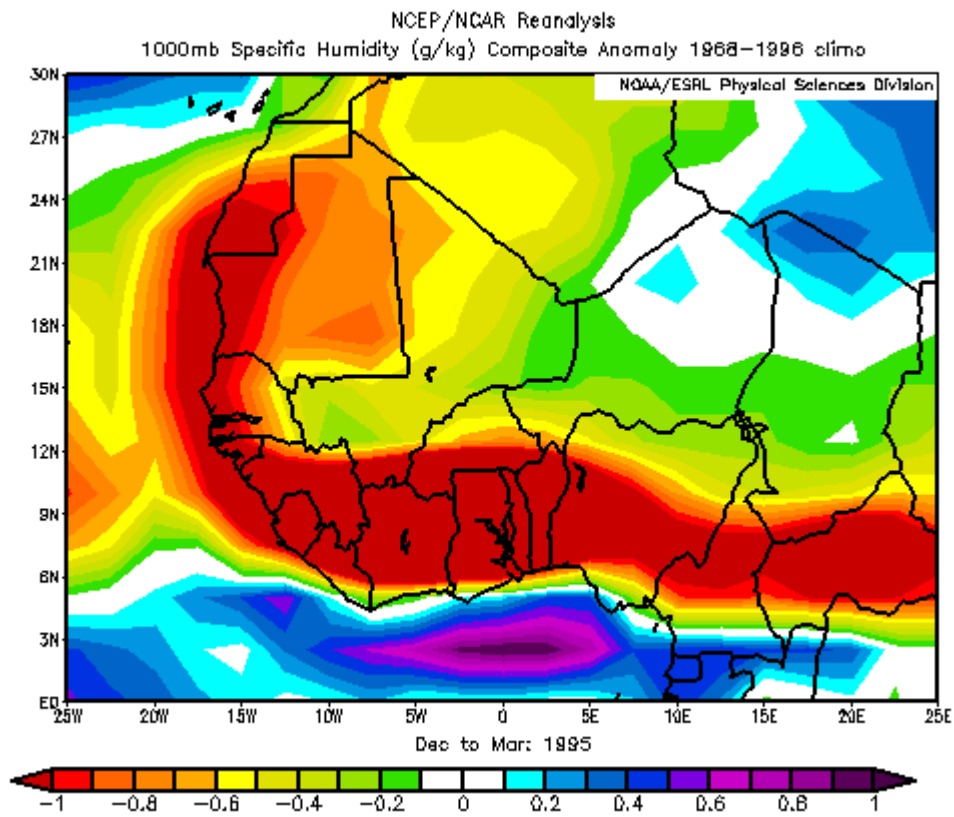
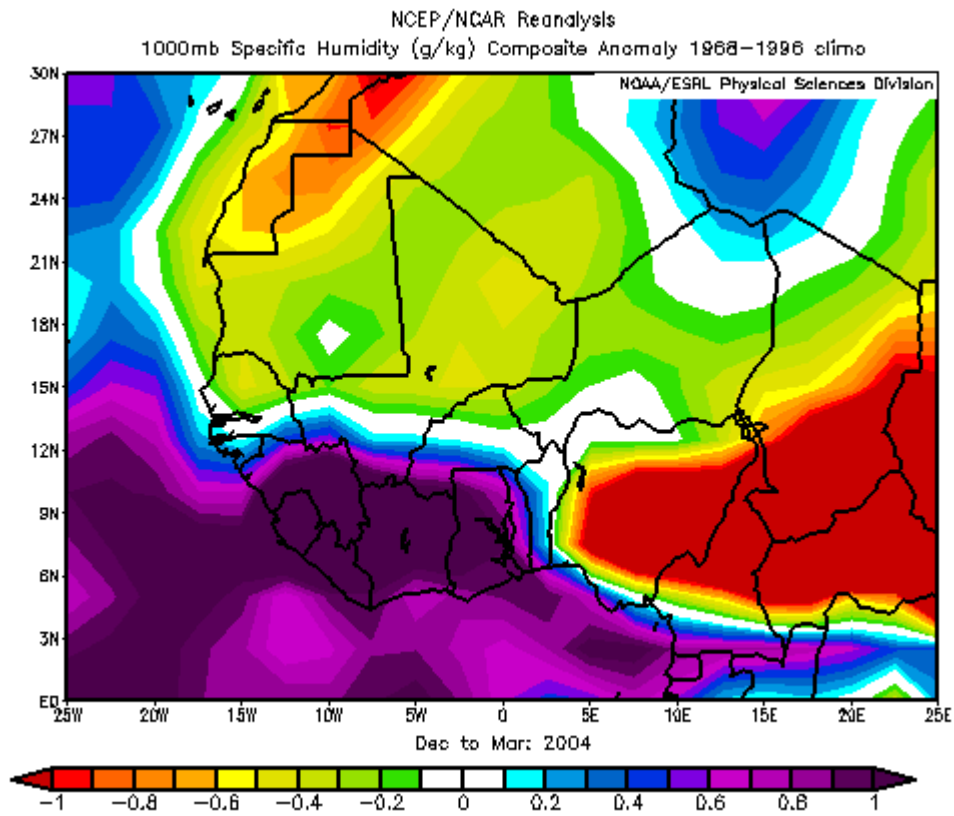


Figure 6.14.; NCEP **Specific humidity (gkg<sup>-1</sup>)** anomalies for December-2003/January-March 2004, a non-epidemic year (up) and anomalies for 1995, an epidemic year (down).

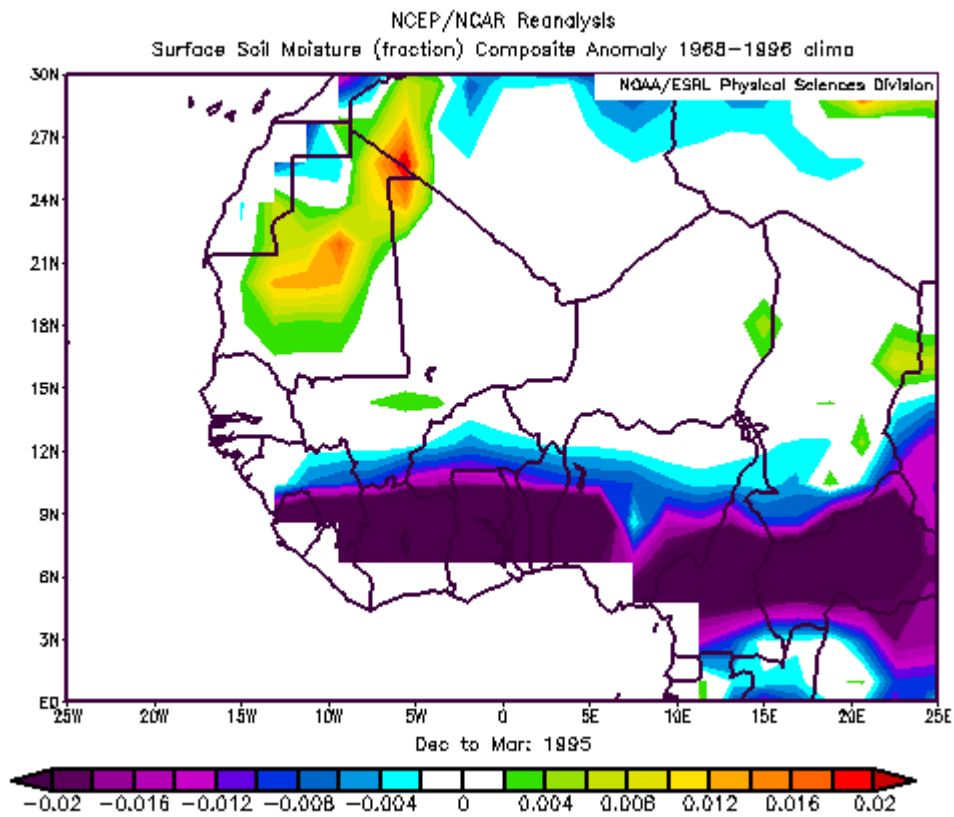
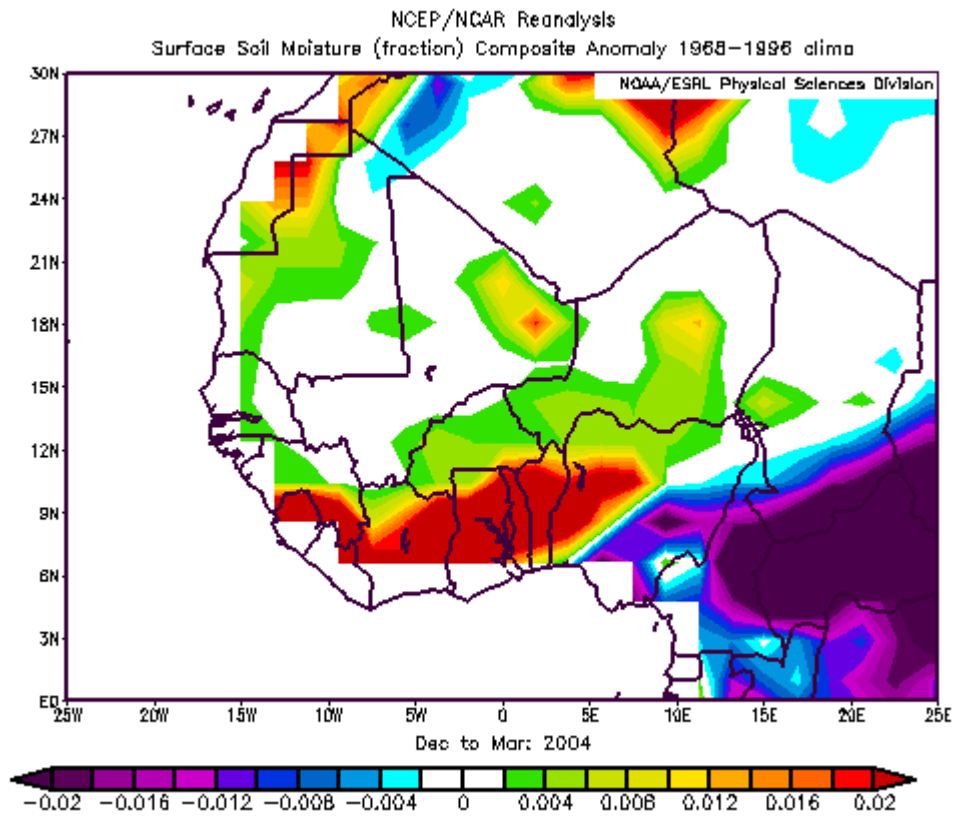


Figure 6.15.; NCEP Soil moisture (fraction) anomalies for March 2004, a Non-epidemic year (up), and for March 1995, an epidemic year (down).

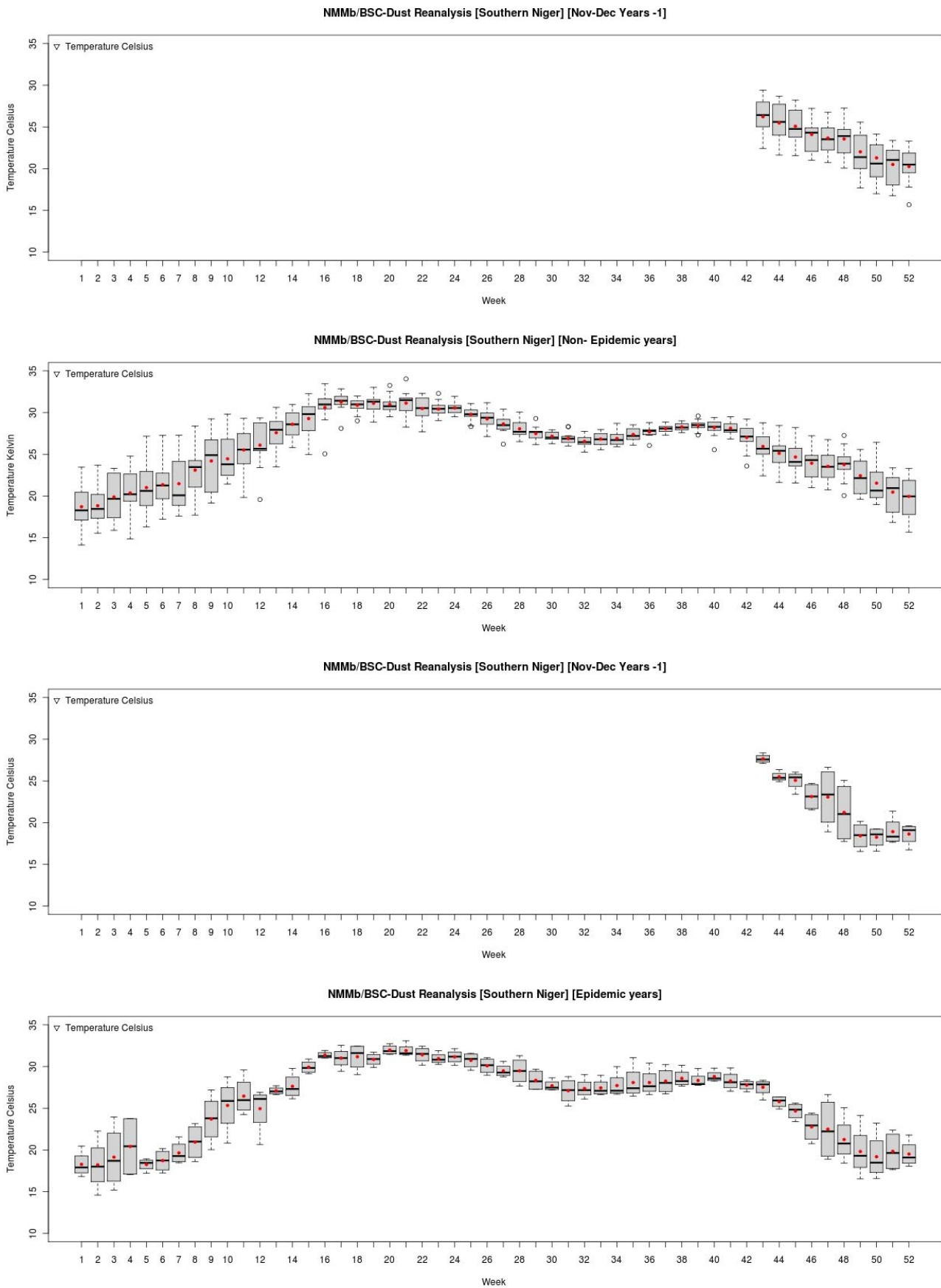
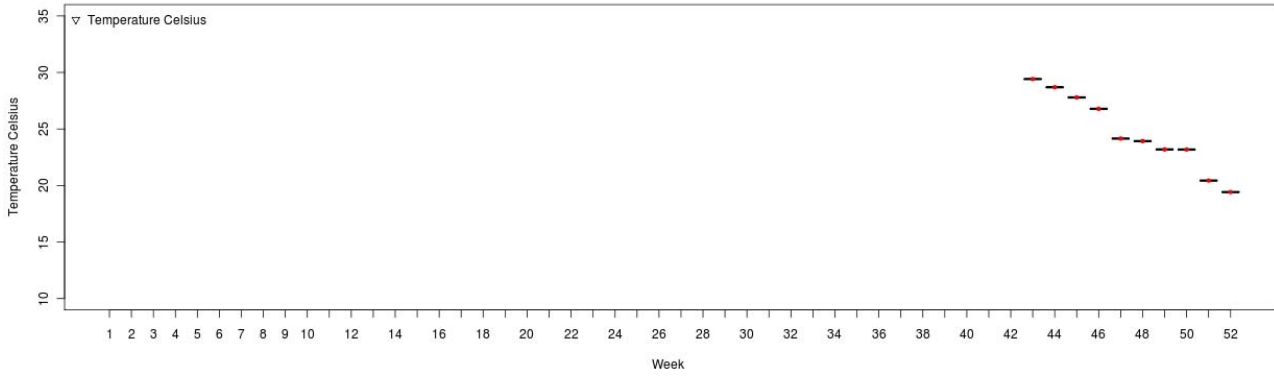
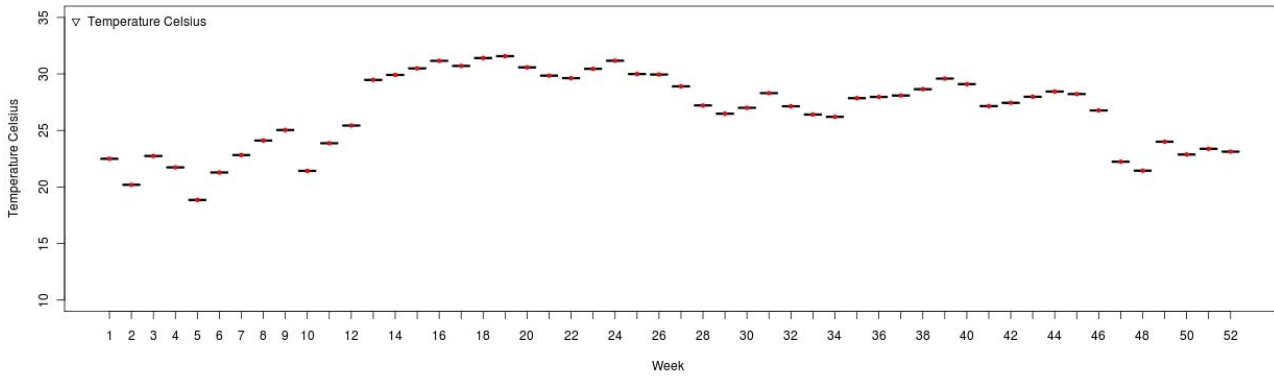


Figure 6.16.; Weekly averages of **temperature (°C)** from NMMb/BSC-Dust reanalysis for non-epidemic years (upper panel) and for epidemic years (lower panel). Notice that weeks 43-52 (November +December) of the corresponding previous years, have been depicted above the respective plots.

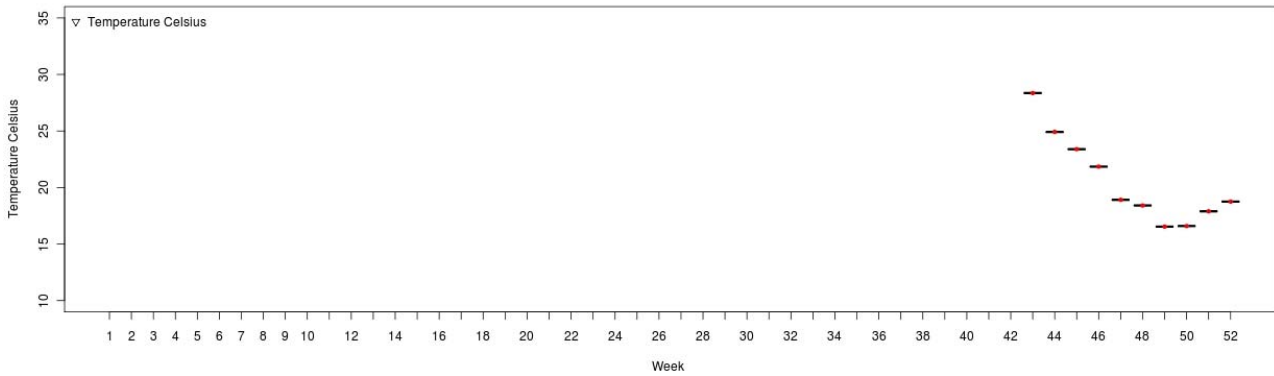
NMMb/BSC-Dust Reanalysis [Southern Niger] [Nov-Dec Years -1]



NMMb/BSC-Dust Reanalysis [Southern Niger] [Non- Epidemic years]



NMMb/BSC-Dust Reanalysis [Southern Niger] [Nov-Dec Years -1]



NMMb/BSC-Dust Reanalysis [Southern Niger] [Epidemic years]

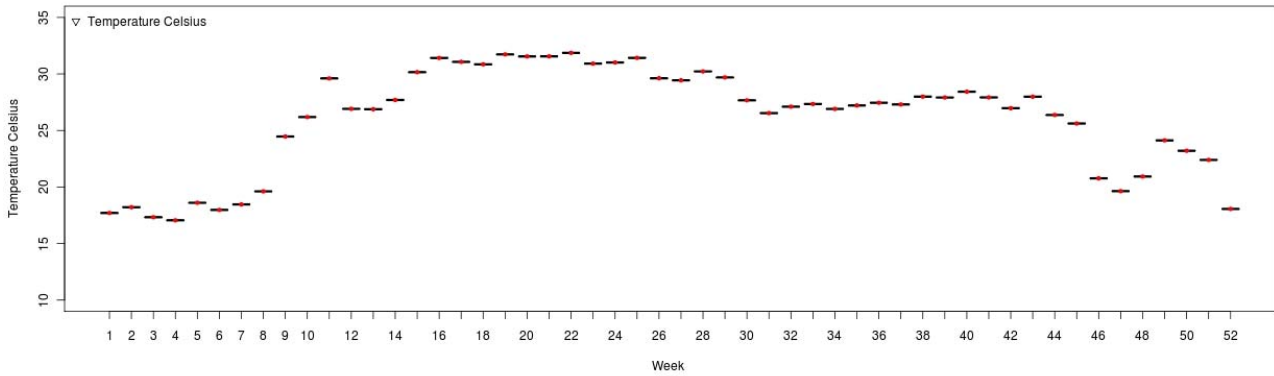


Figure 6.17.; Weekly averages of **temperature (°C)** from NMMb/BSC-Dust reanalysis for 2004, a non-Epidemic year (upper panel), and for 1995, a high epidemic year (lower panel). Notice that weeks 43-52 (November +December) of the corresponding previous years, have been depicted above the respective plots.

## 7. Findings and proposals for MACC

We used an 30-year reanalysis of the new NMMb/BSC-Dust model for this MACC study demonstration trying to find a clear relationship between mineral dust (and environmental conditions) and meningitis epidemics in the Sahel focusing our study to a period of more than 20 years (1986-2008) in southern districts of Niger where meningitis prevalence is highest in winter (dry season). Reanalysis of NMMb/BSC-Dust has been carried out in the BSC (partner of this WP). NMMb/BSC-Dust model will be soon implemented operationally at the Centre contribute to the Sand and Dust Storm Warning Advisory and Assessment System (SDS WAS) Northern Regional Center for Africa, Middle East and Europe. We started working with the DREAM8b-BSC regional model but his behaviour was found not to be optimal in the Sahel region. The new model NMMB/BSC-Dust includes parameterizations that significantly improve the simulations in this region.

First we conducted a preliminar validation and verification of NMMB / BSC-Dust reanalysis. In-situ meteorological information and NCEP reanalysis and ERA-Interim has been used to validate the meteorological outputs of NMMB/BSC-Dust, obtaining good results. AERONET has also been used to validate the AOD in southern Niger (Banizoumbou stations and Niamey). These comparisons show that the model is able to detect the seasonal and interannual variations.

Some comparisons have also been made against semi-quantitative measurements of column aerosol content (AAI from TOMS and OMI) and quantitative measurements (AOD from Deep Blue-MODIS; Figure 5.12). It was verified that the correlations between the AERONET AOD (used as reference), the AOD from NMMb/BSC-Dust reanalysis, and the AAI from TOMS and OMI, were of the same order. However it also highlighted the enormous constraints that satellite-based measurements have for such studies, given the short duration of the series. Satellite-based observations show significant inhomogeneities when changing sensor and method of measurement, preventing analysis of long term series.

Given the almost total unavailability of in-situ measurements of atmospheric dust in the Sahel, and specifically in Niger, we used indirect measurements of visibility of several meteorological stations in Niger, converted into dust concentration by empirical formula, (D'Almeida, 1986), to compare directly to the outputs of surface dust concentration of NMMb/BSC-Dust. The comparisons are very satisfactory showing that the simulations capture rather well the dust events every year, as well as the interannual variations. This verification was complemented with a comparison of actual measurements of in-situ PM-10 performed in the framework of AMMA in the period 2006-2008 (Marticorena et al., 2010). The comparison results are surprisingly good. All these results confirmed the ability of the reanalysis of NMMb/BSC-Dust to perform long-term analysis crossed with meningitis data series.

A second part was focused on identifying relationships between meningitis epidemics and environmental parameters in the Sahel. To this end we performed an exploratory analysis in the southern districts of Niger where the prevalence of meningitis is highest and where a series of data on the number of meningitis cases, disaggregated by district in the period 1986-2008, is available.

Separating the years of the period 1986-2008 into two groups, a low prevalence of meningitis (non-Epidemic years) and a high prevalence of meningitis (Epidemic years) we have seen how high concentrations of dust, low humidity and low temperatures in December of the years before the

firing of meningitis epidemics, may play a significant role in their activation and intensity. However these results are preliminary. In order to understand the role of climate and dust in the onset and intensity of the disease at different spatial and temporal scales we need to account for other very factors such as population density, migration and medical conditions (programs vaccination, other population sensitivity to the spread of meningitis) that play a fundamental role in the activation and intensity of epidemics of meningitis.

There is very poor on-site environmental information in the Sahel region and almost no data of surface dust concentration. On the other hand, there are severe limitations in the systems for remote sensing of atmospheric dust both ground-based (low number of stations with short observation series, with some exceptions) and satellite-based (relatively short series with large gaps and inhomogeneities due to sensor changes and their drifts). Furthermore, total column aerosol measurements may not reflect the conditions of dust near the ground that are affecting people and, trigger meningitis epidemics. Therefore, taking into account the above circumstances, models of high-resolution atmospheric dust become indispensable tools for both long-term reanalysis studies, as shown by the NMMb/BSC-Dust model, and for short and medium term predictions.

Therefore, under MACC-II or under future European atmospheric services, it would be very interesting to include an operational atmospheric dust model system covering the area of the Sahara and the Sahel. This could be easily done (and at non-cost) with dust/aerosols models currently participating in MACC, like MACC-ECMWF, CHIMERE, MOCAGE, LMDZ-INCA, DREAM8b-BSC and others as the used in this work, the NMMb/BSC-Dust, which will be soon incorporated into operational activities through the WMO SDS WAS. This could be an important contribution to the Action Plan on "GMES and Africa" complementing the African Monitoring of the Environment for Sustainable Development (AMESD) Programme, operated by EUMETSAT.

From the point of view of the WMO WAS SDS, early warnings of severe dust intrusions in the Sahel to the National Meteorological and Hydrological Services (NMHS) in the region could be used for making very low-cost actions, such as the distribution of dust masks among the population, which could reduce the number of people affected by meningitis. This could be an important support to the World Health Organization (WHO). On the other hand, it would be desirable to carry out long-term retrospective reanalysis of dust of at least 20 years with MACC-ECMWF in the Sahel to assist in the implementation, that is being conducted, of multidisciplinary systems for meningitis prediction that take into account, in addition, demographic and population factors, medical inputs, and soil conditions.

However, from a strictly meteorological and atmospheric point of view, there are still significant outstanding issues to be addressed. It is necessary to improve the convective parameterization and increase the resolution of the models in the Sahel, one of the most challenging regions of the world for weather forecasting. It is necessary to perform many more validations and verifications of the models, but this requires increasing the in-situ meteorological observations in the Sahel (in quantity and quality) including observations of atmospheric parameters (PM10 concentration, aerosol chemical analysis), and improve satellite observations in areas of high reflectivity, such as large areas of the Saharan region and sub-Saharan Africa.

### **Acknowledgments**

The simulations were run in the Marenostrum Supercomputer at the **Barcelona Supercomputing Center (BSC; [www.bsc.es](http://www.bsc.es))**. The **International Research Institute for Climate and Society, Columbia**

**University (IRI;** <http://portal.iri.columbia.edu>) is acknowledged for providing the series of cases of meningitis in different districts of Niger (1986-2008) fully validated and standardized. Special mention to **Dr. Didier Tanré** maintaining a well-kept long series of AOD in Niger (**Banizoumbou AERONET station;** <http://aeronet.gsfc.nasa.gov>), essential for model validation activities with NMMb/BSC-Dust. **ECMWF** ([www.ecmwf.int](http://www.ecmwf.int)) and **NCEP** ([www.ncep.noaa.gov](http://www.ncep.noaa.gov)) have provided the corresponding long-term **ERA-Interim** and **NCEP** reanalysis used for verification activities of the NMMb/BSC-Dust reanalysis. The authors also appreciate the activities developed under **AMMA project**, and specifically the results obtained by **Dr. Marticorena**, which have helped to increase knowledge about atmospheric processes in the Sahel. The **World Data Center for Remote Sensing of the Atmosphere, WDC-RSAT** (<http://wdc.dlr.de>) and the **Giovanni web-based application** (NASA; <http://disc.sci.gsfc.nasa.gov/giovanni>) have been used to download satellite-based information. In-situ meteorological data has been obtained from **NNDC Climate Data Online** (<http://cdo.ncdc.noaa.gov>).

### **Bibliography**

Cavaliere, O., F. Cairo, F. Fierli, G. Di Donfrancesco, M. Snels, M. Viterbini, F. Cardillo, B. Chatenet, P. Formenti, B. Marticorena, and J. L. Rajot, 2010, Variability of aerosol vertical distribution in the Sahel, *Atmos. Chem. Phys.*, 10, 12005–12023.

Chiapello, I., Bergametti, G., Dulac, F., Gomes, L., Chatenet, B., Pimenta, J., and Santos Soares, E.: An additional low layer transport of Sahelian and Saharan dust over the North-Eastern Tropical Atlantic, *Geophys. Res. Lett.*, 22, 3191–3194, 1995.

D’Almeida, G.A., 1986, A model for Saharan dust transport, *J. Clim. Applied, Meteorol.*, 25:903-916.

Djingarey, M.H., S. Noazin, M. P. Préziosi, C. Lingani, S. Tiendrebéogo, K. Touré, K. Kiari Kaka, W. Perea, E. Bertherat, D. Kandolo, M. LaForce, S. Viviani, K. Kondé, 2008, A 20-year retrospective analysis of epidemic meningitis surveillance data in Burkina Faso, Mali, and Niger, *International Pathogenic Neisseria Conference*, September 2008; Rotterdam, The Netherlands.

Gillies, J.A., W.G. Nickling and G.H. Mctainsh, 1996, Dust concentrations and particle-size characteristics of an intense dust haze event: Inland Delta Region, Mali, West Africa, *Atmos. Environ.*, Vol. 30, 7, Pages 1081-1090.

Ginoux, P., O. Torres, 2003, Empirical TOMS index for dust aerosol: Applications to model validation and source characterization, *J. Geophys. Res.*, VOL. 108, NO. D17, 4534, doi:10.1029/2003JD003470.

Goudie, A. S. and Middleton, N. J., 1992, The changing frequency of dust storms through time, *Climatic Change*, 20, 197–225.

Haywood, J. M., et al., 2008, Overview of the Dust and Biomass-burning Experiment and African Monsoon Multidisciplinary Analysis Special Observing Period-0, *J. Geophys. Res.*, 113, D00C17, doi:10.1029/2008JD010077.



- Holben, B.N., T.F. Eck, I. Slutsker, J.P. Buis, A. Setzer, E. Vermote, J.A. Reagan, Y. Kaufman, T. Nakajima, F. Lavenu and A. Smirnov, 1998, AERONET - A federated instrument network and data archive for aerosol characterization. *Remote Sens. Environ.*, vol.66, No.1, pp.1-16.
- Hsu, N. C., S. C. Tsay, M. D. King, and J. R. Herman, 2004, Aerosol properties over bright-reflecting source regions, *IEEE Trans. Geosci. Remote Sens.*, 42, 557-569.
- Jaenicke, R., 1985, Aerosols Physics and Chemistry, In Landolt-Börnstein, Numerical Data and Functional Relationships in Science and Technology, New Series (Edited by Fisher G.), pp 391-457, Wiley, New York.
- Knippertz, P., Ansmann, A., Althausen, D., Müller, D., Tesche, M., Bierwirth, E., Dinter, T., Müller, T., von Hoyningen-Huene, W., Schepanski, K., Wendisch, M., Heinold, B., Kandler, K., Petzold, A., Schütz, L., and Tegen, I., 2009, Dust Mobilization and Transport in the Northern Sahara during SAMUM 2006 — a meteorological overview, *Tellus 61B*,
- Lapeyssonie, L., 1963, La méningite cérébro-spinale en Afrique, *Bull OMS*, 28 (suppl): 1-100.
- Lerner, J.A., D.L. Westphal, and J.S. Reid, 2004, Quality controlled surface visibility observations used to validate predicted surface aerosol concentration for southwest Asia, P 4.3, 20th Conference on Weather Analysis and Forecasting/16th Conference on Numerical Weather Prediction.
- Mahowald, N. M., and J. L. Dufresne, 2004, Sensitivity of TOMS aerosol index to boundary layer height: Implications for detection of mineral aerosol sources, *Geophys. Res. Lett.*, 31, L03103, doi:10.1029/2003GL018865.
- Marticorena, B., B. Chatenet, J. L. Rajot, S. Traoré, M. Coulibaly, A. Diallo, I. Koné, A. Maman, T. NDiaye, and A. Zakou, 2010, Temporal variability of mineral dust concentrations over West Africa: analyses of a pluriannual monitoring from the AMMA Sahelian Dust Transect, *Atmos. Chem. Phys.*, 10, 8899–8915, 2010, doi:10.5194/acp-10-8899-2010.
- McFarlane, SA, El Kassianov, JC Barnard, CJ Flynn, and TP Ackerman, 2009, Surface shortwave aerosol radiative forcing during the Atmospheric Radiation Measurement Mobile Facility deployment in Niamey, Niger; *J. of Geophys. Res. D. (Atmospheres)* 114: Art. No. D00E06. doi:10.1029/2008JD010491.
- Molesworth A, Cuevas LE, Morse AP, Herman JR, Thomson MC, 2002, Dust clouds and spread of infection. *Lancet* 359: 81–82.
- Molesworth AM, Thomson MC, Connor SJ, Cresswell MP, Morse AP, et al., 2002, Where is the Meningitis Belt? Defining an area at risk of epidemic meningitis in Africa. *Trans R Soc Med Hyg* 96: 242–249.
- Molesworth, A. M., L. E. Cuevas, S. J. Connor, A. P. Morse, and M. C. Thomson, 2003, Environmental risk and meningitis epidemics in Africa, *Emerging Infectious Diseases* 9:1287-1293.
- N'Tchayi, G. M., Bertrand, J., Legrand, M., and Baudet, J., 1994, Temporal and spatial variations of the atmospheric dust loading Throughout West Africa over the last thirty years, *Ann. Geophys.*, 12, 265–273, doi:10.1007/s00585-994-0265-3.

O'Neill, N. T., T. F., Eck, A. Smirnov, B. N. Holben, S. Thulasiraman, 2003, Spectral discrimination of coarse and fine mode optical depth, Vol., 108, J. Geophys. Res., No. D17, 4559-4573, 10.1029/2002JD002975.

Ozer, P., Impact of dust processes on air quality in Niamey, Niger, and consequences on human health, 2008, Combating desertification: Assessment, adaptation and mitigation strategies, pages 125-134, ISBN: 978-90-5989-271-2, Bruxelles, Belgique.

Perez C., Haustein K., Jorba O., Janjic Z., Basart S. and JM. Baldasano, 2009, Atmospheric Mineral Dust Modeling from Meso to Global scales with the NMMB/BSC-DUST, AAAR 28th Annual Conference.

Pérez, C., K. Haustein, Z. Janjic, O. Jorba, N. Huneus, J.M. Baldasano, T. Black, S. Basart, S. Nickovic, R.L. Miller, J. Perlwitz, M. Schulz, and M. Thomson, Online atmospheric dust modeling from meso to global scales with the NMMB/BSC-Dust: 1. Model description, annual simulations and evaluation, submitted to Atmos. Chem. Phys., 2011.

Savory, E. C., L. E. Cuevas, M. A. Yassin, C. A. Hart, A. M. Molesworth, and M. C. Thomson, 2006, Evaluation of the meningitis epidemics risk model in Africa, Epidemiology and Infection 134:1047-1051.

Sultan, B., K. Labadi, J. F. Guegan, and S. Janicot, 2005, Climate drives the meningitis epidemics onset in West Africa, PLoS Medicine 2:43-49.

Thomson, MC, Molesworth AM, Djingarey, MH, Yameogo, KR, Belanger, F, Cuevas, LE, 2006, Potential of environmental models to predict meningitis epidemics in Africa. Tropical Medicine & International Health 11(6), 781-788.

Washington, R., and C.T. Martin, Atmospheric controls on mineral dust emission from the Bodélé Depression, Chad: The role of the low level jet, Geophys. Res. Lett., VOL. 32, L17701, doi:10.1029/2005GL023597, 2005.

World Health Organization (WHO), 1998, Emerging and other Communicable Diseases, Surveillance and Control; Control of epidemic meningococcal disease. WHO practical guidelines. 2<sup>nd</sup> edition; WHO/EMC/BAC/98.3; This document has been downloaded from the WHO/EMC Web site <http://www.who.int/emc>

World Meteorological Organization (WMO), Guide to meteorological instrument and observing practices, WMO-8 TP.3 4th ed., Geneva, 1971.

World Health Organization (WHO); 2000, WHO Report on Global Surveillance of Epidemic-prone Infectious Diseases, WHO/CDS/CSR/ISR/2000.1; Department of Communicable Disease Surveillance and Response; This document has been downloaded from the WHO/CSR Web site <http://www.who.int/emc>